NTNU
Det skapende universitet

Halvt nedsenkbar tørrtre plattform

Koblingen mellom det hydro-pneumatiske stigerørsstrekk-systemet, stigerørene og kjølen.

Thomas Skorpen
Marianne-Isabelle Falk

Marin teknikk
Innlevert: Juni 2012
Hovedveileder: Marilena Greco, IMT
Medveileder: Eilif Pedersen, IMT

Norges teknisk-naturvitenskapelige universitet
Institutt for marin teknikk

NTNU Trondheim
Norwegian University of Science and Technology
Faculty of Engineering Science and Technology
Department of MarineTechnology

MASTER THESIS IN MARINE TECHNOLOGY

SPRING 2012

FOR

Marianne-Isabelle Falk & Thomas Skorpen

Dry tree semisubmersible platform: coupling between the hydro-pneumatic riser tensioning system, the risers and the hull

(Tørt tre halvt nedsenkbare plattformen: kopling mellom hydro-pneumatisk riser tensioning system, stigerør og skroget)

The interactions of a riser system with the connected semisubmersible are relevant, especially when the water depth is large. The consequences are both on the platform motions and on the working conditions of the risers, and need to be properly quantified. For instance, riser-tensioner hysteresis can have a damping effect in the heave motion of the semisubmersible and affect indirectly the loads acting on the riser itself. Another important issue is connected to the effect of stick-slip friction at the contact point between risers and hull, particularly at the keel guide and in the riser tensioners. The challenge is that for small sea states, the static friction between risers and hull may be larger than the forces "anchoring" the semisubmersible with the risers. This leads to a pronounced reduction of the heave motion and is relevant for the fatigue life of the riser system. In both examples, heave response of the semisubmersible is of primary interest, with slowly-varying roll/pitch being second most important. The semisubmersible-riser interactions are expected to be less important for the other platform motions.

Objective

The aim of the thesis is to identify a proper modelling of the riser tensioning system and to analyse the behaviour of the dry tree semisubmersible accounting for the coupling between the riser tensioning system, the risers and the hull. The tensioner hysteresis and the friction phenomena associated with this platform concept should be examined and the consequent effects should be quantified. In particular, the damping mechanisms should be modelled mathematically and included in the equation of motions. Nonlinear effects should be examined and possible simplified solution strategies of the problem should be assessed.

The work should be carried out in steps as follows:

1. Give an overview of previous work, with main focus on state-of-the-art models for riser tensioners and coupled analysis of platform behaviour. Topics that have been discussed in the pre-project need not to be repeated in the Master Thesis report unless found useful for the discussion.
2. Evaluate the possibility of simplified modelling of tensioners in frequency domain and develop a frequency domain model including improved estimates of the hysteresis and friction (in the tensioner and at the keel guide).

3. Assess accuracy of the developed linearized model in frequency domain and use this to estimate the importance of hysteresis and other coupling effects on the semisubmersible motions.
4. Develop a nonlinear platform motion analysis in time domain with suitable riser tensioner model and compare the results for relevant selected cases with the frequency-domain results.
5. Examine extreme response behaviour of the platform.
6. Study effect of stick-slip friction phenomenon and its effects.

The work may show to be more extensive than anticipated. Some topics may therefore be left out after discussion with the supervisor without any negative influence on the grading.

The candidates should in their report give a personal contribution to the solution of the problem formulated in this text. All assumptions and conclusions must be supported by mathematical models and/or references to physical effects in a logical manner.

The candidates should apply all available sources to find relevant literature and information on the actual problem.

The thesis should be organised in a rational manner to give a clear presentation of the work in terms of exposition of results, assessments, and conclusions. It is important that the text is well written and that tables and figures are used to support the verbal presentation. The thesis should be complete, but still as short as possible. In particular, the text should be brief and to the point, with a clear language. Telegraphic language should be avoided.

The thesis must contain the following elements: the text defining the scope (i.e. this text), preface (outlining project-work steps and acknowledgements), abstract (providing the summary), table of contents, main body of thesis, conclusions with recommendations for further work, list of symbols and acronyms, references and (optional) appendices. All figures, tables and equations shall be numerated.

The supervisor may require that the candidates, in an early stage of the work, present a written plan for the completion of the work. The plan should include budget for the use of computer and laboratory resources that will be charged to the department. Overruns shall be reported to the supervisor.

From the thesis it should be possible to identify the work carried out by the candidate and what has been found in the available literature. It is important to give references to the original source for theories and experimental results.

The thesis shall be submitted in two copies:
- The copies must be signed by the candidate.
- This text, defining the scope, must be included.
- The report must appear in a bound volume or a binder.
- Drawings and/or computer prints that cannot be included in the main volume should be organised in a separate folder.
- The bound volume shall be accompanied by a CD or DVD containing the written thesis in World or PDF format. In case computer programs have been made as part of the thesis

work, the source codes shall be included. In case of experimental work, the experimental results shall be included in a suitable electronic format.

Supervisor :Marilena Greco
Submitted :16 January 2012
Deadline :15 June 2012

Marilena Greco
Supervisor

Preface

This thesis is written as a final work on our M.Sc. study in the Department of Marine Technology at Norwegian University of Science and Technology, with specialization in Marine Hydrodynamics. The thesis is carried out in the last semester of the study, and is weighted with 30 units.

During the fall 2011 a project thesis was written, which was meant to bring a foundation and basic understanding of the theory and principles for further work covered in this thesis. Therefore it can be useful to read both reports to get a full understanding of problems and theory covered, as many parts of this report refer to the Project thesis. It is assumed that persons reading this thesis have some background knowledge to the theory presented in this report.

In the Project thesis the computational solver WADAM was used to calculate hydrodynamic coefficients and excitation forces for a semi-submersible model given by Aker Solutions. MATLAB was used for the post-processing in the frequency domain and to plot the RAOs. Simple damping models for viscous flows and Coulomb friction forces were examined in combination with the nonlinear stiffness of hydro-pneumatic tensioners. This thesis carries the work further on, but focuses on time-domain analysis using regular waves with different wave heights and periods, to get a full inclusion of the nonlinear terms caused by the tensioner system.

Acknowledgements

This work has been carried out under supervision of Professor Marilena Greco at the department of Marine Technology, Norwegian University of Science and technology. She deserves a very special thank for her dedication and interest in our work, and for always taking her time for us. She has guided us through our master thesis in the most conceivable way, and the cooperation has been greatly appreciated.

We also want to thank our supervisors Rolf Løken & Christian Juell Gudbrandsen at Aker Solutions for their time and cooperation. They have both showed great interest in our work, and always taken their time to help us with any questions along the way. We are grateful to be provided with office spaces and coffee at the headquarters of Aker Solutions at Fornebu, and we want to thank all other associates at the marine division for good company throughout the semester and all their encouragement. Especially Kjell Hagatun and Ragnvald Børresen deserves a special thank for their meetings and guiding.

In February we were visiting Aker MH in Horten, where they produce riser tensioner systems. They paid big interest in our work, and we are thankful for the visit and guided tour by Rolf Bendiksen, and for all further questions and analysis provided by Ronny Sten.

We also want to thank Eilif Pedersen at the department of Marine Technology, NTNU, for point of views and discussions regarding behavior of the riser tensioner system.

Abstract

The hydro-pneumatic riser tension system will work as a passive heave compensator with a gas/oil accumulator to account for the relative motions between a semi and riser. Stroke of the cylinder will cause an expansion or compression of the gas, depending on direction of response, which is based on ideal gas laws. This causes an additional nonlinear stiffness. This stiffness is also dependent on the gas volume, and the impact of the semi response for a tensioner system with variable gas volume has been evaluated.

The flow of hydraulic fluid between cylinder and accumulator creates a viscous damping in combination with the gas flow between accumulator and gas reservoir bottles. These frictional forces are dependent on diameters and lengths of piping, valves and components in the hydraulic/pneumatic system. In this thesis simplified calculation models assumed to give approximate results are used. A numerical method has been developed to calculate the pressure loss based on Bernoulli's equation and conservation of mass and momentum.

A numerical method has been implemented to solve the equation of motion in time, including nonlinear spring rate and damping terms from the hydro-pneumatic tensioner system. Series of different regular wave heights and periods have been analysed to better separate the different contributions from the tensioner system, thus more easily find trends and contexts defining the system. In the project thesis RAOs was calculated for a few different scenarios. This is important and widely used information in an early design phase. Based on several time domain analyses for different wave heights and periods, new RAOs was extracted by plotting the max responses in the steady-state parts of time simulations.

Frictional forces are found in different contact points between moving elements on the semi. The friction between risers and keel guides and also in seal packers found in tensioner cylinders will influence the response of the semi, especially for small sea states. As the friction forces gets larger than the excitation forces the semi will be effectively "moored" by the risers. Accordingly, the excessive loads on the risers may reduce their expected lifetime. It has been analysed for which regular waves the semi will be stuck. For a "stuck" state of the semi, the stiffness will be dramatically increased and the natural period likely reduced.

Table of contents

List of figures

List of tables

Notations

Abbreviations

Accumulator	A device in a hydraulic system in which fluid is collected and especially in which it is kept under pressure as a means of storing energy. Example illustrated in Figure 11.
Fitting	Piping or tubing part that can connect two or more larger parts.
Keel Guide	Guiding for risers, which allow relative vertical movements, but keep the riser fixed when it comes to horizontal lateral movements. Sliding between keel guide and riser.
Keel Joint	Where the riser exits from the central structural pipe, a keel joint arrangement is used on the riser to control the bending moment transferred into the riser string due to offsets and motion of the riser.
MODU	Mobile Offshore Drilling Unit.
PD	Production and drilling.
RAO	Response Amplitude Operator
ROV	Remotely Operated Underwater Vehicle.
SCR	Steel Catenary Riser.
Stiction	The static friction that needs to be overcome to enable relative motion of stationary objects in contact.
TLP	Tension Leg Platform.
TTR	Top Tensioned Riser.
Well bay	An area on an oil platform where Christmas trees and wellheads are located.
Well Head	Top of oil well.
XMAS tree	Production manifold with valves, placed on top of Well Head.

List of symbols

A_{33}	Added mass in heave
A_C	piston area
β	Frequency ratio
B	Breadth of the semi
B	Linearized viscous damping
c	Damping coefficient
C_{33}	Damping coefficient in heave
$C_{TTR\ linear}$	Damping coefficient from the tensioner system
c_n	Viscous damping coefficient
C_D	Drag coefficient
d_i	Inner diameter of piping
ϵ_i	Roughness height of surface inside the pipes
η_3	Semi response in heave
F_3	Wave excitation force
$F_{3,M}$	Morison drag force in heave
$f_i(t)$	Darcy's friction factor as a function of time
ϕ	Wave potential
$H_x(\omega)$	Hydrodynamic transfer function
k	Wave number
k	Restoring coefficient
K_{33}	Restoring coefficient in heave
$K_{TTR}(x)$	Spring rate as function of stroke of the cylinder / response of the semi
$\mathrm{K_P}$	Loss coefficient in nitrogen piping
L	Length of the semi
λ	Wave length
m	Mass
m_{piston}	Mass of piston
m_{tree}	Mass of x-mas tree
μ	Total friction coefficient for Coulomb friction in seal packers of cylinder and keel guides
n	polytropic constant
P_0	Forces acting on the system
$p_c(t)$	oil pressure in oil as function of time
$Q_{oil}(t)$	Oil flow rate
R	Gas constant for nitrogen
Re	Reynolds number
ρ	Density of fluid
t	Time
T	Period
$T(t)$	Tension in one tensioner cylinder as function of time
T_0	Initial pretension in each riser
T_0	Constant temperature under working conditions
T_0	Eigen period
θ	Phase angle
$u(t)$	Tensioner cylinder stroke velocity
$\mathrm{u_p}$	velocity of gas in piping
V_{max}	Linearizing velocity amplitude
ΔW	Loss of energy
w	Wave particle velocity in z-direction
ω	Frequency
ω_0	Eigen frequency
x	Used as general response variable in the equation of motion
ξ	Damping ratio
ζ_A	Wave elevation amplitude
z_0	gas volume column in [m] relative to stroke length of cylinder

1. Introduction

The search for oil in ultra-deep waters demands new thinking, new methods and new solutions for production and drilling of oil. A new concept of a deep draft semisubmersible with direct access compensated risers are currently developed and evaluated by Aker Solutions.

Such a system with direct access wells on the topside of platform is referred to as a dry tree system. Todays dry tree installations are few, and limited by two different concepts, the TLP & the SPAR buoy. Over the last decades the semi-submersible with a flexible riser system has proven its excellence for oil- and gas-field development in medium to deep water, harsh environment conditions such as in the North Sea. It is therefore interesting to compare the dry tree semi concept to proven dry tree designs, like the TLP and SPAR buoy.

The semi-submersible design is low cost and easy to build, as it have a limited plate thickness and a conventional platform design based on flat stiffened panels. The biggest edge for the semi is its low transportation and installation costs. Most of the commissioning can be done on the yard, compared to the TLP and SPAR buoy, where a big part of the completion and installation must be done offshore on site.

However, heave motion has the greatest influence on whether dry trees can be used on a floater or not, and the TLP & SPAR buoy have the benefits that they don't respond much in vertical motion compared to the semi. Since the riser tensioning systems have restrictions and limited stroke-length, the heave motions must be minimized. This leads to the biggest challenge on the semi-submersible dry tree concept (Chedzoy & Lim, 2003).This work examines the interaction between riser tensioner system and the semi, and how it influences the heave response of the semi.

During fall 2011 a project thesis focusing on the interaction between the semi and the riser compensator system was carried out. The heave response of the semi was analysed in the frequency domain using WADAM and MATLAB. This thesis carries the work further on, and will give a deeper understanding of the physics of the riser tensioner system and how it will influence the heave response of the semi. Analyses have been performed mostly in self-developed MATLAB codes, but WADAM and SIMO have also been used.

2 – Case study: Deep draft dry-tree semi

The dry tree semisubmersible concept developed by Aker Solutions is a deep-draft semi with top tensioned risers, hereby referred to as TTRs, where the riser tensioner cylinders, XMAS trees and BOP are all placed on the topside. The concept is developed for ultra-deep waters, and based on a regular semisubmersible design but with a deeper draft. This is done because the relative motion between the compensated risers and the semi should be as low as possible, and a deeper draft reduces the wave excitation forces on pontoons. The roll and pitch will also be reduced, which give less bending of the top tensioned risers at the keel guides and less excitation of the steel catenary risers.

Figure 1: Dry tree semisubmersible

Table 1: Boundary conditions for semisubmersible

Operation depth	2 438.4 [m]
Operation draft	42.4 [m]
Weight	122 000 [MT]
Length	112 [m]
Breadth	112 [m]
Stroke-length of tensioner cylinders	12.6m (+/-6.3m)

2.1 Top tensioned riser system

The well bay layout consists of two rows of six steel risers, which serves as a direct vertical connection between the semi-submersible and producing wells. As the semi moves in vertical direction relative to the static sea bed, this must be compensated by use of a riser compensator system. To overcome the weight of the risers and ensure a positive tension in the risers, there must also be a constant initial top tension in all of the risers. This will prevent buckling of the risers and horizontal displacements. The top tension and relative motion will for this case be compensated by use of 4 hydro-pneumatic tension cylinders connected to each riser as described below. The hydro-pneumatic tension cylinders act as a spring-dashpot system, in the same way as a regular suspension system on a car. This system is a commonly used passive heave compensator in the offshore industry.

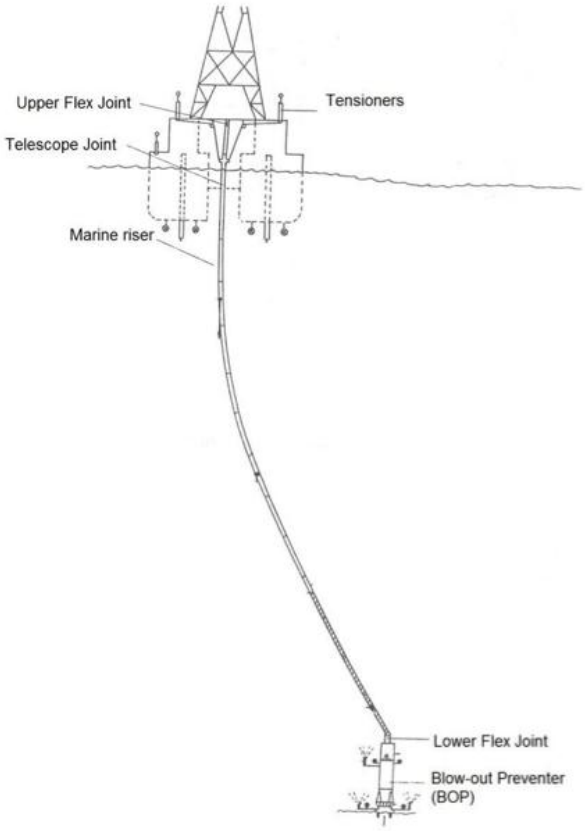

Figure 2: Concept of a riser tensioner compensator

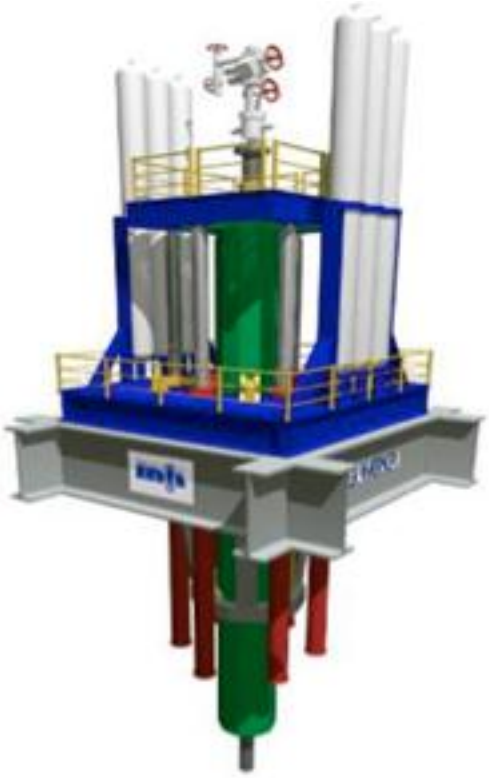

Figure 3: Direct acting riser tensioner system

Each TTR has a RAM-style cassette setup consisting of four hydro-pneumatic tension cylinders placed vertically on the topside. Compared to a conventional direct acting tensioner system, with tensioner cylinders placed below deck with cylinder rods facing downwards this kind of setup protects the risers from incoming waves and weather. Placing the cylinders on the topside will also give easier access for inspection and maintenance of the cylinders.

Each TTR is installed with a given initial pretension. As the fluid side is assumed incompressible, the gas pressure adjusts this pretension in the hydro-pneumatic cylinder system. This defines the stiffness of the system and affects the natural period and response of the semisubmersible. The flow of fluid and gas, leading to the viscous damping in the system, also depends on the pressure in the system. This will be further discussed in theory chapter 3.3. The gas in the accumulator system is chosen to be nitrogen, due to its anti-corrosive and polytropic properties.

Table 2: Top tension riser system data

Number of TTRs	**2 x 6 = 12**
Number of hydro-pneumatic cylinders	4 x 12 = 48
Length of cylinders	12.6 [m] (+/-6.3m)
Inner cylinder diameter	0.560 [m]
Cylinder volume / 2	1550 litres
Initial pretension	840 mT in each TTR
Gas volume	5 x cylinder fluid volume ≈ 7500 litres
Riser stiffness	3600 [kN/m]

2.2 Mooring Configuration

The dry tree semi will be moored by 16 lines, 4 at each corner of the rig. Because of the large water depths most of the anchorlines will consist of polyester fibre ropes to avoid too large loads from the heavy steel anchor chains. Only about 100 meters at each end will consist of anchor chains, as shown in figure 2. With this setup the semi will have a different response than by using anchor chains only, since polyester ropes have a low, non-linear stiffness.

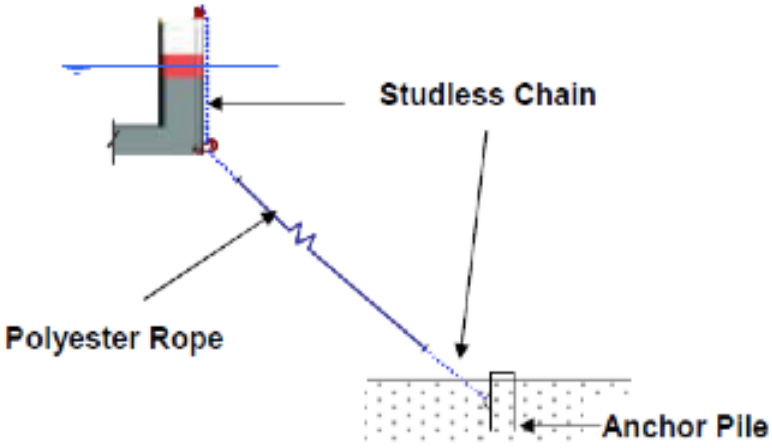

Figure 4: Setup of anchor lines with polyester & studless chain

The pretension of the anchor lines will influence the different Eigen periods and hence affect the response of the semi in every degree of freedom. The distribution between vertical and horizontal stiffness will be close to equal, since the hang-off angle of lines are about 45°.

Table 3: Mooring line data

	R4S Stud less chain	Polyester Rope
Diameter [mm]	133	248
Maximum break load [kN]	16 227	16 752
Anchor chain length [m]	232	3500
Mass [tons]	Not given	Not given
General information		
Number of lines	16 – 4 at each corner	
Pretension [kN/line]	4110	
Hang-off angle [deg]	45.9	
Horizontal stiffness per line [kN/m]	12.9	
Vertical stiffness per line [kN/m]	13.3	

3 – Frequency domain analysis

As far as possible problems are solved in the frequency domain where all values are linearized, hence computational solvers like HydroD may be applied. Being able to apply linear theory normally gives good results and greatly simplifies the calculations and the computational time. It is also easier to divide the problem into different fragments due to super-positioning, and thus look at how one contribution influences the response of the system. The results from frequency domain analysis give a good indication of the sea keeping abilities and vessel characteristics.

In the project thesis a WADAM analysis was done based on a panel model from Aker Solutions. In addition to this a Morison model was created in GeniE to account for the viscous effects, with a drag velocity linearization done for a linearizing velocity of 1.66 [m/s] as discussed more closely in 6.2 – Verification of the solvers. All the hydrodynamic coefficients used in the MATLAB code in the project thesis were gathered from this WADAM analysis (Falk & Skorpen, 2011).

3.1 Theory

3.1.1 The equation of motion and response calculation

The equation of motion can, for a damped system, be described as equation (3.1) below.

$$m\ddot{x} + c\dot{x} + kx = P_0 sin\omega t \tag{3.1}$$

The solution to the homogeneous equation expresses the transient part of the solution and will die out in a damped system. Hence, for marine constructions in waves the homogeneous solution is normally disregarded. The particular solution of the equation of motion is expressed below: (Larsen, January 2009)

$$x_p = C_1 sin\omega t + C_2 sin\omega t \tag{3.2}$$

Which gives us the following expressions when put into equation (3.1):

$$\begin{cases} -m\omega^2 C_1 - c\omega C_2 + kC_1 = P_0 \\ -m\omega^2 C_2 - c\omega C_1 + kC_2 = 0 \end{cases} \tag{3.3}$$

$$\begin{cases} C_1 = \dfrac{P_0}{k} \dfrac{1-\beta^2}{(1-\beta^2)^2 + (2\xi\beta)^2} \\ C_2 = \dfrac{P_0}{k} \dfrac{2\xi\beta}{(1-\beta^2)^2 + (2\xi\beta)^2} \end{cases} \tag{3.4}$$

$$x_p = \frac{P_0}{k} \frac{1}{(1-\beta^2)^2 + (2\xi\beta)^2} [(1-\beta^2) sin\omega t - 2\xi\beta sin\omega t] \tag{3.5}$$

This solution can be represented by one single harmonic function:

$$x_p = R sin(\omega t - \theta) \tag{3.6}$$

$$RAO = (C_1^2 + C_2^2)^{\frac{1}{2}} = \frac{P_0}{k} \frac{1}{(1-\beta^2)^2 + (2\xi\beta)^2} = \frac{P_0}{k} \cdot DAF \tag{3.7}$$

$$\theta = \arctan\left(-\frac{C_2}{C_1}\right) = \arctan\left(\frac{2\xi\beta}{1-\beta^2}\right) \tag{3.8}$$

$$\beta = \frac{\omega}{\omega_0} \tag{3.9}$$

$$\xi = \frac{c}{c_{critical}} = \frac{c}{2m\omega_0} \tag{3.10}$$

$$\omega_0 = \sqrt{\frac{k}{m}} \tag{3.11}$$

The phase angle is a useful tool when looking at the relation between the load and response, and gives much information when looking at the effects of different damping contributions in a system. The phase angle graph plotted against the period is also useful when it comes to estimation of natural periods and to see where the system is mass or stiffness dominated. This is further discussed in Chapter 6.2 and the results Chapter 7.3.

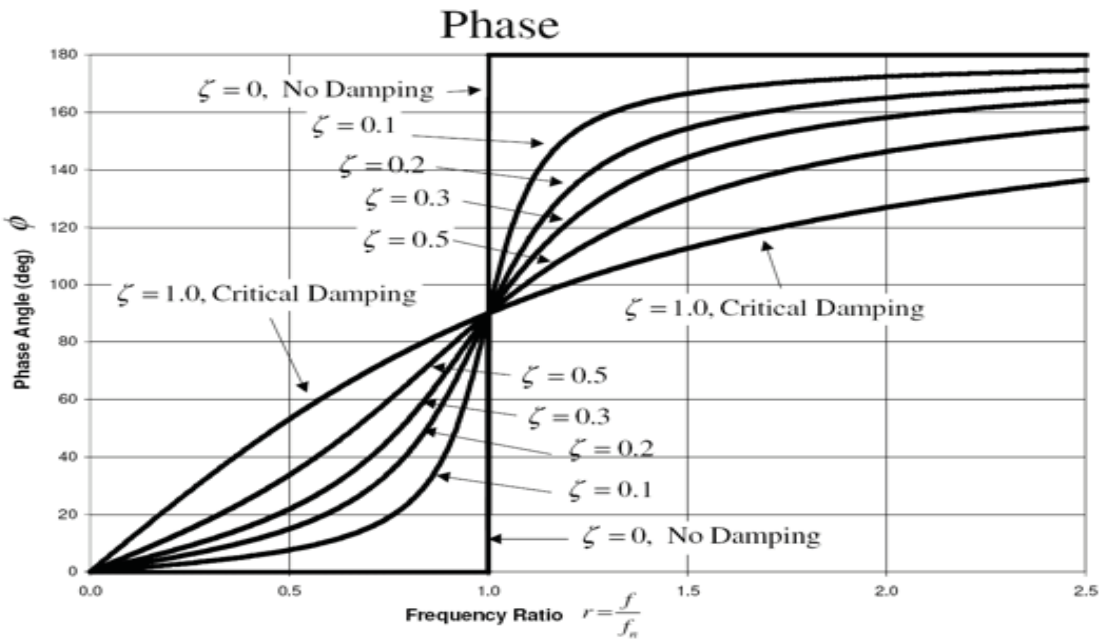

Figure 5: Relation between frequency-ratio, phase shift and damping ratio (Larsen, January 2009)

3.1.2 Drag linearization

In the project thesis the drag force from Morison's equation was linearized by using the drag velocity method in WADAM. B is the linearized viscous damping found from equivalent linearization, with the relative velocity as explained in the project thesis. V_{max} is a linearizing velocity amplitude specified as input to WADAM (Det Norske Veritas).

$$F_{3,M}(t) = \frac{1}{2}\rho C_D DL(w - \eta_3)|w - \eta_3| \tag{3.18}$$

$$B = \frac{1}{2}\rho DLC_D \frac{8}{3\pi} V_{max} \tag{3.19}$$

$$F_{3,M}(t) = B(w - \dot{\eta}_3) \tag{3.20}$$

This linearization makes it possible to split the drag force into two parts, one term which goes into the damping part of the equation of motion, and the other which contributes to the force acting on the body.

$$(m + A_{33})\ddot{\eta}_3 + (c + B)\dot{\eta}_3 + k\eta_3 = F_3 + Bw \tag{3.21}$$

At resonance, the mass term and the restoring term equalize each other; hence the damping term will dominate. Since the damping is the main contribution, which determines how the system reacts over this period range, the linearization is done over the natural period. This is done to get the most accurate results, and the linearized damping value found over this period is used as a constant over the whole frequency-range. In the project thesis B_{heave} was found to be $8.515 \cdot 10^6 \left[\frac{kg}{s}\right]$.

3.1.3 - Damping estimation using free decay test

Decay tests give important information about natural frequencies, added mass and damping of a dynamic system. The system is exposed to a displacement or a constant force pulse, and the response is the undisturbed transient phase until the system reaches its initial condition. To simulate this in MATLAB, the homogeneous part of the system with non-linear damping is considered. This is represented by equation (3.22):

$$M\ddot{x} + B_1\dot{x} + B_2\dot{x}|\dot{x}| + Cx = 0 \tag{3.22}$$

Where M represents the mass and added mass, B_1 is the linear damping and B_2 the quadratic damping and C is the restoring stiffness. Dividing the above equation by M the equation of motion on standard form is obtained:

$$\ddot{x} + p_1\dot{x} + p_2\dot{x}|\dot{x}| + p_3x = 0 \tag{3.23}$$

The analysis of this equation is based on the well-known solution of a linear oscillating system in combination with the technique of equivalent linearization. Equivalent linearization implies that the non-linear damping term is replaced with an equivalent linear term which is determined from the requirement of equal damping energy per cycle. This requirement is satisfied through equation (3.24).

$$p_{EQ} = p_1 + \frac{8}{3\pi}\omega x_0 p_2 \tag{3.24}$$

Where x_0 is the motion amplitude of the relevant cycle and ω is the oscillation frequency. From the above equations, the linearized equation of motion can be written:

$$\ddot{x} + p_{EQ}\dot{x} + p_3 x = 0 \tag{3.25}$$

Assuming that x_{i-1} and x_i are two following amplitudes, the linear damping coefficient, p_{EQ}, is given by:

$$p_{EQ} = -2\omega \frac{\delta}{\sqrt{\pi^2 + \delta^2}} \tag{3.26}$$

$$\delta = ln\left(\frac{x_i}{x_{i-1}}\right) \tag{3.27}$$

$$v_{EQ} = \frac{8\omega x_i}{3\pi} \tag{3.28}$$

p_{EQ} can now be obtained for each cycle from the logarithmic decrement, δ. p_1, which represents the linear damping, is found as the intersection with the abscissa. p_2, which is the quadratic damping, is found from the slope of the curve, if plotted against the relative velocity.

The natural frequency of the damped freely oscillating system, ω_d, found from the natural frequency of the undamped system, ω_0, and the relative damping of the system, κ, given below:

$$\omega_d = \omega_0\sqrt{1-\kappa} \tag{3.29}$$

$$\kappa = \frac{p_{EQ}}{p_{cr}} = \frac{-\delta}{\sqrt{\pi^2 + \delta^2}} \tag{3.30}$$

3.2 Limitations of the frequency domain calculations

The frequency domain is based on linear theory, hence in cases where nonlinearities appear or which is significantly influenced by the history of the response, time domain analysis has to be applied. Only the stationary regime is considered when solving the equation of motion in the frequency domain, thus excluding the transient part expressed by the homogeneous solution. This is especially important when looking at irregular sea states where the memory is applied through the convolution integral, which is non-compatible with the frequency domain.

The calculations cannot be done in the frequency domain if the force is not given as a harmonic function or the principle of linear super-positioning does not apply due to some form of nonlinearities in the system. It is then necessary to do a dynamical analysis in the time domain.

3.3 Case specific limitations

For the dry tree semi the riser tensioner system will cause a nonlinear damping and stiffness dependent on the response. These nonlinearities are due to the flow of hydraulic fluid between cylinder and accumulator which creates a viscous damping in combination with the gas flow between accumulator and gas reservoir bottles. The stiffness of the tensioner system depends upon compression of the gas in the hydro-pneumatic tensioners, which is directly linked to the semi response in heave.

Also, since the objective of the analysis is to see how the tensioner system affects the response of the semi, nonlinear Morison damping has to be applied. This is because the linearized Morison damping is done over the resonance period, and is therefore significantly higher than the real Morison value over the interval in question.

4 - Time domain analysis

As discussed in Chapter 3, a full time-domain analysis must be performed in order to get the correct results in a non-linear system where the coefficients vary in time. Since the heave motion will have the most effect on the tensioner system, only one degree of freedom has been analysed. Roll and pitch motions will also have some impact on the system, though very little compared to heave, and are therefore neglected in this report. This is because the general vertical translational movements affect the stroke length more than the vertical movements generated by rotation, even if the risers are placed far from each other so that the momentum arm is long.

For sinusoidal motions, the equation of motion in heave for the semi can be written as:

$$\big(m + A_{33}(\omega)\big)\ddot{\eta}_3(t) + C_{33}(\omega)\dot{\eta}_3(t) + K_{33}\eta_3(t) = F_{3,exc}(t) \tag{4.1}$$

The hydrodynamic coefficients were found from the WADAM analysis done in the Project thesis. Both the added mass- and damping-coefficients are frequency dependent, and the mass and restoring terms are constant. These coefficients are given in *APPENDIX D: Results from WADAM*. The wave excitation forces were found by applying the hydrodynamic transfer function using regular waves, discussed more closely in chapter 4.2. The additional nonlinear viscous Morison damping is further discussed in chapter 4.3.

The riser tensioning system will include extra stiffness and damping. By including these terms the total equation of motion can be written as:

$$F_{3,exc} = \big(m + A_{33}(\omega)\big)\ddot{z}(t) + (C_{33}(\omega) + C_{TTR\ linear})\dot{z}(t) + (K_{33} + K_{TTR}(x))z(t) \tag{4.2}$$

In equation (4.2) z represents the heave response on the semi, and x the stroke length in the tensioner system. These values are in essentials the same, but to separate the two systems they are given two different notations.

The stiffness of riser system will include both the spring force caused by gas pressure in accumulator and stiffness of the risers. As the risers are much stiffer than the accumulators, the accumulator spring force will be dominating. Total stiffness for two springs in serial is given by:

$$K_{TTR,total} = \frac{1}{\frac{1}{K_{TTR}(z)} + \frac{1}{K_{Risers}}} \tag{4.3}$$

It should be noted that the equation of motion will have both frequency-dependent and response-dependent variables. The frequency-dependent coefficients are solved in advance using WADAM. For irregular waves with several frequencies, a convolution integral can be applied to include the frequency dependence for added mass and damping. The response-dependent variables, i.e. variables depending on the tensioner system or the nonlinear Morison drag force, have to be solved by iteration.

4.1 - Numerical integration by 4th order Runge-Kutta

To get correct results of a nonlinear system, a time domain analysis must be performed. This is done by solving the equation of motion over a time interval, but since it is very difficult to find an anti-derivative to this which is an elementary function, it has to be solved using numerical integration. This is normally a complicated process, especially for systems with many degrees of freedom. What recognizes the methods using numerical time integration is that in all of them the dynamic response is estimated in discrete time steps. The solution might be good in the integration points, but may differ in between as shown in Figure 7. The results contains both the particular and the homogenous solution, hence the transient phase is included in the calculations. Numerical methods also have a limited accuracy depending on which method is used and on the time step size.

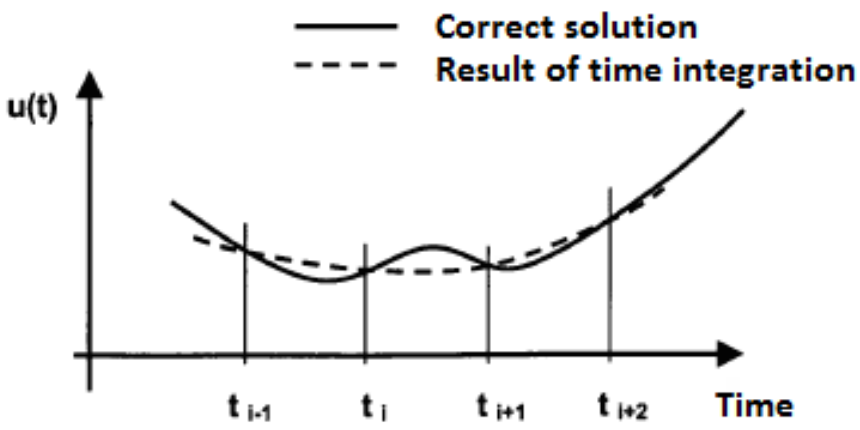

Figure 6: Discrete and continuous solution of time integration (Larsen, January 2009)

The one-degree of freedom equation of motion expressed by equation (4.1) is an initial value problem, where the solution is determined by the initial conditions. The most practical numerical integration methods for these kinds of problems are described by a stepwise process in the chosen time domain, hence it is divided into time steps, h, which are normally of equal length. Given the displacement and velocity of the system at the beginning of an interval in the time domain, one can determine the solution at the end of the interval by assuming the form of the graph over the interval. This solution may now be used to determine the next time step, and thus iterating through the time domain an approximation of the correct solution is found. The precision of the result is closely related to the size of the

time steps. (Langen & Sigbjörnsson, 1979)

$$m\ddot{x} + c\dot{x} + kx = Q(t) \tag{4.4}$$

$$m = m_{semi} + A_{33}$$
$$c = B_{33} + c_n \cdot abs(\dot{u})$$
$$k = K_{33} + k_{TTR}$$
$$Q(t) = F_3 \cdot \zeta_A \cdot sin(\omega t)$$

Where c_n is the viscous damping coefficient and k_{TTR} is the contribution from the risers estimated in the project thesis.

The above equation was solved using the 4th order Runge-Kutta method. The Runge-Kutta methods are a family of explicit and implicit one-step methods, where the displacement and velocity is found for every new time step by integrating the acceleration, $\ddot{x}(t)$:

$$\ddot{x}(t) = \frac{1}{m}(Q(t) - c\dot{x}(t) - kx(t)) \tag{4.5}$$

$$\dot{x}_{k+1} = \dot{x}_k + \int_0^h \ddot{x}(t)dt \tag{4.6}$$

$$x_{k+1} = x_k + \int_0^h \dot{x}(t)dt \tag{4.7}$$

The above integrals are approximated on the following form:

$$x_{k+1} = \dot{x}_k + h\phi_1(t_k, x_k, \dot{x}_k, h) \tag{4.8}$$
$$x_{k+1} = x_k + h\phi_2(t_k, x_k, \dot{x}_k, h) \tag{4.9}$$

Where ϕ_1 and ϕ_2 represents mean values for respectively $\ddot{x}(t)$ and $\dot{x}(t)$ over the time interval. They are estimated as the weighted average values of many different approximations of $x(t)$ and $\dot{x}(t)$ in the interval. There exist many different Runge-Kutta methods which differs with respect to the accuracy and computational time, but for the explicit 4th order method the above problem is solved as follows, where a_i and b_i are approximations to respectively $\ddot{x}(t)$ and $\dot{x}(t)$ at the beginning, in the middle and at the end of the interval (Langen & Sigbjörnsson, 1979):

$$\dot{x}_{k+1} = x_k + \frac{h}{6}(a_1 + 2a_2 + 2a_3 + a_4) \tag{4.10}$$

$$x_{k+1} = x_k + \frac{h}{6}(b_1 + 2b_2 + 2b_3 + b_4) \tag{4.11}$$

$$a_1 = \frac{1}{m}(Q_k - kx_k - c\dot{x}_k)$$

$$a_2 = \frac{1}{m}\left(Q_{k+\frac{1}{2}} - k\left(x_k + \frac{1}{2}hb_1\right) - c(\dot{x}_k + \frac{1}{2}ha_1)\right)$$

$$a_3 = \frac{1}{m}\left(Q_{k+\frac{1}{2}} - k\left(x_k + \frac{1}{2}hb_2\right) - c(\dot{x}_k + \frac{1}{2}ha_2)\right)$$

$$a_4 = \frac{1}{m}(Q_{k+1} - k(x_k + hb_3) - c(\dot{x}_k + ha_3))$$

$$b_1 = \dot{x}_k$$

$$b_2 = \dot{x}_k + \frac{1}{2}ha_1$$

$$b_3 = \dot{x}_k + \frac{1}{2}ha_2$$

$$b_3 = \dot{x}_k + ha_3$$

For every time step it is necessary to calculate four velocities and four accelerations, hence there are significantly more operations than for example in Newmark's or Euler's method. This is also an explicit method, which is conditionally stable.

In general the accuracy of the integration methods depends on the dynamic loads, the physical parameters acting on the system and the step length. To get a picture of the accuracy one looks at a free decay test of the system without damping. This normally shows typical faults like period errors or decreasing amplitude caused by artificial damping. For systems with one degree of freedom conditional stability is no drawback, since the step length must necessarily be less than the stability limit to get a sufficient accuracy.

Loss of stability in a numerical integration gives a very great deviation from the correct solution. This error may show itself as uncontrolled oscillation around the exact result, the numerical values might become unrealistic and the integration process will stop due to overflow in the computer. Stability cannot be controlled with damping, but by the time step size. In a conditionally stable system the time step size must be strictly smaller than a certain value depending on the Eigen period of the system.

4.2 - Wave excitation forces by linear wave theory

Linear wave potential theory is used throughout the study for calculations of excitation forces on the semi. According to Airy´s wave theory, the wave potential is written as (Faltinsen, 1990):

$$\phi = \frac{\zeta_A g}{\omega} \frac{\cosh k(z+d)}{\cosh kd} \cos(\omega t - kx) \tag{4.12}$$

For deep water waves, i.e. $depth > \frac{\lambda}{2}$, a simplification can be done:

$$\frac{\cosh k(z+d)}{\cosh kd} \rightarrow e^{kz} \tag{4.13}$$

Irregular sea was considered, but to better see trends that may be found, regular waves with different heights was chosen. The wave elevation can be written as:

$$\zeta(t) = \zeta_A \sin(\omega t - \mathrm{kx}) \tag{4.14}$$

Particle velocity and acceleration:

$$w = \frac{d\phi}{dz} = \omega \zeta_a e^{\mathrm{kz}} \cos(\omega t - \mathrm{kx}) \tag{4.15}$$

$$a_z = \frac{dw}{dz} = -\omega^2 \zeta_a e^{\mathrm{kz}} \sin(\omega t - \mathrm{kx}) \tag{4.16}$$

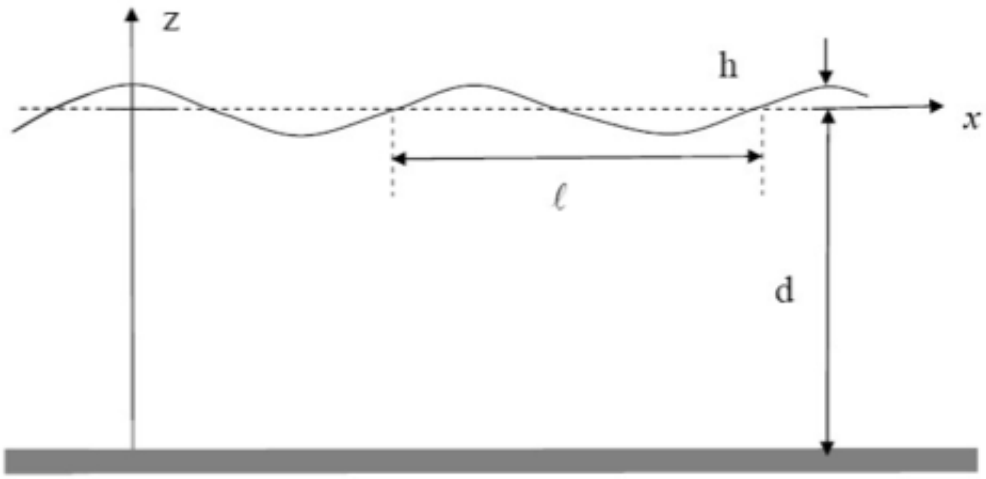

Figure 7: Linear wave theory (Faltinsen, 1990)

The wave excitation loads, consisting of Froude-Kriloff and diffraction forces, were calculated in WADAM and a hydrodynamic transfer function $H_X(\omega)$ were obtained. By applying the transfer function the excitation forces on the semi were found. The hydrodynamic transfer function is found in *APPENDIX D: results from WADAM*

$$F_{3,exc}(\omega, t) = \zeta(t)H_x(\omega) = \zeta_A \cos(\omega t)\, H_x(\omega) \tag{4.17}$$

As the semi was analysed in regular waves with a single frequency, the wave excitation force will vary sinusoidal.

4.3 - Nonlinear Morison damping

As the frequency domain considers a linearization of the drag term in Morison´s equation, B, which is constant for all frequencies, there will be an error compared with the real quadratic Morison damping term as seen in Figure 8. Since this error is especially prominent for $T \in [5s\,, 20s]$, the additional damping from the linearization over this interval may dominate the damping from the tensioner system. To get the most accurate results concerning the importance of hysteresis in the tensioner system, nonlinear Morison damping has been used.

The exact solution can be found by considering the time varying Morison drag force on a strip of length dz, which is expressed as equation (4.18) below. Since the semi is not a fixed body, it is important to consider the relative velocity between waves and the semi. The relative velocity increases as the wave height increases, and the Morison drag force augments with the square of that, hence nonlinear Morison drag force becomes more significant for higher sea states.

$$F_{3,M}(t) = \frac{1}{2}\rho C_D DL(w - \eta_3)|w - \eta_3| \tag{4.18}$$

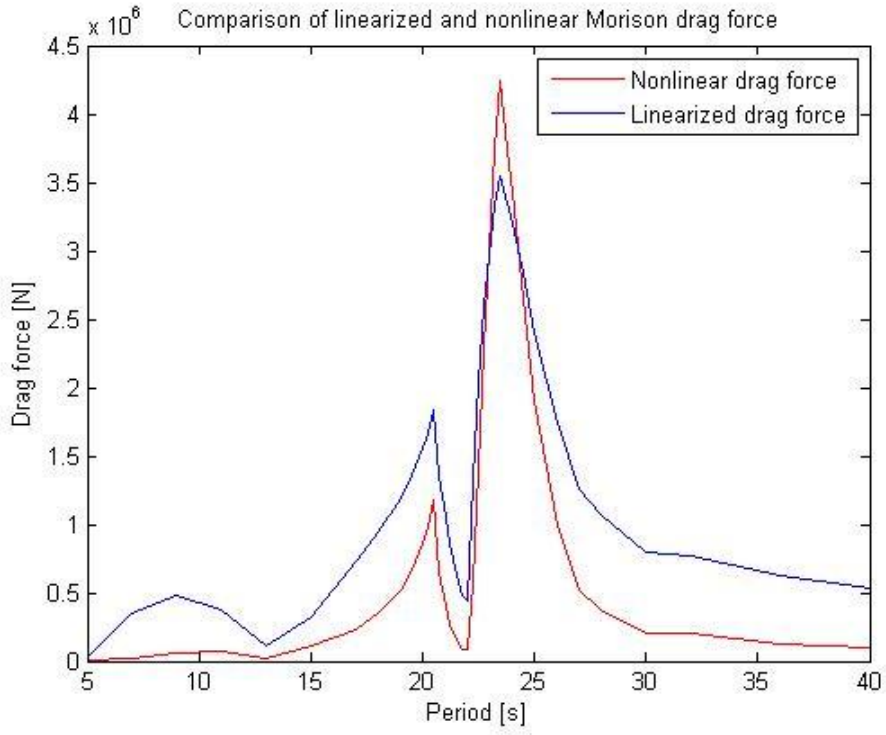

Figure 8: Comparison of linear and non-linear Morison drag force in 2m wave height

4.4 - Solution of equation of motion by convolution integral

Irregular wave analysis was discussed at an early stage and some basic theory on this is therefore included in this report for further analysis. Analysing the equation of motion in irregular sea with multiple frequencies brings in difficulties with frequency dependent coefficients. This can be solved by adapting the convolution integral.

Assuming linear theory, an arbitrary load history can be represented by a super-positioning of impulse loads acting over a short time duration dt. Every impulse load generates a response, and the response of the system will be the sum of all these response contributions (Langen & Sigbjörnsson, 1979).

Dirac's delta function is used to describe one impulse load unit:

$$\delta(t-a) = 0|_{t\neq a} \tag{4.19}$$

$$\int_{-\infty}^{\infty} \delta(t-a)dt = 1 \tag{4.20}$$

This means that δ equals zero for all $t \neq a$, and when $t \to a$ the δ-function go towards infinity. Hence the above integral equals zero for all t, except when $t = a$. Accordingly, the load function for an arbitrary impulse I can be expressed:

$$Q(t) = I\delta(t-\tau) \tag{4.21}$$

Using Dirac's delta function the following relation is found:

$$\int_{-\infty}^{\infty} Q(t)dt = \int_{-\infty}^{\infty} I\delta(t-\tau)dt = I\int_{-\infty}^{\infty} \delta(t-\tau)dt = I \tag{4.22}$$

Assuming one unit load acting on a one degree of freedom system at the time $t = 0$:

$$m\ddot{x} + c\dot{x} + kx = Q(t) = I\delta(t) \tag{4.23}$$

The response is hereby referred to as the impulse-response function, $h(t)$:

$$x(t) = h(t) \tag{4.24}$$

The response for an arbitrary impulse I at the time τ with a load $Q(t) = I\delta(t-\tau)$ is expressed:

$$x(t) = I \cdot h(t-\tau) \tag{4.25}$$

For physical systems $h(t-\tau) = 0$ for $\tau > t$.

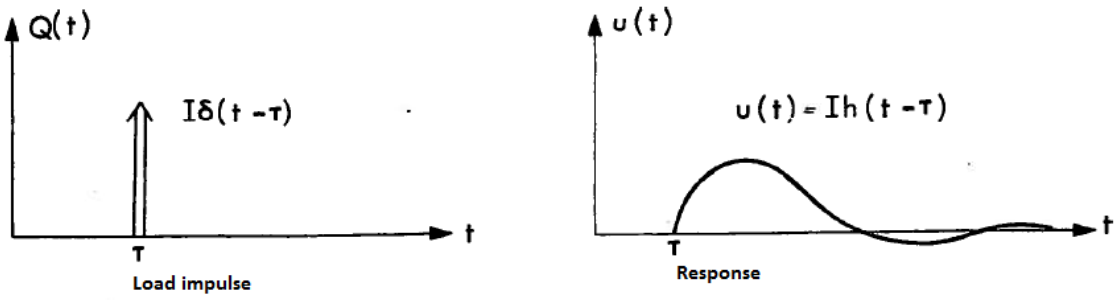

Figure 9: Load and response for a unit load impulse (Langen & Sigbjörnsson, 1979)

It is possible to find the response for an arbitrary load using the impulse-response function. The load history is divided into a sum of load impulses acting over $\Delta\tau$ as seen in Figure 9. Here an impulse acts at the time $t = \tau$ with the impact of $Q(\tau)\Delta\tau$. The corresponding force can be written:

$$Q(\tau)\Delta\tau\delta(t-\tau) \tag{4.26}$$

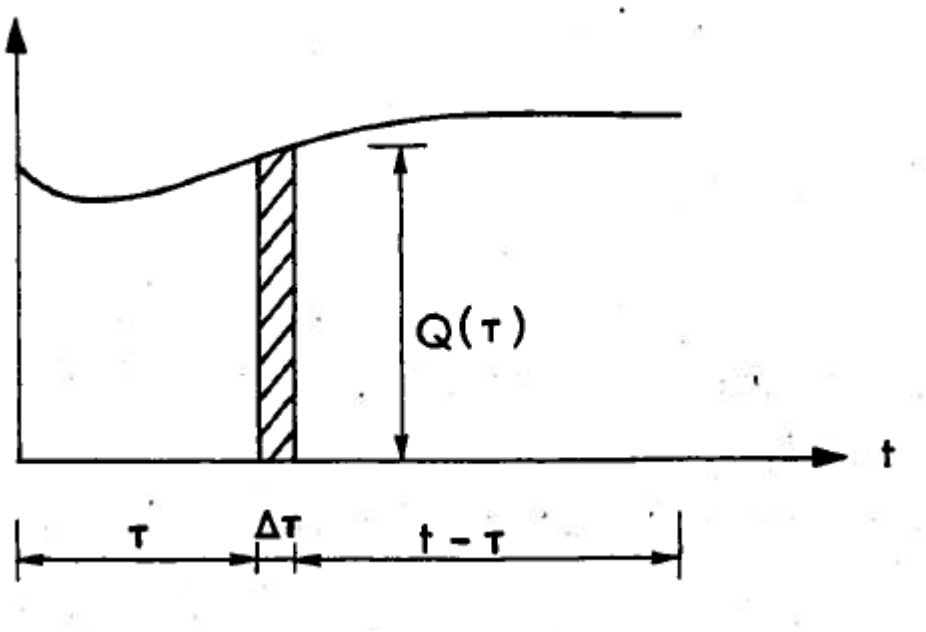

Figure 10: Arbitrary load impulse in a load history (Langen & Sigbjörnsson, 1979)

Using equation (4.25) and (4.26), the response at the time t can be written:

$$x(t,\tau) = Q(\tau)\Delta\tau h(t-\tau) \tag{4.27}$$

Summing up all the impulses, the above equation is expressed:

$$x(t) = \lim_{\Delta\tau\to 0}\sum Q(\tau)h(t-\tau)\Delta\tau \tag{4.28}$$

$$x(t) = \int_0^t h(t-\tau)Q(\tau)d\tau \tag{4.29}$$

The above integral is also known as the convolution integral. This integral brings memory into the system, and is necessary when looking at irregular seas.

5 – Theory: Hydro-pneumatic cylinders

In offshore applications the hydro-pneumatic cylinder concept is often used as a passive heave compensator (Falk & Skorpen, 2011). For the case described in this report, the TTR compensator system will have two important contributions that will influence response of the semisubmersible; additional damping and increased stiffness. The damping is mainly caused by viscous friction of the fluid and gas in the system, but frictional forces found in seal packers will also contribute. The nonlinear stiffness is caused by compression of an ideal gas.

Hydraulic and pneumatic systems have different areas of application, but their governing equations and fundamental principles are the same. The main difference is that hydraulics is assumed incompressible, and pneumatics use highly compressible gas fluid. Still their basic principles are the same; conservation of mass, energy and momentum. This is described in basic fluid mechanics (White, 2002).

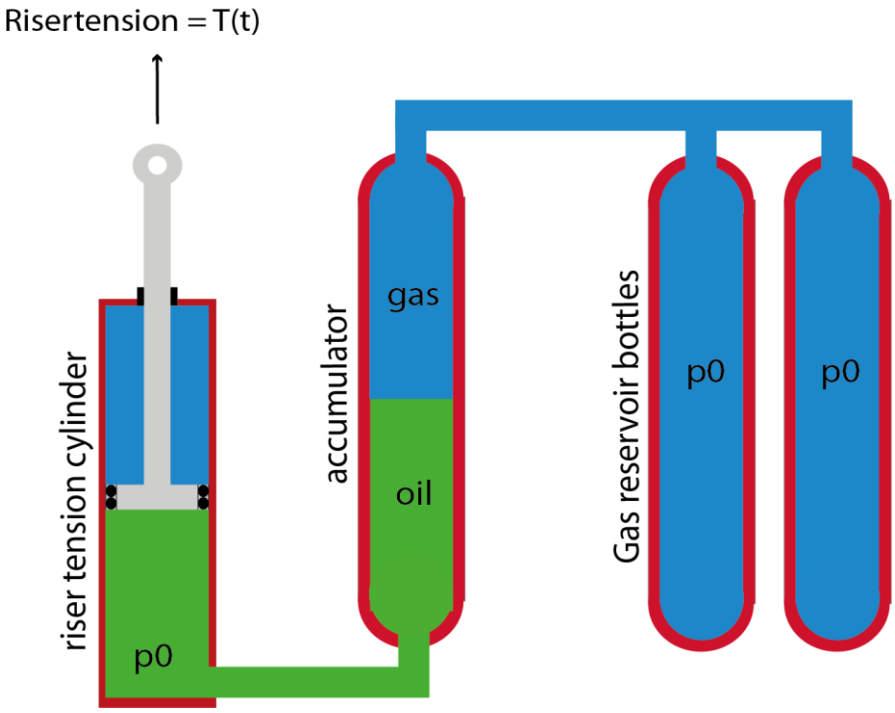

Figure 11: Hydro-pneumatic cylinder concept as used in riser tensioner system.

Figure 11 shows a basic hydro-pneumatic compensator cylinder widely applied in the offshore industry. For the riser compensator system on the dry-tree semi-submersible, four of these cylinders are attached to each riser. This is described and illustrated in chapter 2.1

The mathematical theory behind flow of fluids in the system can be complex and difficult to calculate exactly. Often CFD analyses are used, which gives the most exact results, but are time consuming. In the following chapter simplified calculation models to calculate the behaviour and pressure loss in the system are described. This theory is later implemented in a MATLAB-code to make estimations of tension variation in the top tensioned risers caused by viscous and frictional forces, hence the damping found in the system.

The tension in each riser as function of time can be calculated as

$$T(t) = 4 * \left(p_c(t)A_C + \mu T_0 sign\left(u(t)\right) - m_{piston}g\right) - m_{tree}\mathrm{g} + k_{TTR}\left(x(t)\right)x \qquad (5.1)$$

$T(t)$ = Tension in one tensioner cylinder as function of time

$p_c(t)$ = oil pressure in oil as function of time

A_C= piston area on oil side of cylinder

μ = total friction coefficient for Coulomb friction in seal packers of cylinder and keel guides

T_0 = Initial pretension in each riser

$x(t)$ = tensioner stroke velocity = semi heave velocity

m_{piston} = mass of piston = 5 tonnes

m_{tree} = mass of xmas tree

k_{TTR} =spring rate as function of stroke of the cylinder / response of the semi

In the following sub chapters the theory behind calculation of pressure loss for an oscillating hydro-pneumatic cylinder is presented. The calculation is split in two; calculating the fluid and gas parts separately.

5.1 Nonlinear stiffness

Compression of the hydro-pneumatic tensioners will cause a change in stiffness, caused by the pressure increase. This means that spring force is related to the stroke of the piston. In an isotherm compression, where temperature stays constant, change of stiffness due to the stroke of cylinder will be linear. As few gases will compress without developing some heat, the basic polytropic relationships for compression of gases must be used (Giliomee, 2005).

$$PV^n = constant \quad \rightarrow \quad P_1V_1^n = P_2V_2^n \tag{5.2}$$

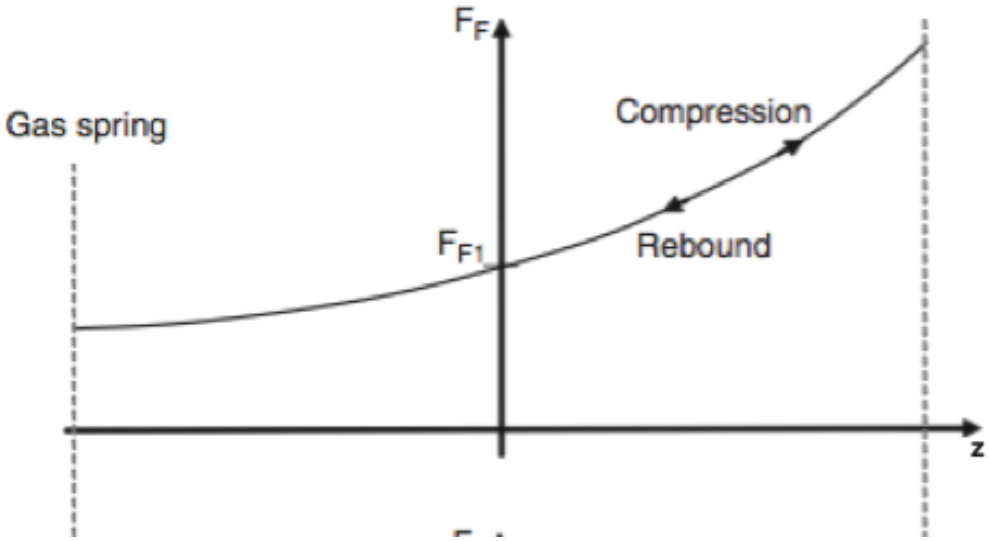

Figure 12: Spring rate of hydro-pneumatic cylinder as function of stroke length

In project thesis the following expression for spring rate was derived: (Falk & Skorpen, 2011)

$$k(z) = T_0 n \frac{z_0^n}{(z_0 - z)^{n+1}} \tag{5.3}$$

n = polytropic constant, for this case nitrogen with n = 1.4 is used (isentropic)

z_0= gas volume column in [m] relative to stroke length of cylinder

This equation is the fundamental of how the spring rate of a hydro-pneumatic cylinder behaves. It should be noted in this equation that geometry plays no role for the spring rate, only the volumes. But then again volume is based on geometry. (Falk & Skorpen, 2011)

5.2 Damping

The damping found in the hydro-pneumatic tensioner cylinder can roughly be divided into two contributions, which will be further discussed and described in this chapter.

First contribution is the damping caused by friction of both gas and oil flowing between cylinder, accumulator and gas bottles. These frictional forces are highly dependent on velocities; hence the largest viscous damping will be experienced for larger waves. Chapter 5.2.1 & 5.2.2 describes a calculation method to find the pressure loss by use of Bernoulli´s equation and conservation of mass and momentum. In chapter 5.2.3, two simplified damping models that can be used to represent the viscous damping are explained. These damping models can easily be put into the equation of motion, to represent both quadratic and linear viscous damping.

The second damping contribution is from static and dynamic friction forces found in seal packers in cylinders and friction between risers and keel guides. These damping forces are nearly constant and only dependent upon the sign of velocity, and they tend to dominate for small sea states. A Coulomb friction model that represents this damping is described in chapter 5.2.5.

5.2.1 Pressure loss in oil flow between cylinder and accumulator

The oil flow between the hydro-pneumatic cylinder and accumulator is written: (White, 2002)

$$Q_{oil}(t) = A_C u(t) \tag{5.4}$$

$Q_{oil}(t) = \ oil\ flow\ rate\ [m^3/s]$
$A_C = piston\ area\ in\ one\ cylinder\ [m^2]$
$u(t) = \ tensioner\ cylinder\ stroke\ velocity = semi\ heave\ velocity\ [m/s].$
$d_i = inner\ diameter\ of\ piping\ [m]$

Reynolds number at any given time for each pipe section "i" between cylinder and accumulator

$$Re_i(t) = \frac{u_i(t) d_i}{\nu_{oil}} = \frac{Q(t) d_i}{\nu_{oil} A_i} = \frac{4\,Q(t)}{\nu_{oil}\,\pi\,d_i} \tag{5.5}$$

The Darcy's friction factor is a dimensionless quantity used in fluid dynamics to describe the friction losses in open channel and piping flows, as for this case. The formulas are based on both experimental data and basic flow theory. The friction factors are calculated for each part of the piping system, and are in this case simplified to 2 x 30[m] pipes with an inner diameter of $d_i = 0.2$[m]. The Colebrook equation for solving the Darcy's friction factor implicit is given as:

$$\frac{1}{\sqrt{f_i(t)}} = -2\log\left[\frac{\epsilon_i}{3.7\mathrm{d_i}} + \frac{2.51}{Re_i(t)\sqrt{f_i(t)}}\right] \tag{5.6}$$

$f_i(t) = Darcys's\ friction\ factor\ as\ a\ time\ function\ [-]$
$\epsilon_i = Roughness\ height\ of\ surface\ inside\ of\ piping\ [m]$

The Haaland equation (5.8) can be used to solve the friction factor directly and is valid for a full flowing circular pipe, as found in the flow between hydraulic cylinder and gas bottles.

$$\frac{1}{\sqrt{f_i(t)}} = -1.8\log\left[\left(\frac{\epsilon_i}{3.7\mathrm{d_i}}\right)^{1.11} + \frac{6.9}{\mathrm{Re_i(t)}}\right] \tag{5.7}$$

Bernoulli´s equation can be used to calculate the pressure loss between the cylinder and accumulator by summing all contributions from different piping parts: (Blevins, 1984)

$$\Delta p_{loss,1}(t) = p_c(t) - p_{acc}(t) = \frac{1}{2}\rho_{oil}\sum_{i=1}^{N}\left(\frac{f_i(t) L_i}{d_i}\right) u_i(t) u_i(t) \tag{5.8}$$

5.2.2 Pressure loss in nitrogen flow between accumulator and gas reservoir bottles

Since the oil is incompressible, the nitrogen volume in accumulator and its change of volume can be written:

$$V_{acc} = V_{0,gas} + u(t)A_C \tag{5.9}$$

$$dV_{acc}(t) = u(t)A_C \tag{5.10}$$

The equations above describe the gas and its compression in time. The figures below illustrate this compression of gas and its relation to the semisubmersible response. A response of the semi in positive vertical direction gives compression of gas and increased stiffness as based on equation (5.3).

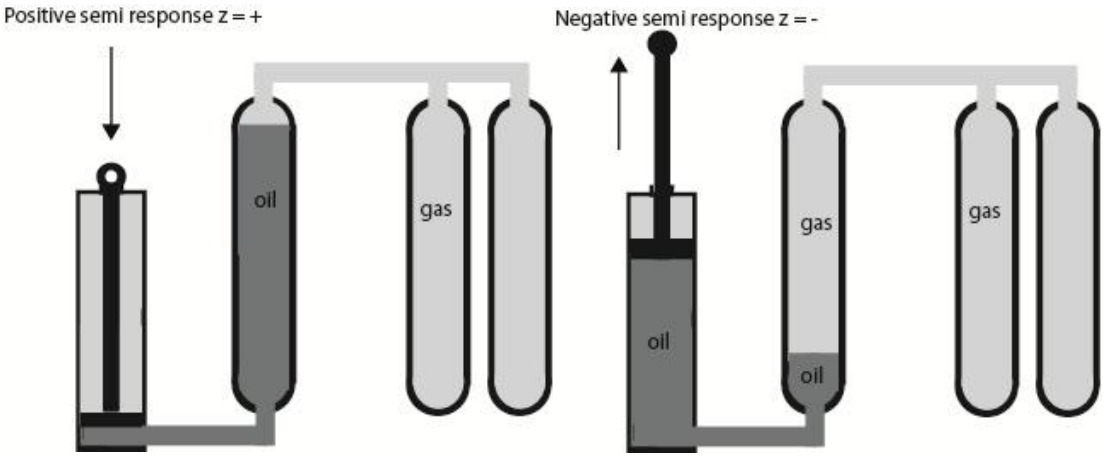

Figure 13: Relation between semi response and flow/compression of gas

By considering conservation of mass, and considering that the system is closed, the change of nitrogen mass between accumulators and gas bottles is then:

$$\frac{\mathrm{dm_A}}{\mathrm{dt}} = \frac{d\rho}{dt}V_{Acc}(t) + \rho\frac{dV_{Acc}(t)}{dt} \tag{5.11}$$

By assuming that the temperature will be constant, which is reasonable when reaching a steady operation oscillation, the ideal gas law can be used to give a relationship between pressure and density of the gas:

$$p_A(t) = \rho_A(t) R T_0 \tag{5.12}$$

$$p_V(t) = \rho_V(t) R T_0 \tag{5.13}$$

$$R = gas\ constant\ for\ nitrogen = 297 \left[\frac{J}{kgK}\right]$$

$T_0 = constant\ temperature\ under\ working\ condition$

The velocity of gas flowing through piping between accumulator and gas reservoir bottles can be written as, where positive u_p is flowing towards gas reservoir bottles:

$$u_p(t) = \sqrt{\frac{2}{p_0 K_p(t)} |dP_{gas}|} \tag{5.14}$$

$$K_P = \sum_{i=1}^{N} \left(\frac{f_i(t) L_i}{d_i}\right) \left(\frac{A_P}{n_i A_i}\right)^2 \tag{5.15}$$

$$dP_{gas}(t) = p_A(t) \left(1 + \frac{V_A}{V_{V0}}\right) - p_0 \left(1 + \frac{V_{A0}}{V_{V0}}\right) \tag{5.16}$$

Pressure loss between accumulator and gas bottles can then be calculated by Bernoulli's equation:

$$\Delta p_{loss,2} = p_{acc}(t) - p_{gas}(t) = \sum_{i=1}^{N} \left(\frac{f_i(t) L_i}{d_i}\right) \frac{1}{2} \rho_0 |u_p(t)| u_p(t) \tag{5.17}$$

K_P = loss coefficient in nitrogen piping

u_p = velocity of gas in piping

5.2.3 Damping model: Linear viscous damping

The linear viscous damping model gives simple mathematical results and is commonly used in the equation of motion for a big range of problems. The model can physically be represented by a shock absorber where the damping force is proportional and in phase with the velocity

$$F_D = c\,\frac{du}{dt} \tag{5.18}$$

$c = damping\ coefficient\ [Ns/m]$

When we plot the force against displacement a closed loop will be represented, as seen in figure 1(a). The area of this loop denotes the energy dissipated by the damper in a cycle of motion, and is called a hysteresis loop. This loss of energy for each cycle can be written as (Langen & Sigbjörnsson, 1979)

$$\Delta W = \oint F_D\,du = \pi c\omega u_0^2 \tag{5.19}$$

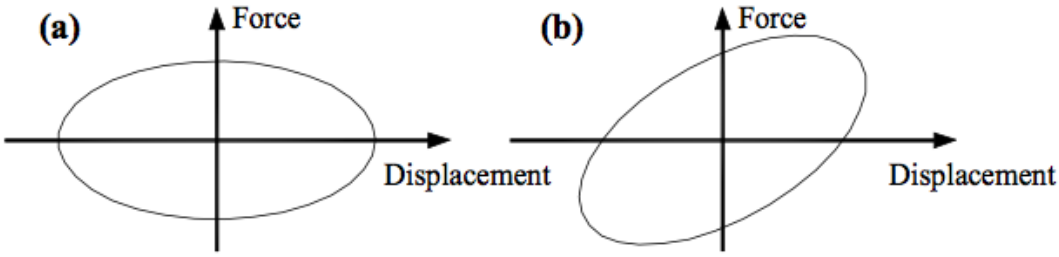

Figure 14: Hysteresis loops for a linear viscous damper.

The force is written as

$$F_D = \pi c\omega\cos(\omega t - \phi) = c\omega\sqrt{u_0^2 - u^2} \tag{5.20}$$

If restoring forces are added to the hysteresis-loop in figure 14(a) the Voigt-Kelvin model which is a spring and damper in parallel will be modelled, as in figure 14(b). This hysteresis-loop is then said to be viscoelastic and the force for this system can be written as

$F = F_D + ku$

5.2.4 Damping model: Non-linear viscous damping

In some cases the damping force is assumed to be in phase with and proportional to the square of the velocity. A non-linear viscous damping model will be more correct for such cases, and damping force can then be written as (Langen & Sigbjörnsson, 1979)

$$F_D = C_N * \frac{du}{dt} * |\frac{du}{dt}|, \tag{5.21}$$

C_N = Problem dependent coefficient $\left[N/\left(\frac{m}{s}\right)^2\right]$

A non-linear viscous model is often used for systems that oscillate in fluids. The hysteresis-loop for this model is made of two parabolas and the energy dissipated by the damper in a cycle of motion can be written as

$$\Delta W_D = \frac{8}{3} C_N \omega^2 u_0^3 \tag{5.22}$$

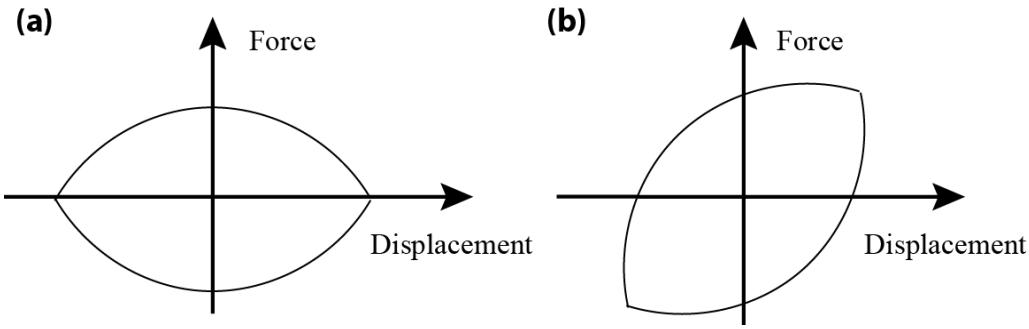

Figure 15: Hysteresis-loop for non-linear viscous damping model.

In the same way as for the linear viscous damper, the hysteresis loops are shown both with and without the spring-rate contribution in figure 15 (a) and (b)

5.2.5 Damping model: Coulomb friction

The Coulomb friction force is a retarding force with constant amplitude with respect to velocity. As soon as two bodies start to slide on each other, Coulomb friction will be present. It is written as:

$$F_{f,col} = \mu_{col} F_N sign(u) \tag{5.23}$$

μ_{col} = a dynamic friction coefficient.

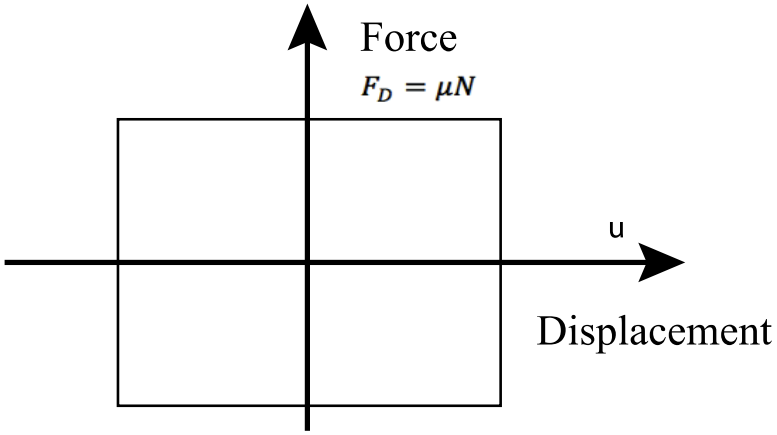

Figure 16: Coulomb friction force as function of displacement.

In hydro-pneumatic cylinders the Coulombs friction is found in seal packer element, and in between cylinder and piston. Friction coefficients are difficult to obtain mathematically and have to be measured experimentally in order to get exact results. Pressure, temperature and surface roughness are all factors that affect the frictional forces. In the analysis done in this study the Coulomb friction force is varied between 2-6% of the initial riser tension. This range is meant to include the static friction coefficient when there is no response in the system.

The static friction plays an important role in the hydro-pneumatic cylinder. It determines the minimum excitation forces needed to make the system move and oscillate. When the static friction force is dominating and there is no oscillation the risers will be subjected to the excitation loads and fatigue damage must be considered. The static friction forces are found in seal areas, and depend on the pressure in system.

The normal forces on seals increase as pressure increase, and the exact friction coefficients are hard to predict. In a design phase the static friction coefficient is roughly said to be 50% higher than the dynamic; $\mu_{static} = 1.5\mu_{dynamic}$ (Løken, R. Personal Communication 2012)

6 - The solvers

This chapter contains the approach and verification of the solvers used in this master thesis. All input like the hydrodynamic coefficients, dimensions of the semisubmersible and environmental data is taken from the WADAM analysis done in the project thesis, and a thorough review of this can be found in that report.

Two programs were written in MATLAB;
- *RK.m:* solves the nonlinear equation of motion with a Runge-Kutta time iteration method.
- *TensionerDamping.m:* calculates the pressure loss in oscillating accumulator, based on Bernoulli and conservation of mass in gas and fluid.

To get correct analysis these two programs has to coincide.

6.1 - Approach

The problem was mainly solved in MATLAB. Both HydroD and SIMO was considered and tested out, but since these are pre-made programs they did not offer the flexibility needed to properly solve the problem.

The hydrodynamic excitation forces, added mass, potential damping and potential stiffness was taken in from a HydroD analysis without a Morison model , see Appendix D. The equation of motion was solved by Runge-Kutta time iteration, which was programmed manually to be able to take in the nonlinearities. The viscous drag force was represented by the nonlinear Morison drag term and the stiffness contribution from the tensioner system by equation based on ideal gas law. To get a correct damping coefficient for the tensioner system an iteration process between RK.m and TensionerDamping.m had to be done. An analysis was done in RK.m with an approximate damping coefficient, then the velocity from the most probable sea state domain was chosen and used as input for a new analysis in TensionerDamping.m. The tension variation due to the viscous damping is plotted against the velocity as seen in Figure 17, and the damping coefficient is given as follows:

$$c_{TTR,lin} = \frac{A}{B} \tag{6.1}$$

If $c_{TTR,lin}$ equals the $c_{TTR,lin}$ used in RK.m, the first analyze was correct, if not one chose the $c_{TTR,lin}$ given by TensionerDamping.m and run a new analyze in RK.m, thus iterating until the correct tensioner damping value is found. This is used in a linear hysteresis model, which is added to the damping term in the equation of motion.

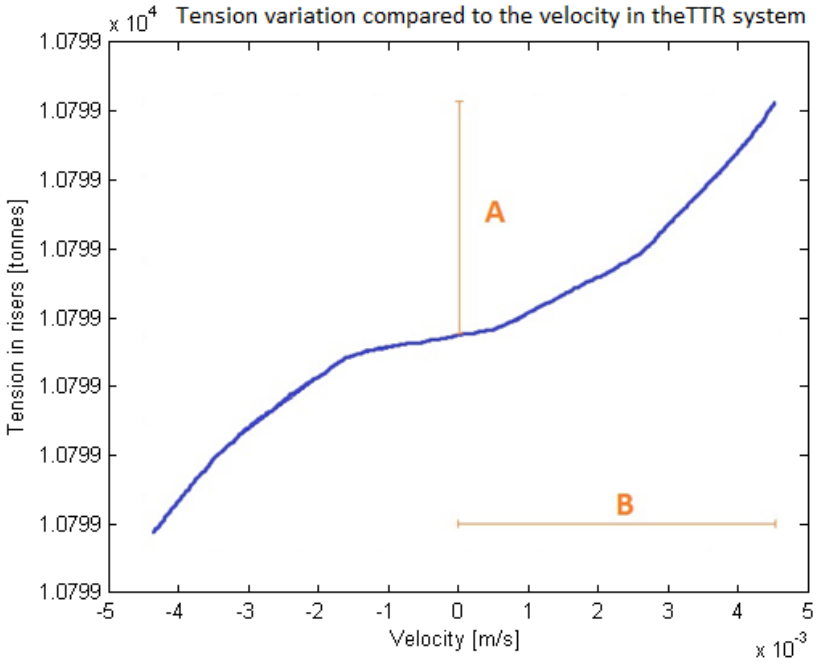

Figure 17: Tension variation plotted against the velocity of the piston

To get the RAO from the time domain analysis the steady-state domain is considered, and the response is gathered for each frequency. Hence the solution can be compared to the frequency domain, and it is possible to filter out the different contributions to look at the effects these has on the overall system.

6.2 – Verification of the solvers

Before the results can be considered it is important that the program is verified. Since the results from the frequency domain were already calculated in HydroD, it was natural to compare the initial RK.m runs to these.

To demonstrate that the MATLAB script was correct, the Runge-Kutta code was first checked against MATLAB's own built-in differential function solver: ode45, which is based on the Runge-Kutta 4th order method. When the results matched, hydrodynamic coefficients from a HydroD analysis with a Morison model included was taken into RK.m, and an analysis for a small sea state was done. This was compared and found equal to the RAO from the SESAM post-processing program Postresp. Then hydrodynamic coefficients from a HydroD analysis done without a Morison model were taken in, and a linearized Morison damping was added to RK.m. This run was also verified against the Postresp RAO to ensure that the code with the linearized damping was correct.

6.2.1 – Morison damping

Nonlinear Morison damping was used in all the analyses in this thesis, except when simulating decays where the super-positioning of the linearized Morison drag term was a necessity.

To check that the nonlinear Morison damping was reasonable, a sea state of two meters wave height was run. This sea state was chosen since the nonlinear Morison damping increases with the square of the relative velocity between the semi and the wave, and it can best be compared to the linearized damping in small sea states. The comparison is shown in Figure 18 below. Three analyses were run, the first shows how the nonlinear Morison drag force varies over the period, the two others illustrates the linearized Morison damping force, $F_{3,M}(t) = B(w - \dot{\eta_3})$, for a $V_{max} = 1.00$[m/s] and $V_{max} = 1.66$ [m/s].

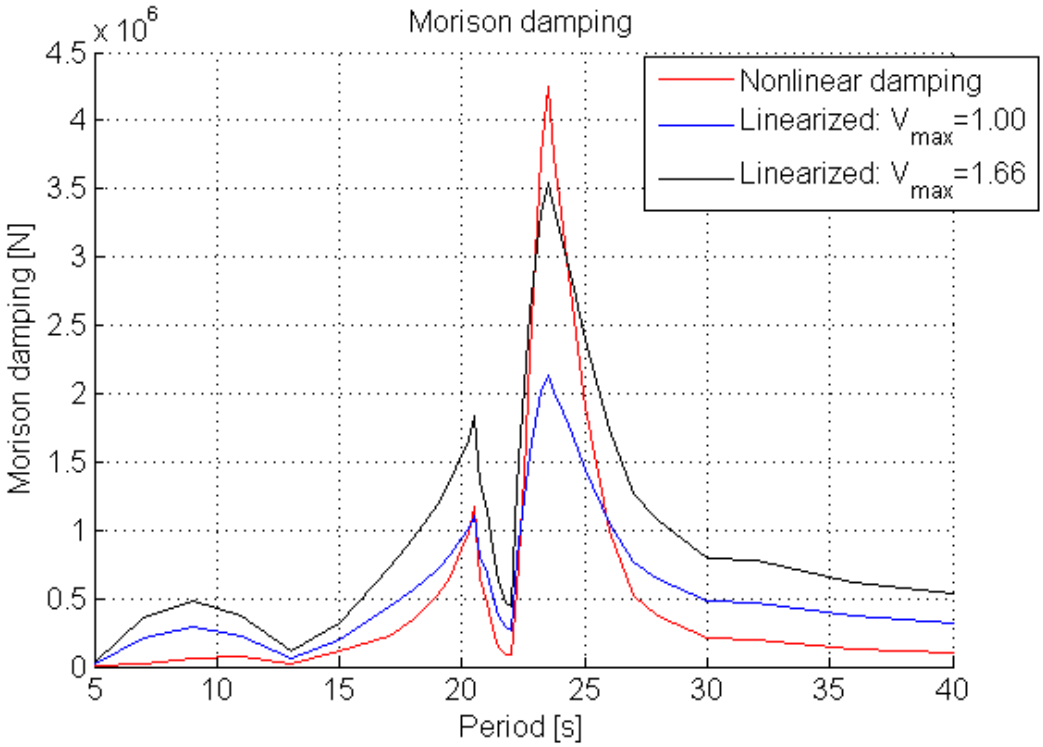

Figure 18: Variation in the Morison damping force over the period.

The linearizing velocity amplitude specified as input to WADAM in the project thesis is 1.66 [m/s], which gives higher Morison damping contribution than the WADAM default value of 1.00[m/s]. This linearizing velocity was chosen in the project thesis because it gave results similar to the one Aker Solutions had obtained. This is also very close to the nonlinear Morison drag force found in this thesis. As previously assumed the nonlinear Morison damping gives a lower contribution in the significant frequency domain but has a higher peak in the resonance area than the linearized damping force.

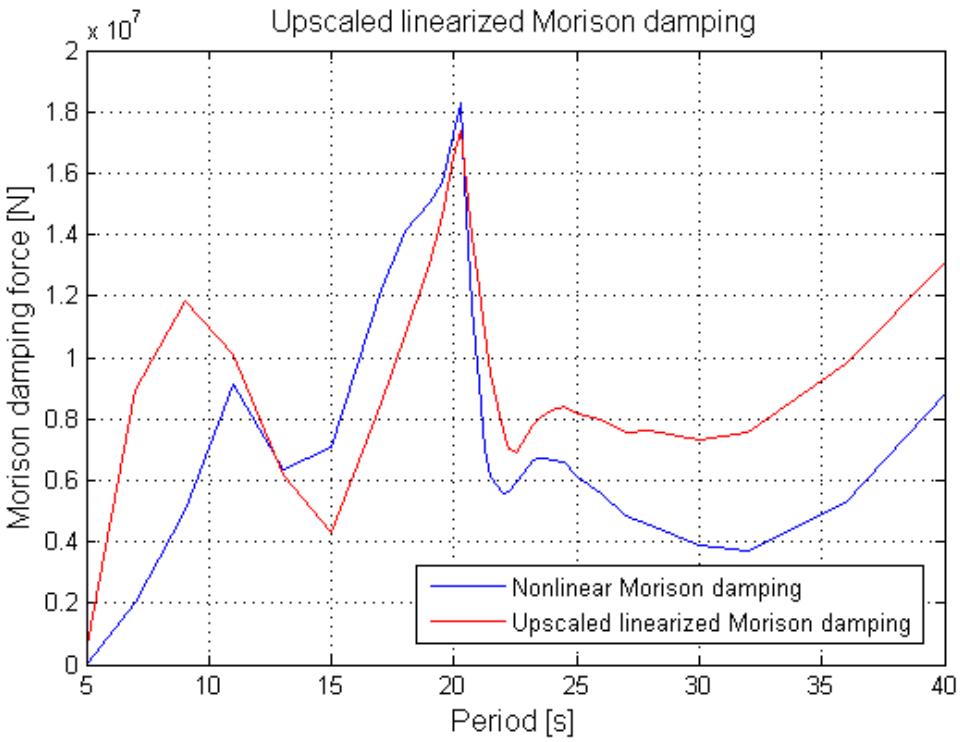

Figure 19: Up-scaled linearized Morison drag force

When increasing the wave height, the nonlinear Morison damping will be greatly affected, hence one cannot use the linearized Morison value from WADAM. An analysis for a wave height of 20 [m] was done, and the linearized Morison value, B, was upscaled until it fitted the nonlinear Morison drag force over the resonance period. The best fit was found for $B = 2.2 \cdot 10^7 \left[\frac{kg}{s}\right]$, which is the linearized Morison damping value used for the decay simulations for 20 [m] sea state. This is shown in figure 19.

6.2.2 – Phase angle

Another important aspect to verify is the phase angle between the load and response, which is given in chapter 3.1.1 and is a function of the frequency ratio. Since nonlinear Morison damping cannot be super-positioned, the phase angle is based on the linearized Morison value from the WADAM analysis in the project thesis with a linearizing velocity of 1.66 [m/s]. The program also uses linearized damping and stiffness, which gave good results when comparing the RAO's from the linearized and nonlinear analysis.

$$\theta = \arctan\left(\frac{2\xi\beta}{1-\beta^2}\right) \tag{6.2}$$

$$\beta = \frac{\omega}{\omega_0} \tag{6.3}$$

$$\xi = \frac{C_{33} + C_{Morison} + C_{viscous\ linearized}}{2m\omega_0} \tag{6.4}$$

$$\omega_{0\ lin} = \sqrt{\frac{K_{33} + K_{ttr\ linearized}}{mass + A_{33\ linearized}}} \tag{6.5}$$

As expected, the plot of the phase angle without Morison damping and TTR system has almost no damping because the only damping contribution is diffraction of the waves. The damping ratio is around 1%, which corresponds well to what was expected. When introducing Morison damping to the system, the damping ratio augments, and the phase angle graph evens out a little. With the tensioner system included, the Eigen period will be affected, and the inflection point will move to the left due to a stiffer system.

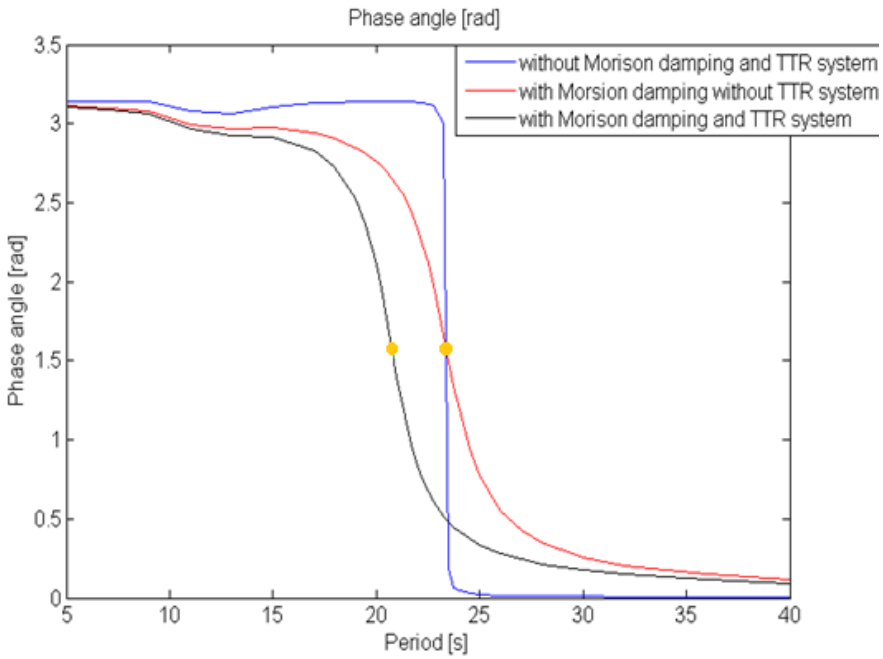

Figure 20: Phase angle with and w/o TTRs. Inflection point moves from 23.4s to 20.7s.

6.2.3 – Decay simulation

To make sure that the iteration loop converges towards a steady state, decay simulations were run. This is done by introducing a static force of $F_3 = 1 \cdot e^6$ $[N]$ the first 50 $[s]$ of the analysis, and let the system react to that. The wave force- and Coulomb damping force-contributions are neglected to see how the freely oscillating system reacts. If the response converges towards zero, there is damping in the system.

Since the nonlinear Morison damping cannot be super-positioned and is therefore implemented in the system as a force, the decay simulation uses the linearized Morison value to account for the Morison damping. An up-scaled linearized Morison damping value is used for sea state 20 [m] to account for the increased relative velocity. The Coulomb damping is constant and will not contribute to any difference between the two sea states.

Table 4 - Damping ratio with and without TTR-system

Wave height [m]	TTR-system	ξ
2	No	6.42 %
2	Yes	6.52 %
20	No	16.74 %
20	Yes	23.09 %

The above table shows the damping ratios found from the plots in Figure 21 and Figure 22. These figures show the decay in two different sea states, and the damping ratio is calculated by the use of the logarithmical increment as explained in Chapter 3.1.3.

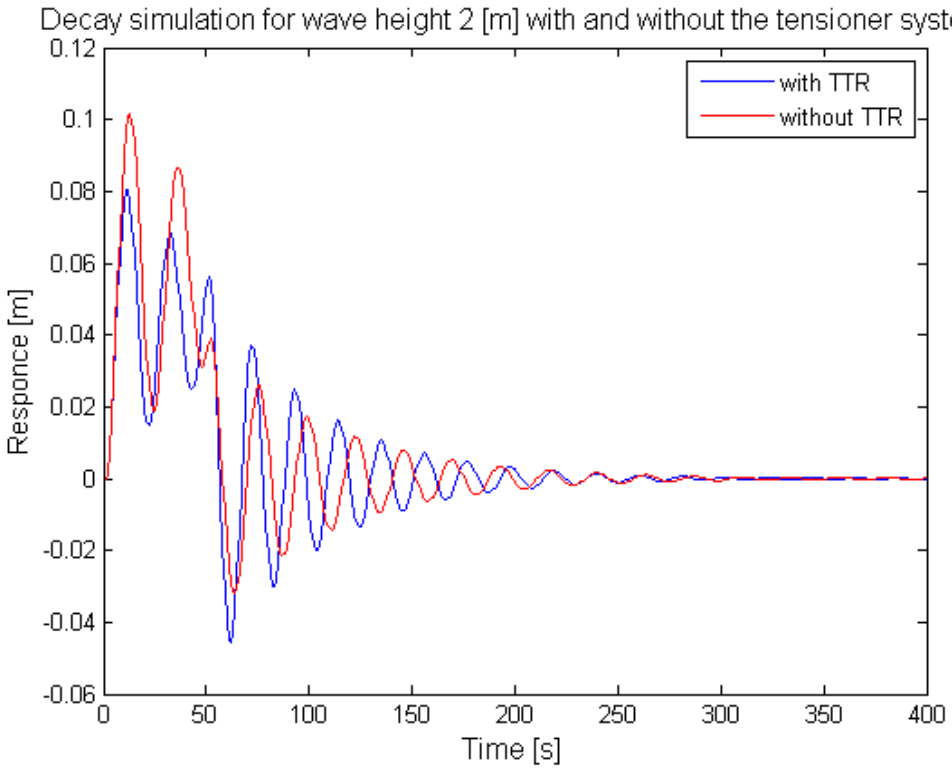

Figure 21: Decay simulation for a wave height of 2m.

In 2 [m] sea state, there is little difference in the damping ratio for the system with and without a tensioner system. This is seen in Figure 21, where the two plots die out at the same time. The tensioner system contributes with an increase in damping ratio of $0.10\ \%$, hence the system is almost not affected by it. Since there is very little damping in the system this spring force will dominate. Hence the stiffness of the riser tensioner system contributes to a larger response after the initial loading is gone, due to the fact that energy will be stored in the compressed gas.

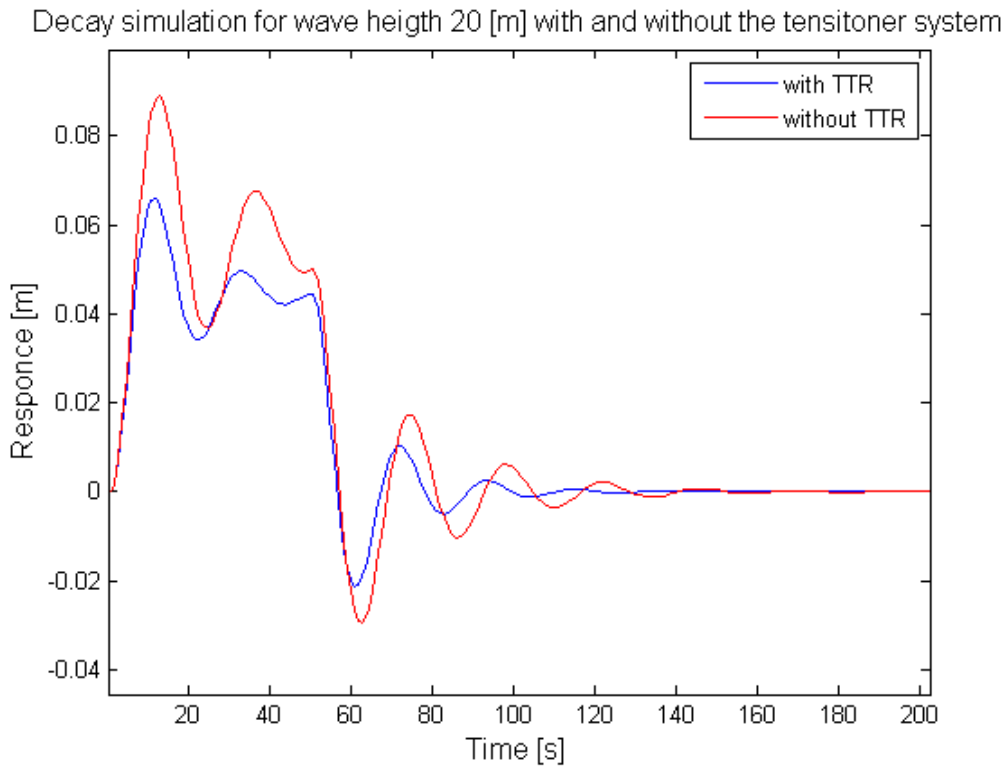

Figure 22: Decay simulation for a wave height of 20m.

The viscous effects in the tensioner system become more prominent in higher sea states. For 20 [m] sea state the system decays faster, however this do not affect the Eigen period. Without the tensioner system there is a great increase in the damping ratio, from 6.42 % to 16.74 % due to a higher relative velocity and therefore higher Morison damping. With the tensioner system included the damping ratio is 23.09 % which is an increase of 6.35 %, hence the damping from the tensioner system affects the semi more in higher sea states. This increased damping also affects the response of the semi. The damping force is no longer dominated by the stiffness of the tensioner system, therefore the response is lower for the semi with TTR-system than for the one without in Figure 22.

Table 5: Comparison of natural periods.

	Linearized $T_{0\,lin}$ [s]	Mean T_0 [s]	T_0 from decay [s]
Without TTR system	23.41	23.38	24
With TTR system	20.74	20.89	21

The mean ω_0 from Table 5 is found by looking at how the Eigen period varies over the different periods, and take the mean value of that. This variation in the Eigen period is mostly due to frequency depended added mass but is also affected by variations in the tensioner system stiffness and in the nonlinear Morison drag force. Figure 23 show how the Eigen period changes over the period with and without the tensioner system for different wave heights. The Eigen period found from the decay simulations are not exact values due to the size of the time steps in the analyses.

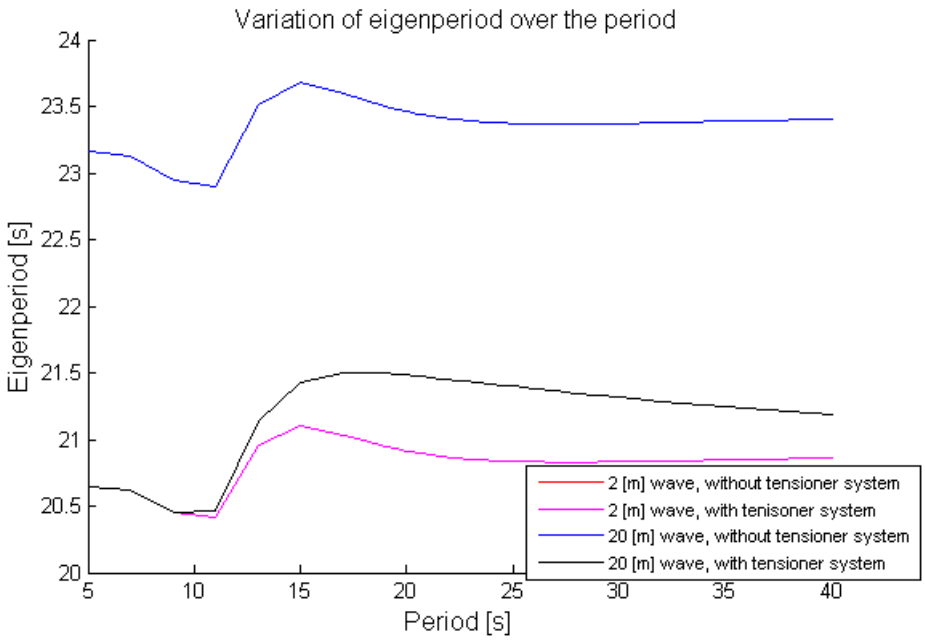

Figure 23: Variation of Eigen period with and w/o TTR system for 2m and 20m wave.

The decays give the damped Eigen periods in calm water. As the high damping ratio for high sea states suggest, this Eigen period should be used for further analyses. However, the MATLAB code uses the natural period found from the stiffness and mass in the analysis, which gives a small error in extreme sea states.

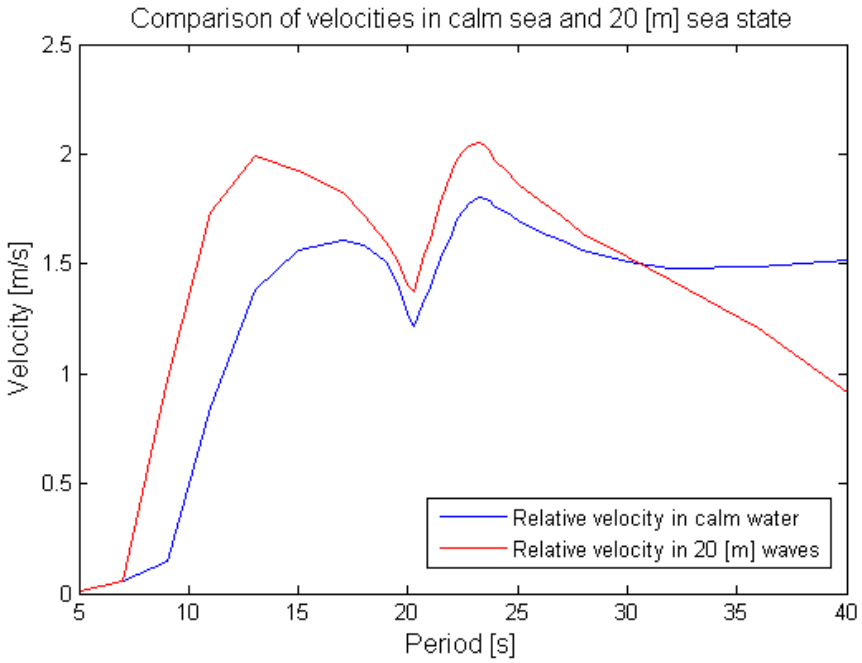

Figure 24: Comparison of relative velocities

The above graph shows the relative velocity between the wave and the pontoon in 20 [m] sea state and between 20 [m] sea state response and the water line. This is done to point out that there will be a lower Morison damping in 20 [m] sea state decay than in a real 20 [m] sea state, hence the damping ratio is higher in the analysis done in RK.m

7 – Results and discussion

The results section is divided into 6 parts, which systematically describes the results from various analyses done. All results are obtained from developed MATLAB codes, which use input defined in the code and from analysis done in WADAM. A brief description of each subchapter will be given below:

7.1 - Nonlinear stiffness and influence on system response: Examines the nonlinear stiffness caused by compression of gas. Calculations are based on ideal gas law expression for the spring rate $k_{TTR}(x, V_{gas})$, from equation (5.3). Different plots show how the additional stiffness influences the natural period and response of semi by varying the gas reservoir volume. Linearization of the spring rate values is obtained.

*7.2 - Damping in hydro-pneumatic system***:** Using potential flow theory and Bernoulli's equation, as described in theory chapter 5.2.1, the time dependent pressure loss and tension variations have been calculated.

*7.3 - Time-domain analysis***:** The damping and nonlinear stiffness from the riser tensioner system has been implemented in the dry-tree semi model, and a new equation of motion established. The full equation of motion has been solved using a developed MATLAB code, which uses a 4^{th} order Runge-Kutta numerical integration method. Analyses have been done using series of regular waves, wave heights ranging from 2 – 30[m] and period 5 – 40[s].

7.4 - Frequency analysis based on time-domain analysis: Based on the time-domain analysis for a range of different wave heights and periods, the max values of responses in the steady state are plotted against the wave periods to gain new RAOs.

7.5 – Tension variation in risers: Based on equation (5.1) the total riser tension variation as a function of time was calculated based on the mathematical models of spring rate and damping described in chapter 5.1, 5.2.3, 5.2.4 & 5.2.5

7.6 – Coulomb friction forces: A Coulomb friction force is used to simulate the seal friction between seal packers in tensioner cylinders and friction found between risers and keel guides. For low sea states and waves, the wave excitation forces will be less than friction forces and the semi will be effectively moored by the risers.

7.1 – Nonlinear stiffness influence on system response

The additional stiffness caused by compression of gas will significantly affect the natural period and response. For all analysis done a gas reservoir volume of five times the cylinder stroke volume is used. This equals 5 * 1551 litres ≈ 7500 litres, which is a reasonable design assumption for the system *(Ronny Sten, Personal communication, 2012).* By varying this volume, new natural periods and responses are attained. An increased gas-volume will decrease the stiffness, causing a ”softer” system and vice versa. The gas used in the system is nitrogen, which has an adiabatic coefficient of 1.4.

In this chapter, the change of gas volume shall be evaluated and its influence on the spring-rate, natural period and RAOs. Three different gas-volumes will be examined; 4.000 litres, 7.500 litres and 15.000 litres. In an ideal system the gas reservoir volume will be infinitely large, but this is of course a design criteria limited by available space.

Figure 25 below shows how the stiffness varies with stroke of the cylinders when the gas reservoir volume is changed from 4.000 to 15.000 litres.

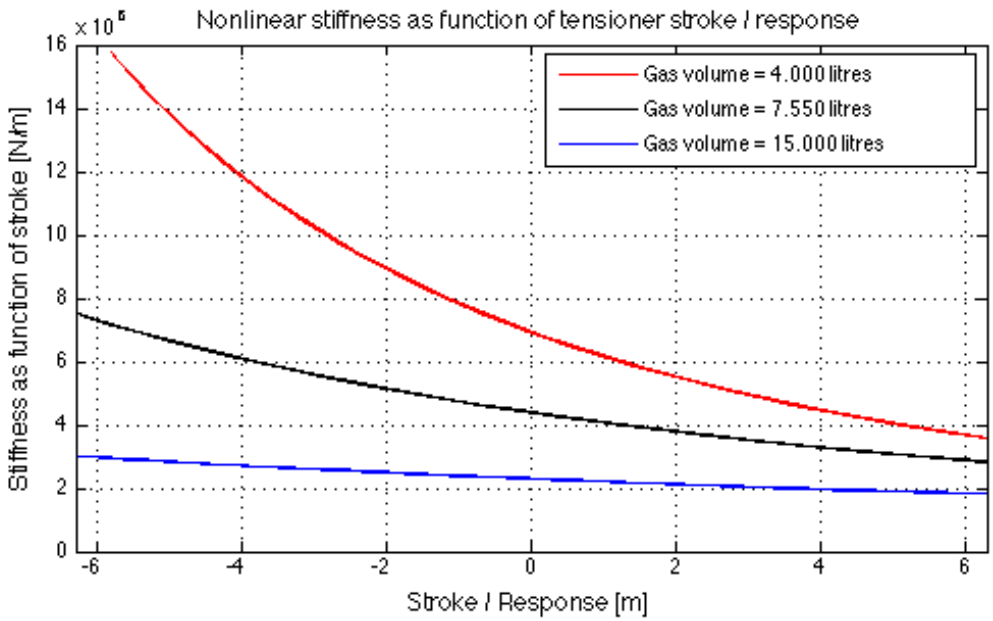

Figure 25: Relation between gas volume and spring rate for max stroke/response

Table 6 presents data obtained and relations between spring rate for initial condition, linearized spring rate and natural periods, and the deviations between linearized and initial spring rate values.

The initial spring rate $K_{TTR,0}$ is found by reading the k-value from the plot in Figure 25 for the stroke length equals zero.

The linearized stiffness for a response with full stroke-length/response-amplitude of 6.3m was found by integrating the time varying stiffness over one period and divide by the length of the period

$$K_{TTR,linearized} = \frac{1}{T}\int_0^T k_{TTR}(t)dt \qquad 7.1$$

Table 6: Spring rate values and correlations

Gas volume	$K_{TTR,0}$	$T_N(K_{TTR,0})$	$K_{TTR,linearized}$	$T_N(K_{TTR,lin})$	ΔK_{TTR} in %
4.000 litres	6.9216e+06	19.86	8.6272e+06	19.21	24.6%
7.500 litres	4.6148e+06	20.86	4.8749e+06	20.75	5.3%
15.000 litres	2.3069e+06	22.02	2.3591e+06	22.00	2.0%

From the table it is shown that the largest deviations between initial and linearized spring rate is found for a stiff system, here given as a gas reservoir volume of 4.000 litres. For this case the deviation in % is given as $\frac{\Delta K_{TTR}}{K_{TTR,0}} = \frac{8.6272-6.9216}{6.9216} * 100\% = 24.6\%$. This is an important consideration if using the linearized value for small sea states, where the heave response and the stroke of cylinders are small.

By comparing RAOs made by use of the real-time values and the linearized values, a rough estimate can be done whether the linearized spring rate values can be used or not. Figure 26 compares two RAOs based on time-domain simulations for various wave periods, in the same way as described in chapter 7.4. One is based on the real-time values of $K_{TTR}(x)$, and the other one use the linearized value $K_{TTR,lin}$. Both a soft system; gas volume = 15.000 litres, and a stiff system; gas volume 4.000 litres are presented in the figure.

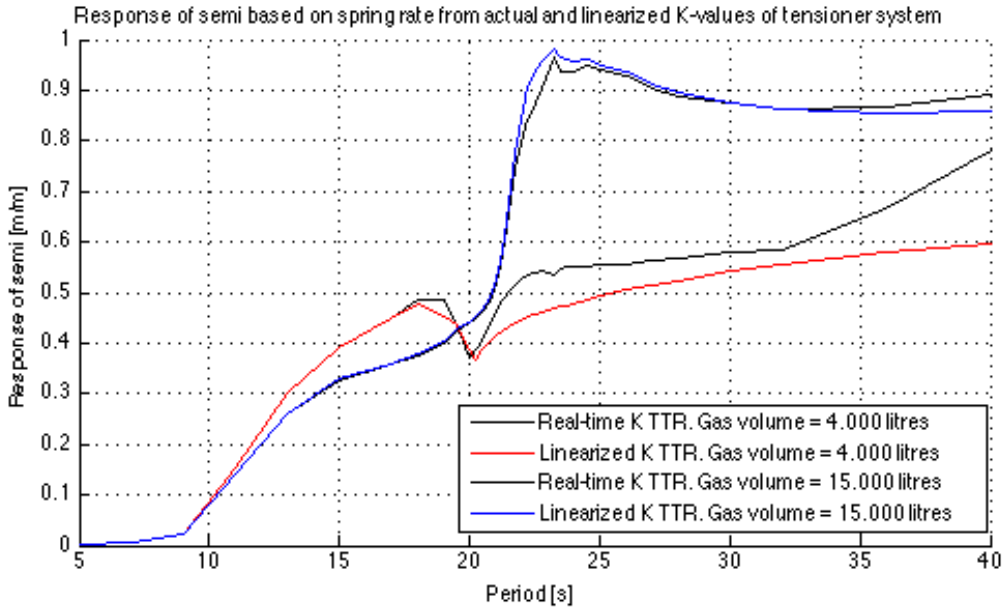

Figure 26: RAOs based on real and linearized spring rate for stiff and soft TTR system.

The linearized values give accurate results in the mass dominated period range. In the stiffness dominated period range, which is above the natural period T>21[s], there are deviations for the stiff system of 4.000 litres gas reservoir volume. These values gives accurate results in the period range before resonance, in which the system is inertia dominated. This is also the most interesting response period array, as it is the most common wave period range.

To get an idea of how the gas reservoir volume will influence the response of the semi, RAOs with variable gas volume are plotted for two different wave heights in the figures below.

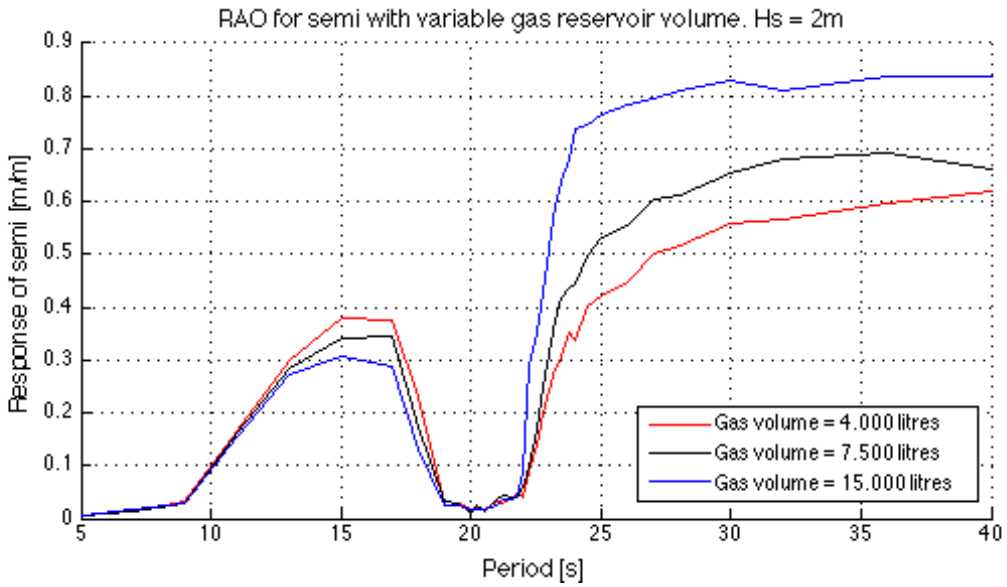

Figure 27: RAOs for variable gas volume in hydro-pneumatic TTR system. Hs=2m

Figure 27 shows the RAOs with variable gas volume for a wave height of 2[m]. A Coulomb friction force of 2% of initial tension is added, which causes the semi to be effectively moored by the risers, for a period range near the cancellation period. This is later referred to as stiction, and further described in chapter 7.6.

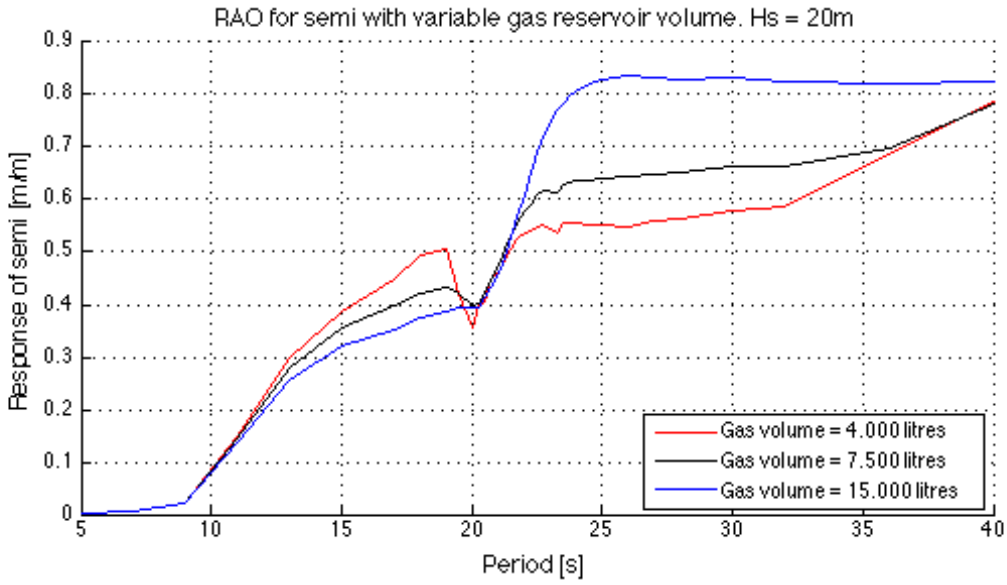

Figure 28: RAOs for semi with variable gas volume. Hs=20m. Friction 2%

Figure 28 shows that responses for a 20[m] wave height are larger than for 2[m] in the inertia-dominated period range 14-18[s]. This is mainly due to the increased nonlinear stiffness and Coulomb damping. The nonlinear stiffness will increase the excitation forces in this range, and the Coulomb damping will have less importance for this wave height as the wave excitation forces are much larger than the friction forces. This is further described in Chapter 7.6

7.2 - Damping in hydro-pneumatic compensator system.

The tension variation as function of both displacement and velocity have been calculated for different scenarios by use of a MATLAB code; TensionerDamping.m. The theory for this script is described in chapter 5 and the approach in chapter 6. The amplitudes and periods used for the calculations were chosen by looking into RAOs calculated for different wave heights, and choose points to analyse in the RAOs where the biggest velocities in the most interesting period range 10 – 20 [s] occurred. This was done in an iterative loop as described in *APPENDIX B: Routine for MATLAB code.*

The pressure loss caused by friction in the piping is dependent on several variables. As the oscillating tensioner system will have a time variable fluid flow and fluid velocity, the Reynolds number and Darcy's friction factor will be calculated as time functions. Results below are shown for an extreme case with Hs = 30 [m], T = 18 [s]. Each cylinder is for this case pre-charged to 91,34 [bars] to give an initial tension of 840 [tonnes] on each riser. The system analysed have been simplified by using 2 x 30 [m] flow lines for hydraulic oil and gas with an inner diameter of 0.2 [m].

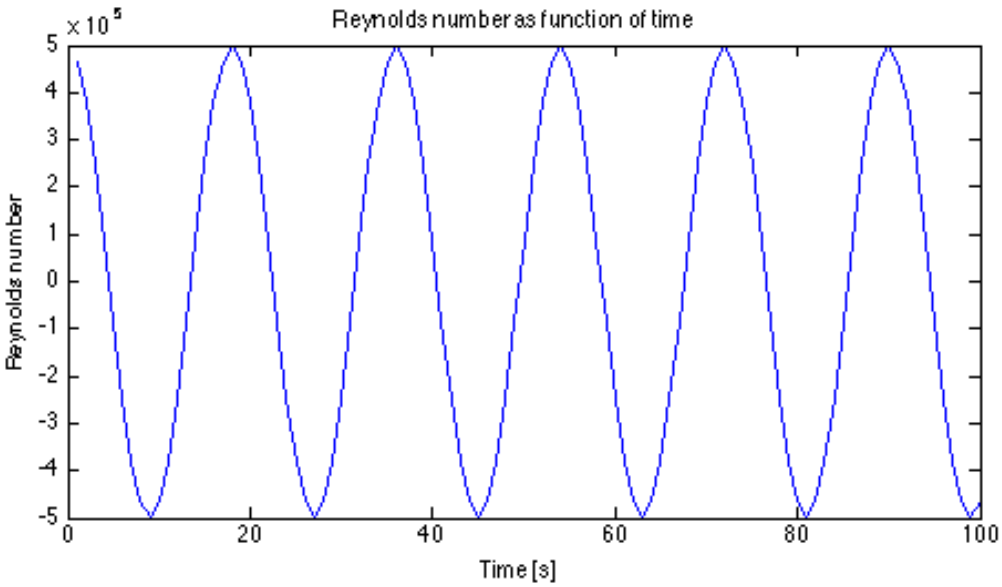

Figure 29: Reynolds number as function of time. Extreme case of Hs=30m, T=18s

Figure 29 shows how the Reynolds number oscillates as a function of time due to the change in fluid velocity. The Reynolds number will be in phase with fluid velocity, ref. equation (5.5).

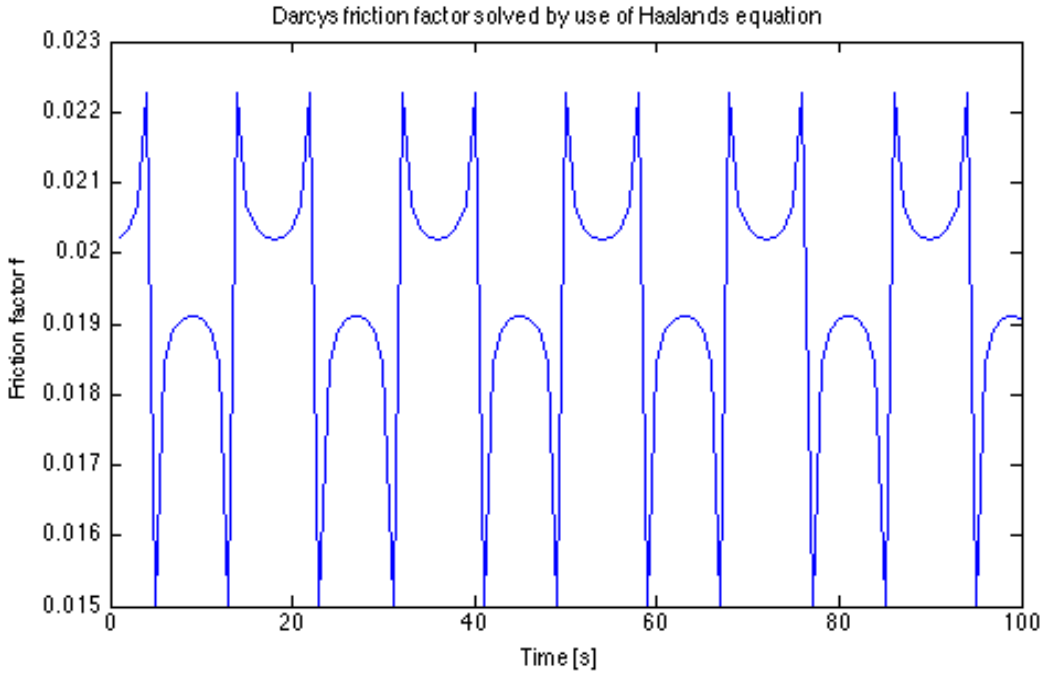

Figure 30: Darcys friction factor solved by use of Haalands equation. Hs=30m, T 18s

Figure 30 shows how the Darcy's friction factor varies as the fluid in hydraulic system oscillates. The friction factor is calculated using Haaland's equation (5.7).

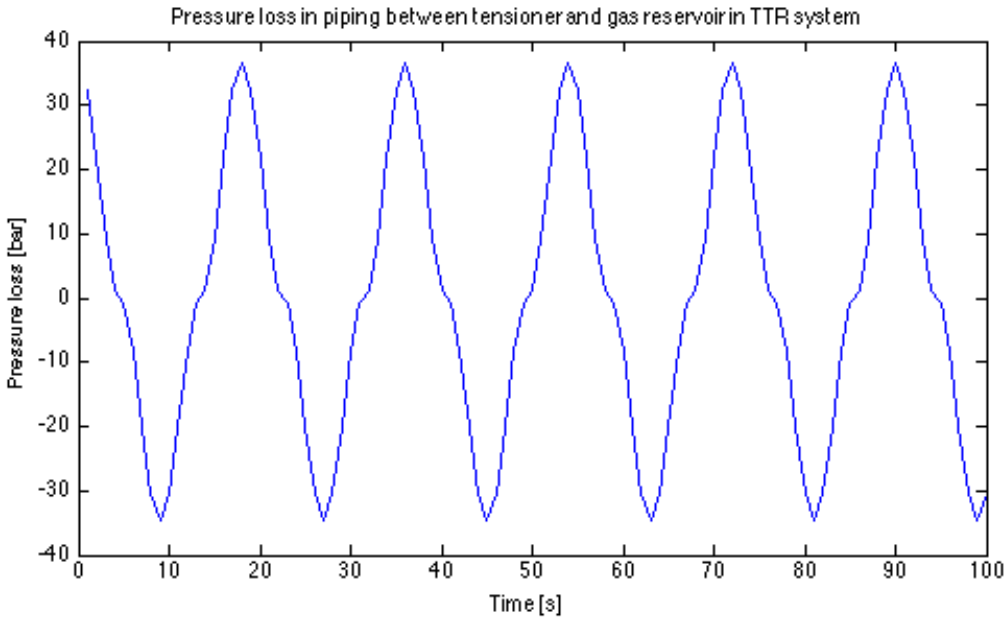

Figure 31: Total pressure loss in piping between hydraulic cylinder and gas reservoir.

Figure 31 shows the pressure loss, $\Delta p_{loss}(t)$, given in bars. It shows a typical nonlinear behaviour. By knowing the pressure loss at any given time, the tension variation caused by viscous damping in the system can easily be found by use of Bernoulli.

By plotting the tension as a function of stroke length, the hysteresis loops that represent the damping in the system are found. Below are different figures showing the tension variation caused by the viscous friction from oil and gas-flow in the tensioner cylinders. They are calculated for different wave heights and periods.

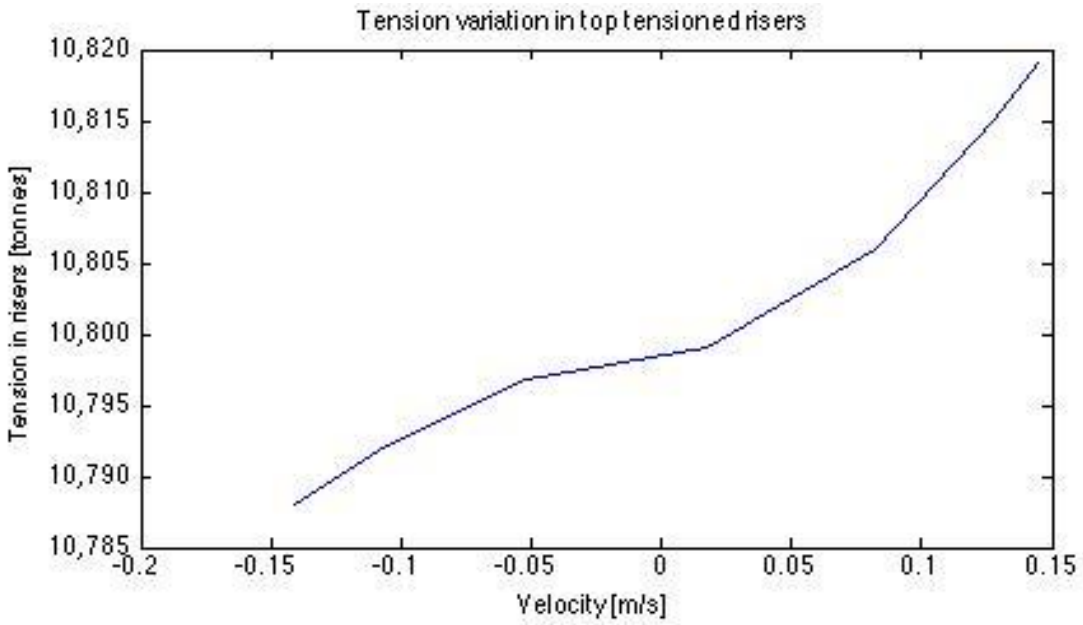

Figure 32: Tension variation in TTRs due to damping. Hs= 2m, Zmax = 0.3m, T = 13s

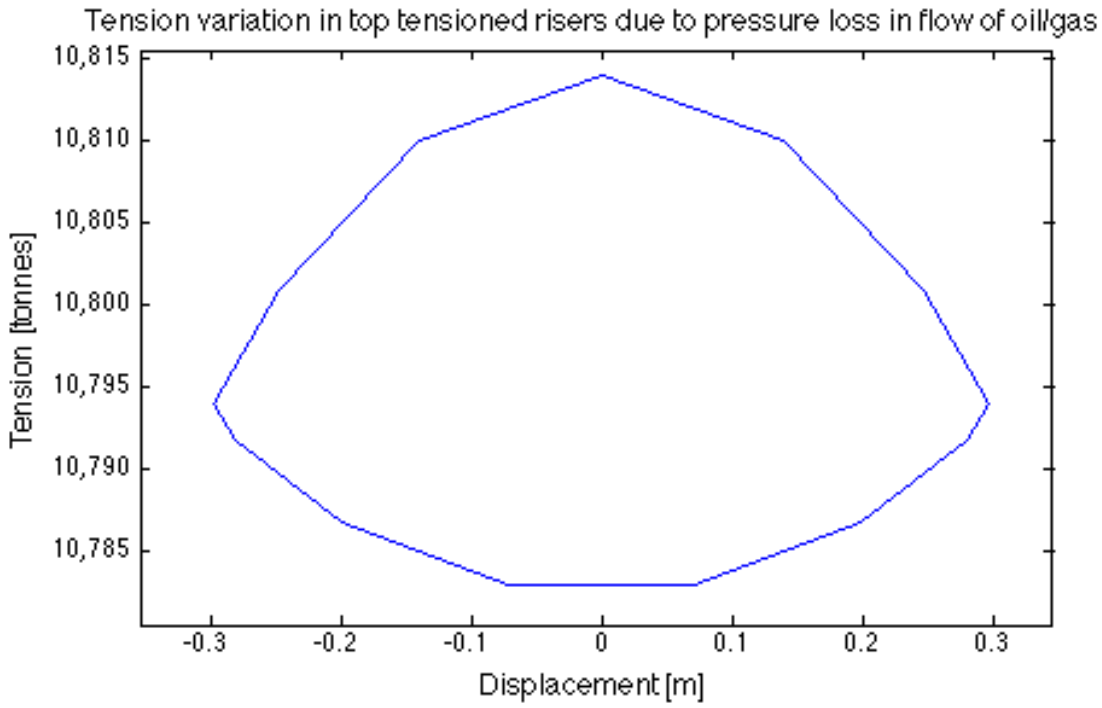

Figure 33: Tension variation in TTRs due to damping. Hs = 2m, Zmax = 0.3m, T = 13s

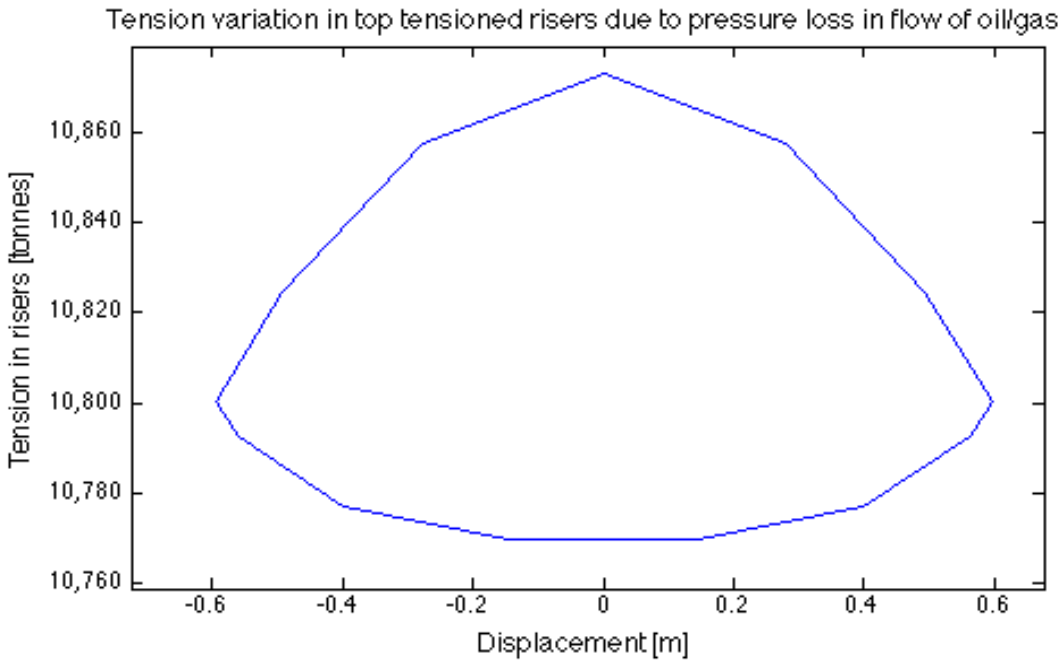

Figure 34: Tension variation in TTRs due to damping. Hs=4m, Zmax=0.6m, T=13s

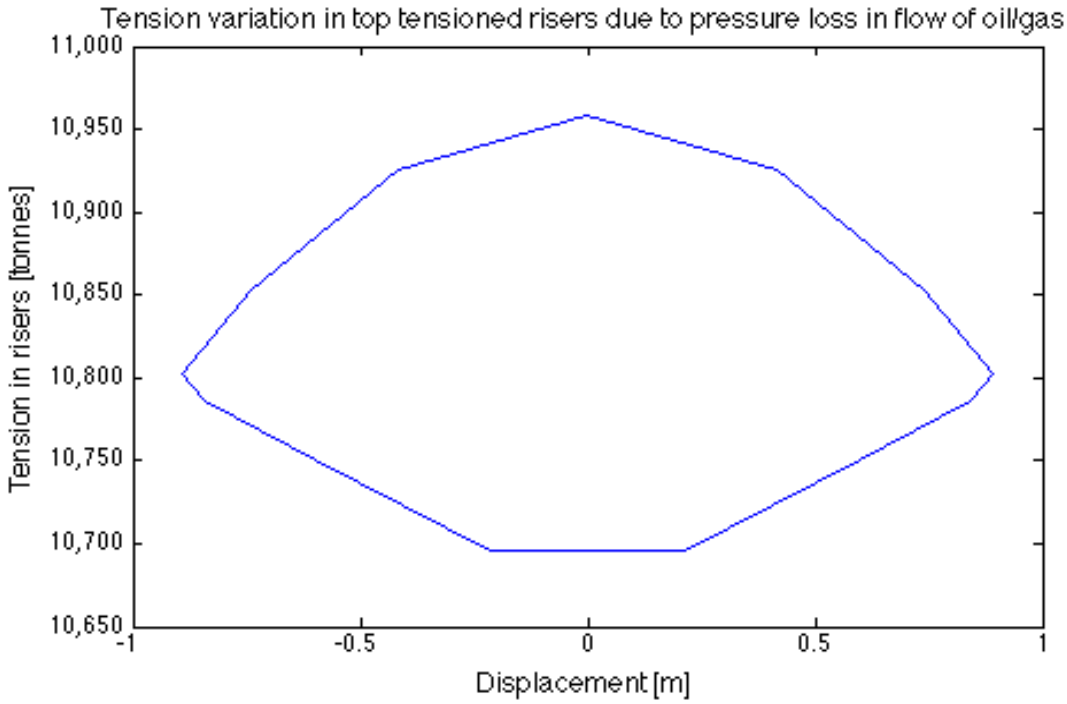

Figure 35: Tension variation in TTRs due to damping. Hs=6m, Zmax=0.9m, T=13s

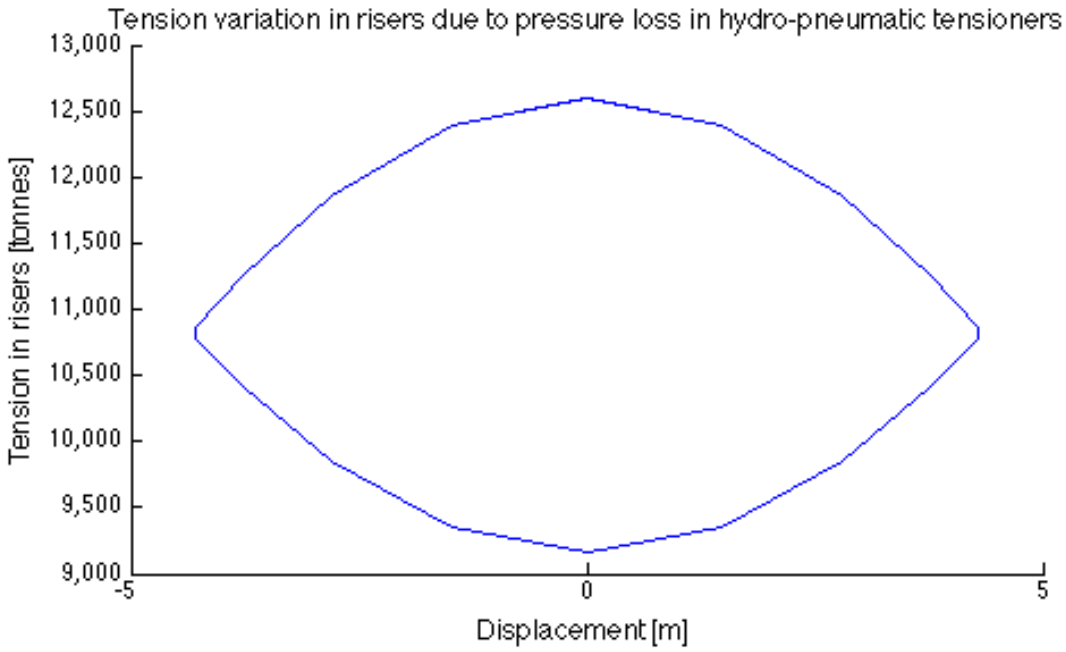

Figure 36: Tension variation in TTRs due to damping. Hs=20m, Zmax=4.35m, T=18s

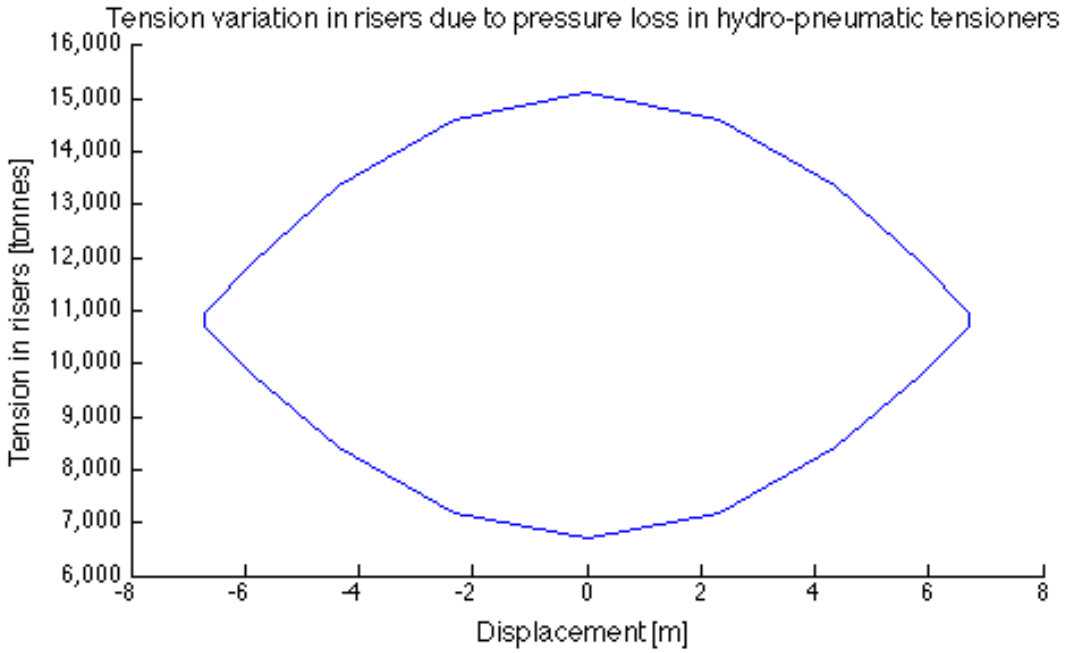

Figure 37: Tension variation in TTRs due to damping. Hs=20m, Zmax=6.8m, T=18s

By analysing the graphs, the tension variation, ΔT_{max} is found as the maximum occuring tension minus the initial tension, which in this case is 10,800 tonnes. From these results both a linear and a nonlinear damping coefficient is calculated by using the relations:

$$C_{linear\ viscous} = \Delta T_{max} / v \quad 7.2$$

$$C_{nonlinear\ viscous} = \Delta T_{max} / v^2 \quad 7.3$$

Table 7: Damping coefficients calculated from tension variation for different sea states

Hs [m]	Response amplitude	Period	ΔT_{max}	Velocity	$C_{TTR,lin}$	$C_{TTR,nonlin}$
2m	0.3m	13s	18t	0.15m/s	$120 * 10^4$	$800 * 10^4$
4m	0.6m	13s	70t	0.30m/s	$233 * 10^4$	$778 * 10^4$
6m	0.9m	13s	160t	0.435/s	$368 * 10^4$	$846 * 10^4$
20m	4.35m	18s	1800t	1.52 m/s	$1184 * 10^4$	$779 * 10^4$
30m	6.80m	18s	4300t	2.38 m/s	$1806 * 10^4$	$807 * 10^4$

The damping is then introduced again in the MATLAB code RK.m as linear & nonlinear viscous damping as described in chapter 5.2.3 & 5.2.4. The most conservative way is to introduce the damping as a linear model, where the equivalent damping will be bigger than for the nonlinear viscous damping model. However the nonlinear damping coefficient is showing a clear trend and one value can be used for all sea states with pretty good accuracy. The damping coefficients used in the RK.m code are:

$C_{TTR,linear}$ = as given in Table 7

$C_{TTR,nonlinear} = 8.000.000N / \left(\frac{m}{s}\right)^2 = 8 * 10^6 kg/m$

7.3 – Time-domain analysis

Time domain analyses have been performed using MATLAB code RK.m, which solves the equation of motion using a numerical Runge-Kutta method as described in chapter 4.1. Additional nonlinear damping and stiffness dependent on responses and velocities of the semi/tensioner system is introduced. This has been done by calculating damping and stiffness using the response and velocity of the last time step, then iterate the current time step.

Figure 38 shows how the phase angle varies over the different periods, and results from the steady-state part of three different time domain analysis is presented below; before, near and after the resonance period, marked A, B and C in the plot below.

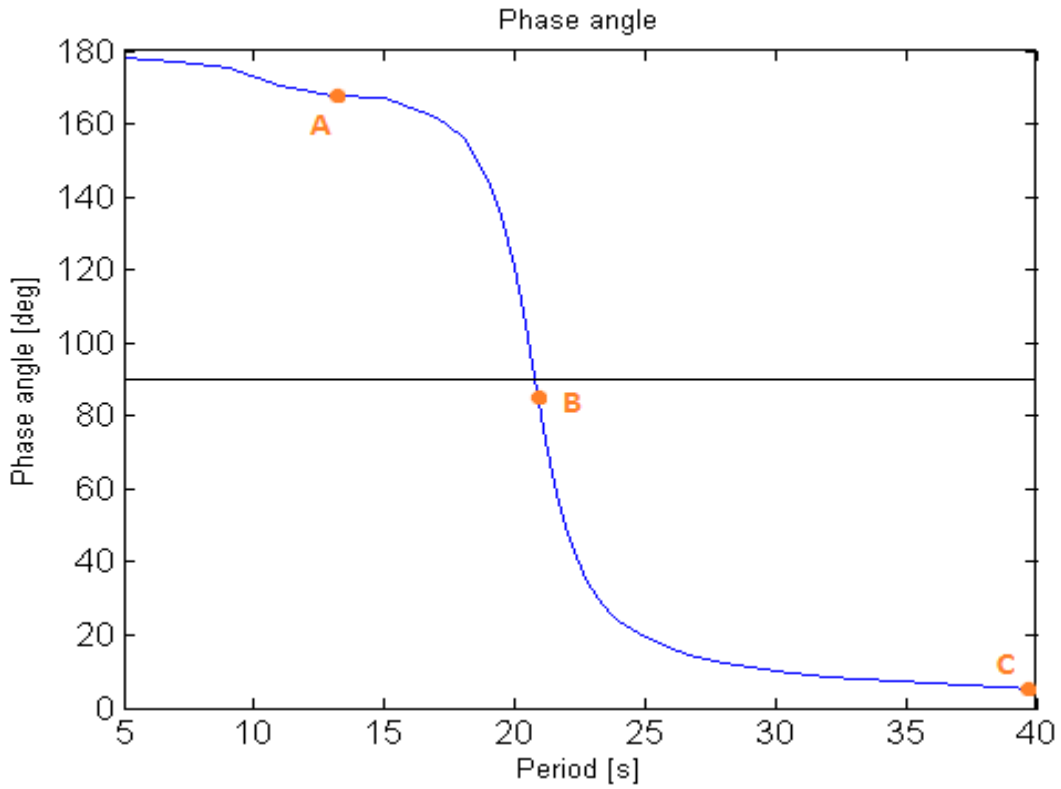

Figure 38: Phase angles used for time simulations

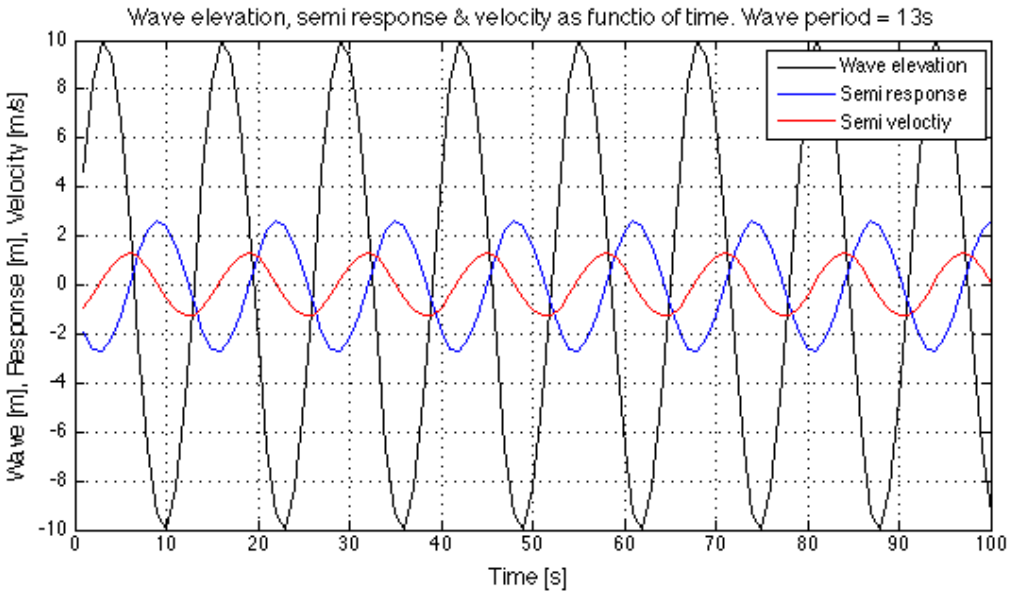

Figure 39: Time domain analysis of semi with TTR system. Hs=20m T=13s

Figure 39 shows how the loads and response varies in the steady-state domain in point A. The phase between load and response is 180° for wave period T = 13s, and the phase between the load and velocity is 90°. The system is clearly inertia dominated.

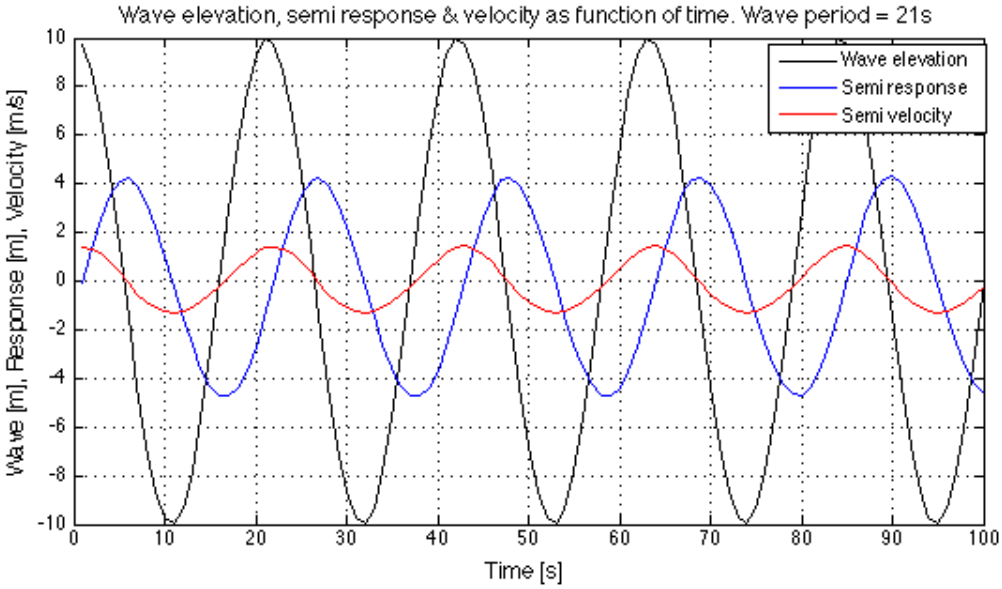

Figure 40: Time domain analysis of semi with TTR system. Hs=20m. T = 21s

Figure 40 shows that phase between load and response is 90° for wave period T = 21s. The load and velocity is almost in phase, which makes it clear that the system is oscillating near the resonance period, which is found in the inflection point of the graph in Figure 38.Hand calculations shows that the natural period of the system is found at T = 20.74 [s].

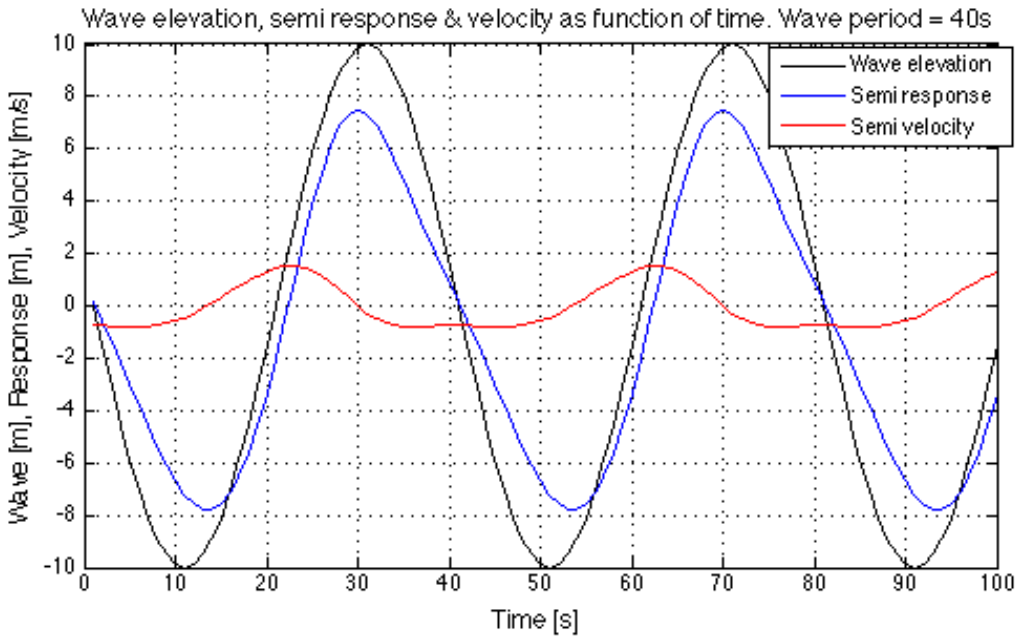

Figure 41: Time domain analysis of semi with TTR system. Hs=20m T=40s.

Figure 41 shows how the load and response is nearly in phase for a high wave period of T=40. The system oscillation is here stiffness dominated. It should also be noted how the additional nonlinear stiffness from the tensioner system affects the response, where the counteracting spring force is larger for a down-stroke of the tensioner cylinders, hence a positive semi-response. This is seen in the above figure, as the maximum response is smaller than the minimum response.

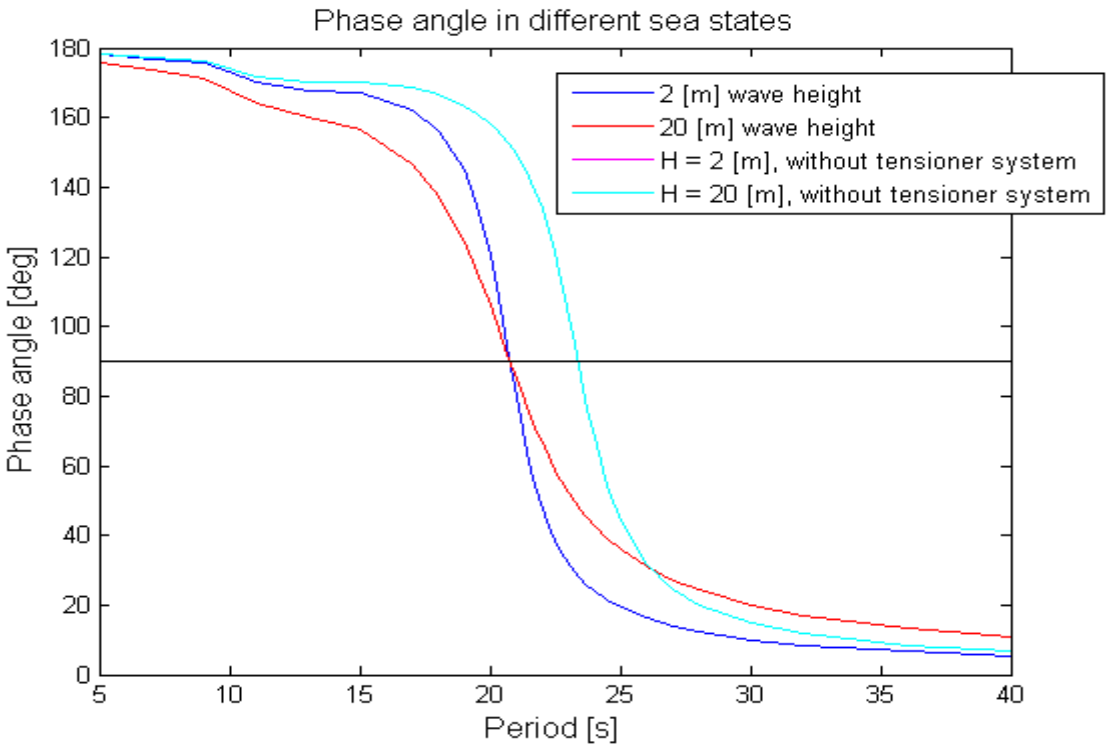

Figure 42: Variation of phase angle in different sea states with and w/o the TTR system.

Figure 42 show how the phase angle varies with different sea states, with and without the tensioner system. The comparison of the different sea states without the tensioner system, marked in magenta and cyan, lies exactly on the top of one another. Without the tensioner system there is no change in the phase angle when changing the sea state, which is due to the use of linearized Morison damping when calculating the phase angle. If a nonlinear Morison damping had been used the increase in wave height would have caused an increase in Morison damping, thus causing the graph to even out without changing the inflection point determining the resonance period.

This is easily seen when looking at the comparison between the different wave heights when the tensioner system is included, marked in red and blue. The loss in the tensioner system augments for greater stroke lengths in higher sea, hence introducing more damping to the system which leads to a smoother variation of the phase angle for higher sea states. Since the natural period do not change due to the sea state, the two graphs crosses at resonance. When comparing the analysis with and without the tensioner system one sees that the natural period is affected. An increase in stiffness when introducing the tensioner system will cause the natural period to decrease from 23.41 [s] to 20.74 [s], and the graph will move to the left since the inflection point always coincide with the resonance which happens at $\theta = 90°$.

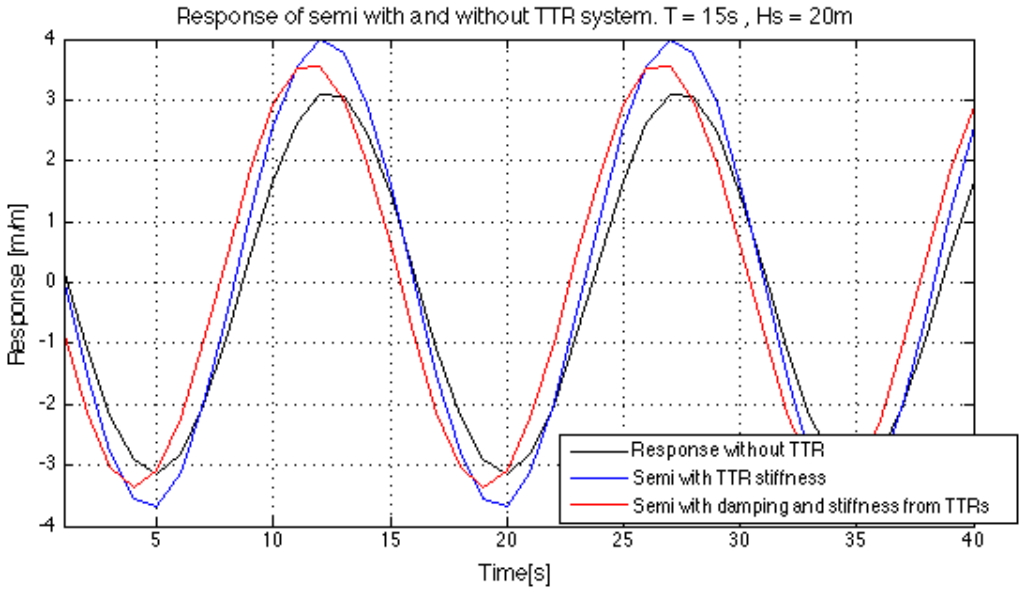

Figure 43: Response of semi with and without TTR system. T=15s. Hs=20m

Figure 43 show the response of the semi for an inertia dominated period of 15[s]. Three cases are compared; a freely floating semi, semi with tensioner stiffness only and semi with full TTR system. Response is decreased when introducing the stiffness, but then again increased as the additional damping is introduced.

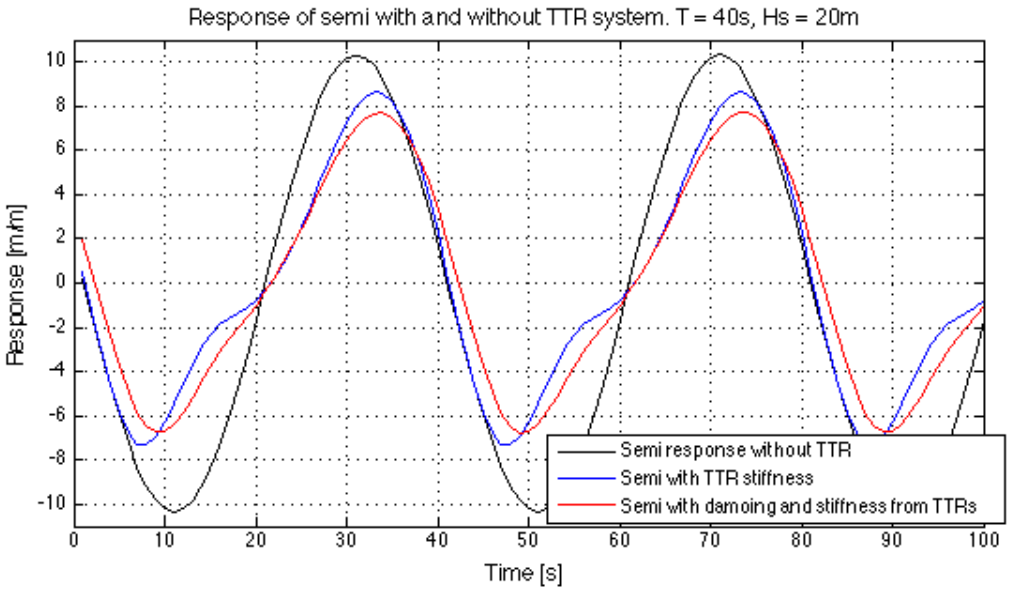

Figure 44: Response of semi with and without TTR system. T=40s. Hs=20m

Figure 44 shows how the response varies with and without stiffness and damping from the TTR system for wave period T = 40. This period is more typical for low wave heights in swell. It is interesting to see how the response of the stiffness-dominated system will be highly affected by the nonlinear stiffness for this wave period.

7.4 – Tension variation in risers

From chapter 5 the tension variation function was derived as equation (5.1). Using nonlinear spring rate, viscous damping, and Coulomb friction force based on time simulations, the tension variations in risers can be calculated based on equation 5.1. The results presented in this sub chapter are how the nonlinear terms are introduced in the dynamic response calculations of the semisubmersible, seen in equation (4.2)

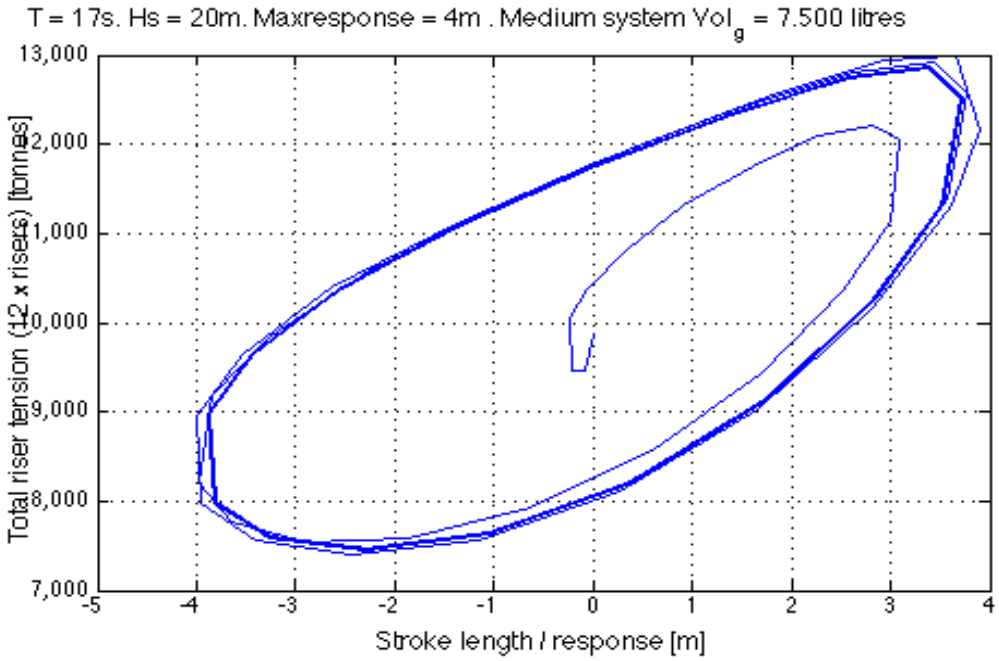

Figure 45: Tension variation for all risers. Hs = 20m. T = 17s. Gas volume = 7.500 litres

Figure 45 above shows the tension variation in time plotted against the response for a medium soft system, with gas volume of 7.500 litres. It should be noted that it is the enclosed area for one period that defines the energy loss for each oscillation in the system, hence damping.

As the gas volume defines the nonlinear stiffness of the tensioner system, by considering three different systems with variable gas volume, the effect of this can be compared.

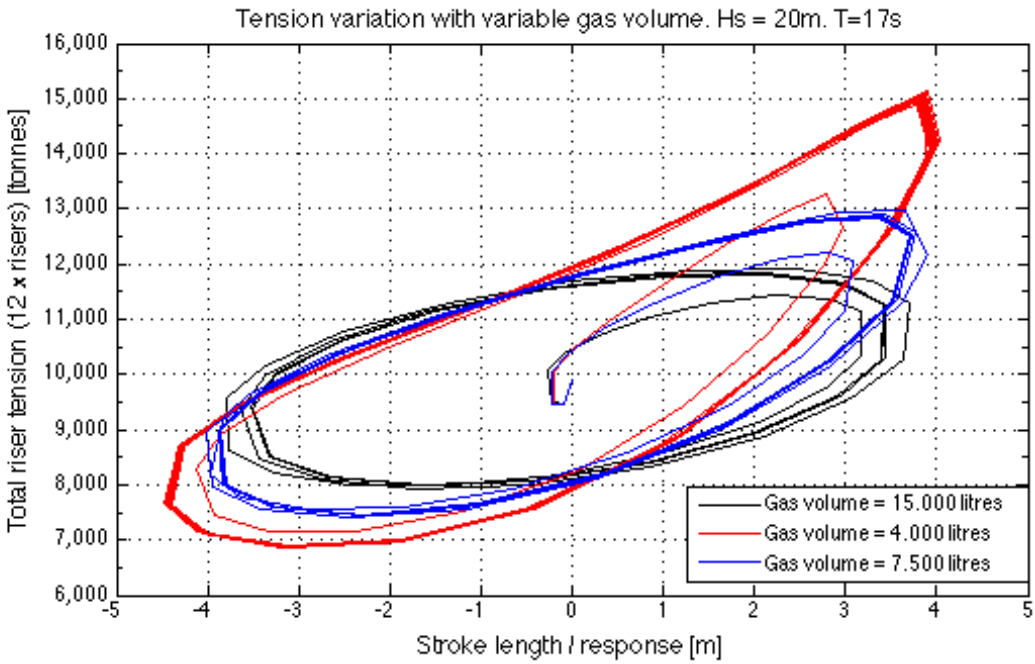

Figure 46: Tension variation in risers using variable gas volume. Hs = 20m. T = 17s

Figure 46 shows how the nonlinearity of the stiffness increase as the gas volume is decreased. It is of big interest to see how the decreased gas volume give a larger response in the inertia-dominated period of T=17s. This will be the opposite for a stiffness-dominated period above the natural period, where a decreased gas volume will give less response. This is also shown in Figure 27 & 28.

From results in chapter 7.1 the nonlinear spring-rates were linearized, and in chapter 7.2 linearized values for the damping were proposed. By comparing the tension variation based on both nonlinear damping and stiffness with the linearized values, differences can be clarified. This is done in the next two figures.

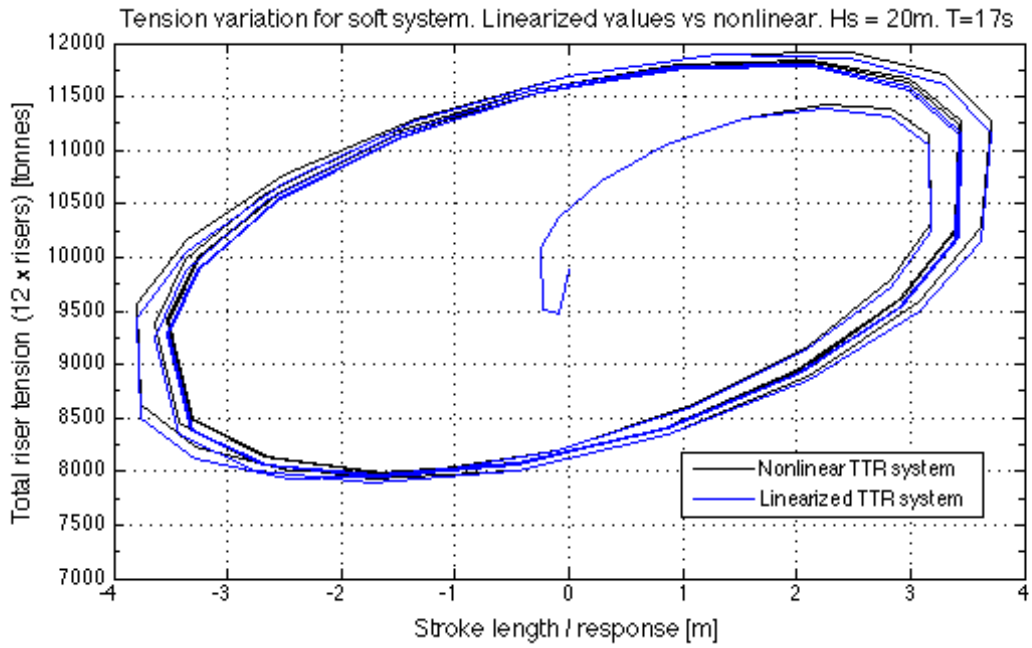

Figure 47: Tension variation for soft system with nonlinear and linearized TTR system

Figure 47 shows that the linearized values give very exact results for a soft tensioner system with gas volume of 15.000 litres. This is expected as the variation between linearized and initial nonlinear stiffness for a soft system was found to be only 2% in chapter 7.1.

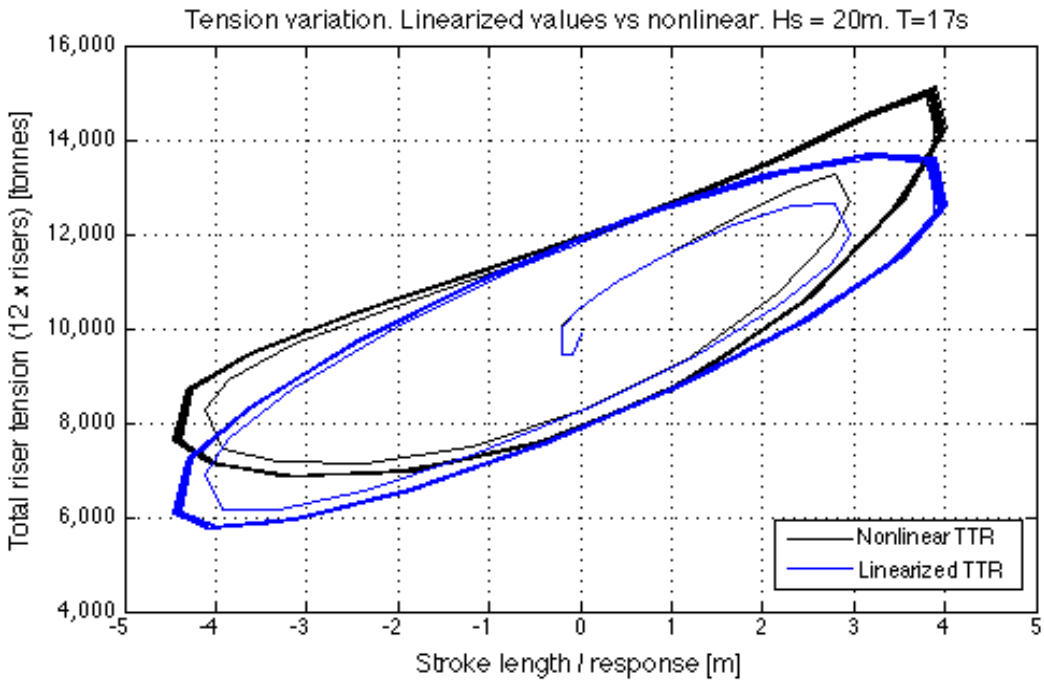

Figure 48: Tension variation for stiff system with nonlinear and linearized TTR system

For a stiff TTR-system with gas volume of 4.000 litres the deviations are larger. It is clear that the nonlinear stiffness seen in the black plot deviates from the linear, but this is also as expected from results presented in Chapter 7.1, Table 6.

7.5 – RAOs based on time-domain results

Based on the time-domain analysis for a range of different wave heights and periods, the maximum values of the response in the steady state are plotted against their respective wave periods. When plotted against the period, these maximum values will form a RAO based on time domain analysis, hence including the nonlinearities. This gives the opportunity to implement the full effect of spring-rate and damping of the riser tensioner system. The isolated results for the tensioner system are given in Chapter 7.4.

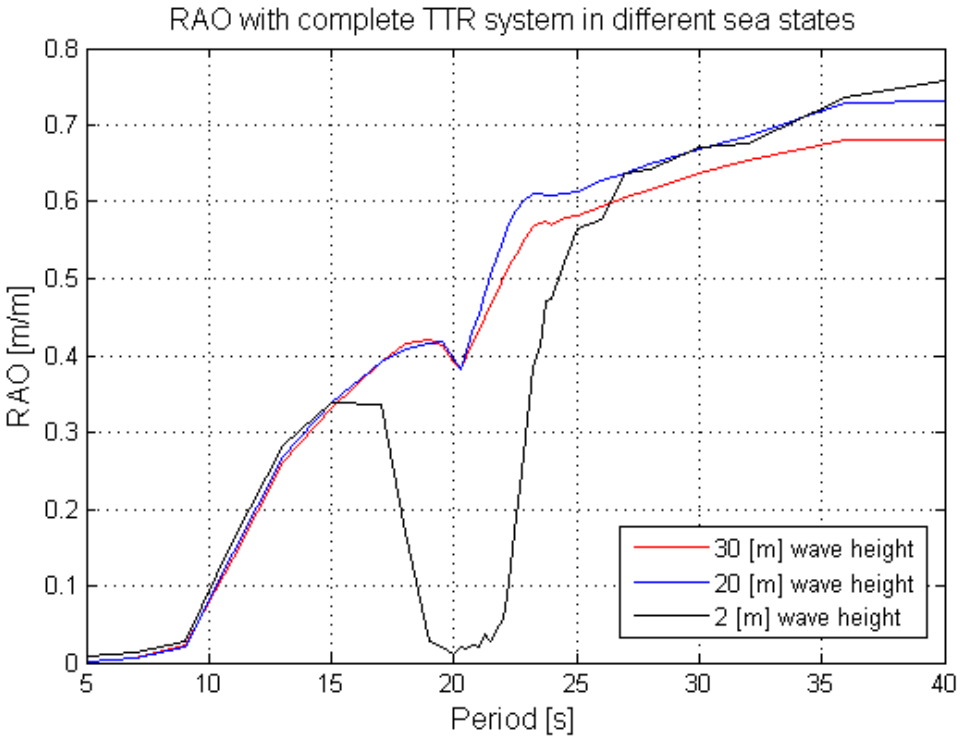

Figure 49: Comparison of RAOs with complete tensioner system in different sea states

The above figure clearly shows how the response is affected by the wave height. For small sea states there will not be enough energy to overcome the Coulomb friction, and we see a stiction effect around the cancellation period. The RAO is more similar for the higher sea states of 20 [m] and 30 [m], mainly due to the augmentation of the Morison drag contribution, which will dominate near the cancellation period and also lower the resonance peak a lot.

For periods higher that the resonance period the RAOs converges towards a response value which is lower than 1. The semi is restrained by the risers in which there is assumed constant tension; hence it will not follow the wave movements perfectly. Since there will be higher tension in the risers in a 30 [m] sea state, the response will converge towards a lower value than for a 20 [m] sea state. This can be compared to a TLP platform with linear tension variation in the tethers in tidal water.

The analysis done in the Figure below have the main focus of comparing the effects of viscous- and Coulomb- damping in the tensioner system, and to demonstrate how these contributions affects the RAO differently in different sea states. Another very important contribution is the stiffness from the tensioner system, which will have a big influence on the RAOs.

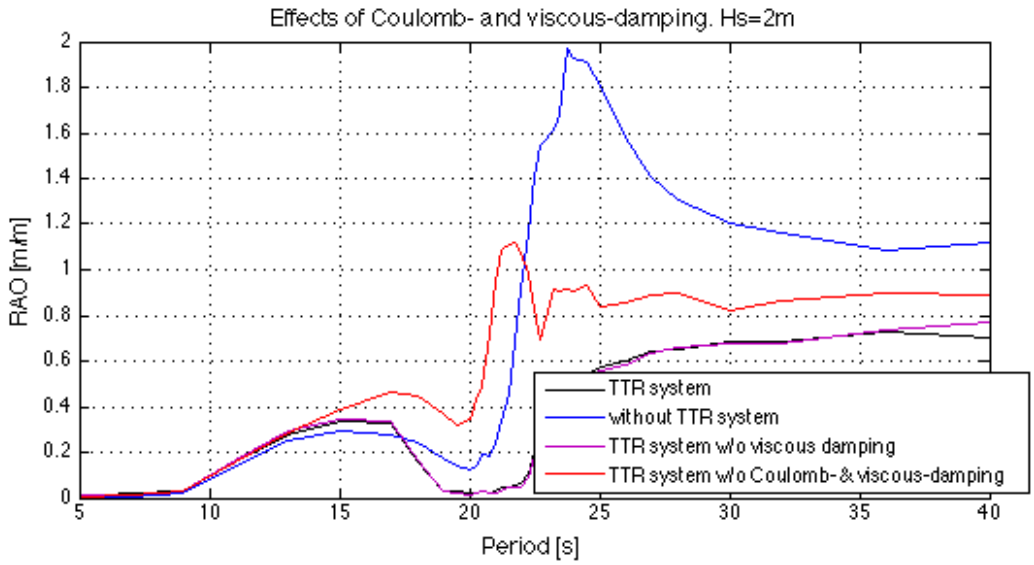

Figure 50: Effects of tensioner system on RAO. Hs=2m

For a 2 [m] wave height the viscous damping from the tensioner system will have almost no effect on the response of the semi due to the low velocities. However, the Coulomb damping will affect the system a lot. This is due to the fact that the Coulomb friction forces are independent on the sea state, and will dominate the wave forces in 2[m] wave height. Since the stroke length of tensioner cylinders is small, the viscous damping from the tensioner system will not be significant for such a small sea state.

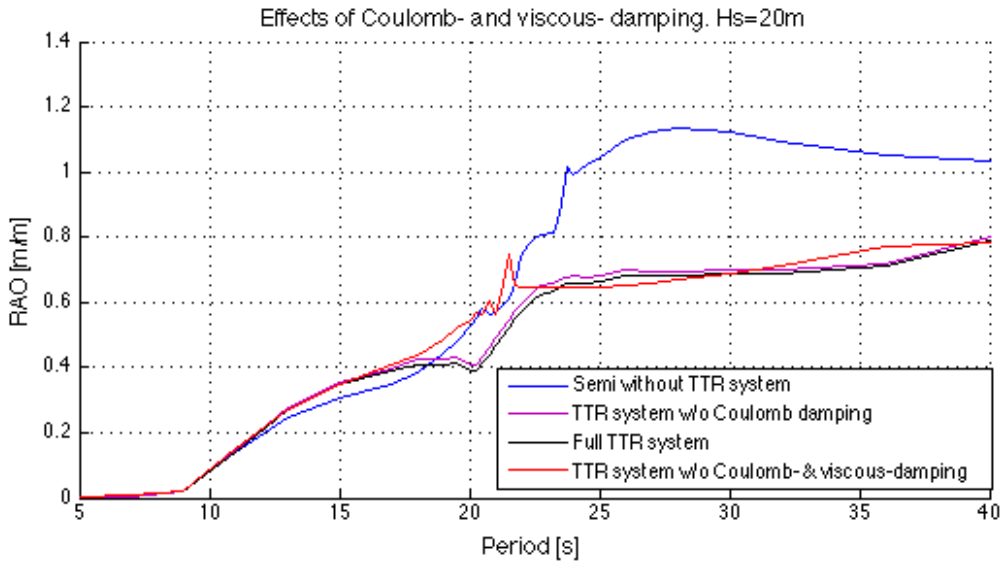

Figure 51: Effects of tensioner system on RAO. Hs = 20m

When looking at the RAOs in 20 [m] waves, it is clear that the wave forces dominate the Coulomb friction forces. In this sea state it is the viscous damping force contribution that has the main impact on the system. Due to greater heave movements of the semi, the stroke length in the tensioner system will increase. This leads to higher pressure loss in the tensioner system, hence more viscous damping.

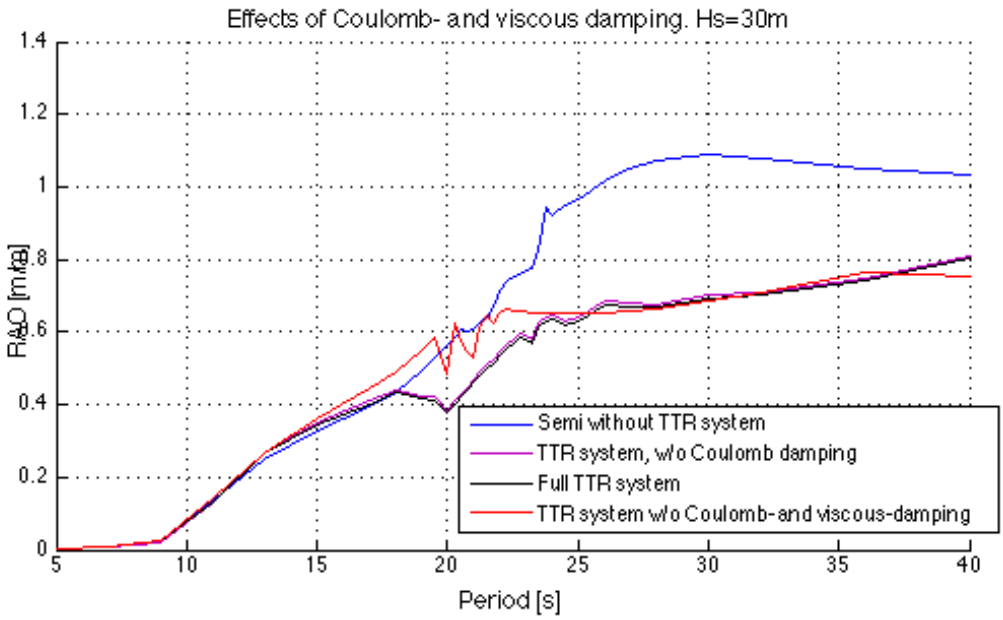

Figure 52: Effects of tensioner system on RAO. Hs = 30m

Based on Figure 51 and 52, extreme responses in heave for the semi can be evaluated. Based on an extreme period of 17[s], the response amplitudes for the semi with TTR system will be 3.88[m] for a 20[m] regular wave, and 6.13[m] for a 30[m] wave. Without the TTR

system, the response amplitudes are 3.49[m] and 5.90[m] for a 20[m] and 30[m] wave. As the tensioner cylinder amplitude length is 6.3[m], the system will in theory be good. But tidal water effects must be considered, and initial stroke of the cylinders will not always be 0[m].

In chapter 7.1 and 7.2 linearized values for the stiffness and damping were proposed. By doing analysis with linear coefficients and compare them to the nonlinear analysis, it can be evaluated if the linearized values can be used with good accuracy. If linear results can be used with good accuracy, the problem can be solved using a frequency domain solver like WADAM. Three different systems with variable gas reservoir volumes, 4.000, 7.500, and 15.000 litres were examined for two different wave heights of 2[m] and 20[m]. The Coulomb friction was not included in these analyses, as it is a constant, and don't include any nonlinearities.

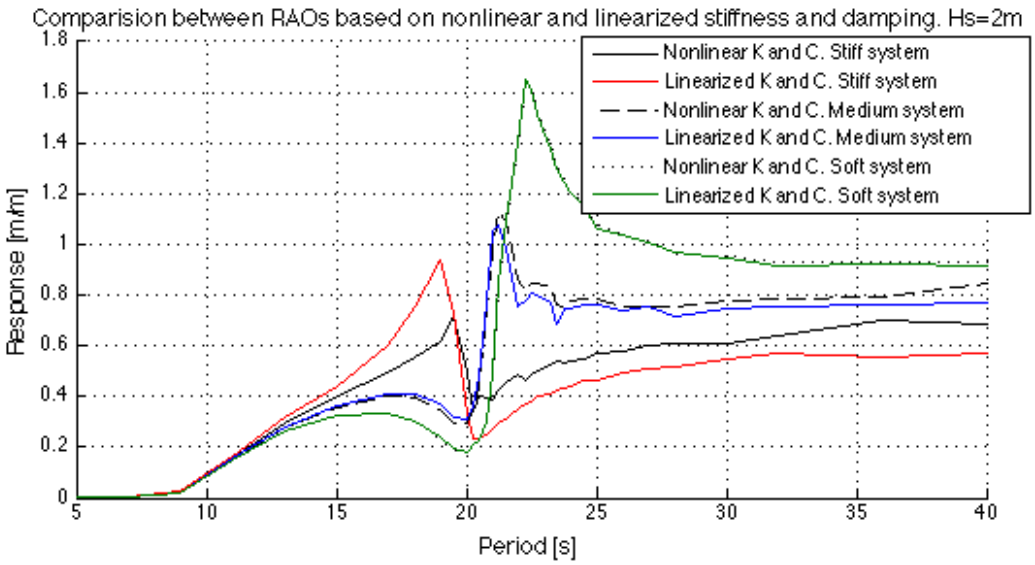

Figure 53: RAO comparison between nonlinear and linearized TTR coefficients. Hs=2m

Figure 53 shows the correlation between linearized and nonlinear stiffness and damping caused by the tensioner system. The stiff system with 4.000 litres gas volume shows big deviations and the linearized values are probably not suitable in a low sea state with small strokes of the tensioner cylinders. Both the medium and soft tensioner system show good accuracy by use of the linearized values. It is then expected that these two systems correlate good in 20[m] as well, as the linearized values are based on a maximum stroke of the cylinders.

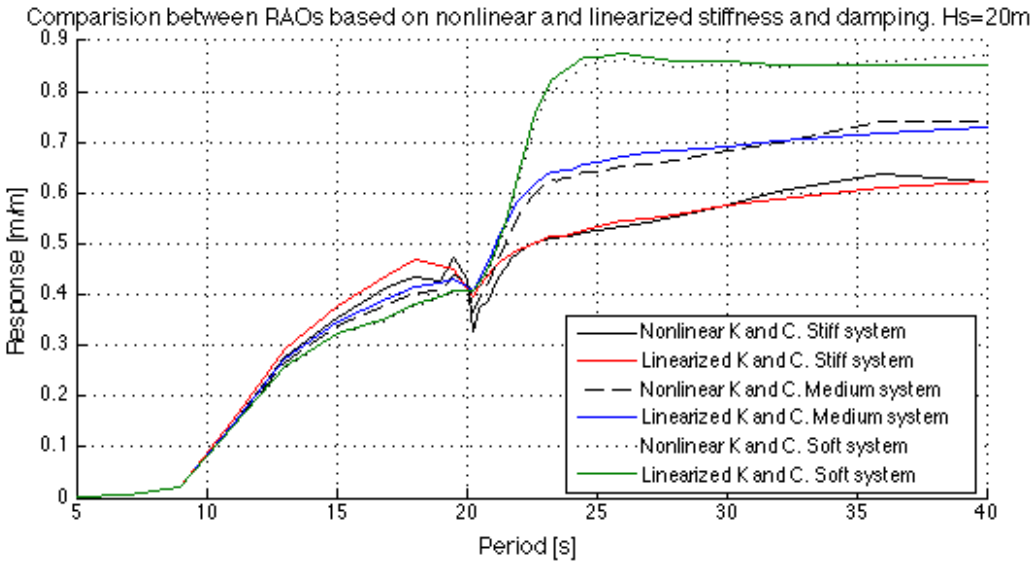

Figure 54: RAO comparison between nonlinear and linearized TTR coefficients. Hs=20m

Figure 54 shows that for a wave height of 20[m] the deviations of the stiff system are smaller than 2[m]. This is expected as the response, hence stroke of cylinders are 70-80% of max piston stroke length for period 18[s], and the linearized values are based on 100% stroke of cylinder pistons. Both the medium and soft system show good accuracy for the linearized coefficients, and the problem can be solved with good accuracy using a frequency domain solver.

7.6 – Coulomb friction forces

By introducing a Coulomb friction force that models the friction found in the seals of the tensioner cylinders and keel guides, responses in low sea states will be highly affected. The Coulomb friction force model is discussed in chapter 5.2.5.

The friction is given as a fraction of the total initial tension in all of the risers and for this case the following values are used

2%: 0.02 * 12 * 840 tonnes = 201,6 tonnes

4% 0.04 * 12 * 840 tonnes = 403,2 tonnes

6%: 0.06 * 12 * 840 tonnes = 604,8 tonnes

As this opposing friction force gets bigger than the exciting forces for a given wave height and period, the semi will be stuck and have zero response. The exciting forces may then cause fatigue of the risers, as the semi will be effectively moored by the risers. This will drastically increase the stiffness of the semi as the elastic stiffness of the risers then will dominate. This will decrease the natural period in heave, roll & pitch. The semisubmersible then may be exposed to resonance oscillations for small sea states. Variable friction coefficients for different wave heights are presented in figures below:

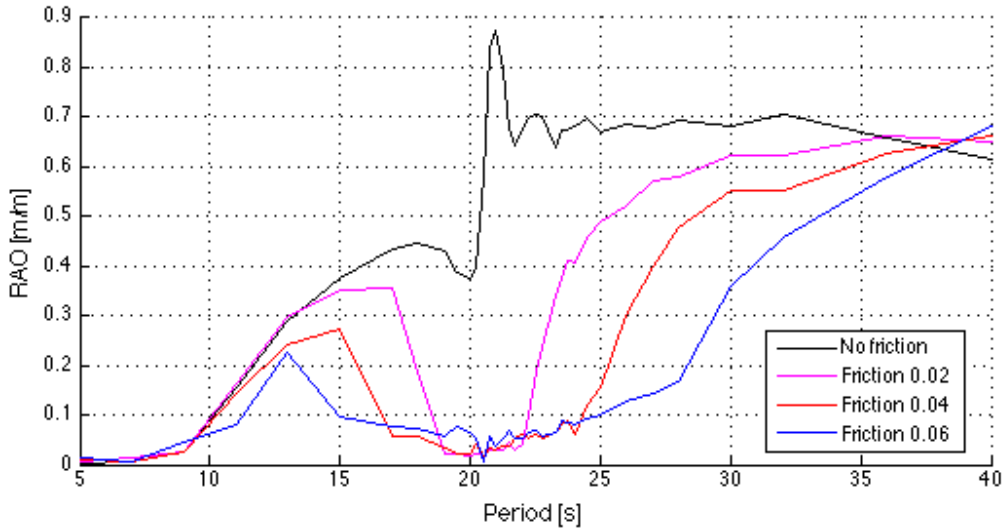

Figure 55: RAO for semi with variable Coulomb friction. Hs=2m

Figure 55 shows how the response will go towards zero for periods near cancellation and resonance. Since the Coulomb friction force will be more than the exciting force, the time domain simulations will use a resulting negative force in the analysis. This will give a low false response for periods where semi is stuck. As the frictional force gets above the excitation force the real RAO is seen in the figure below.

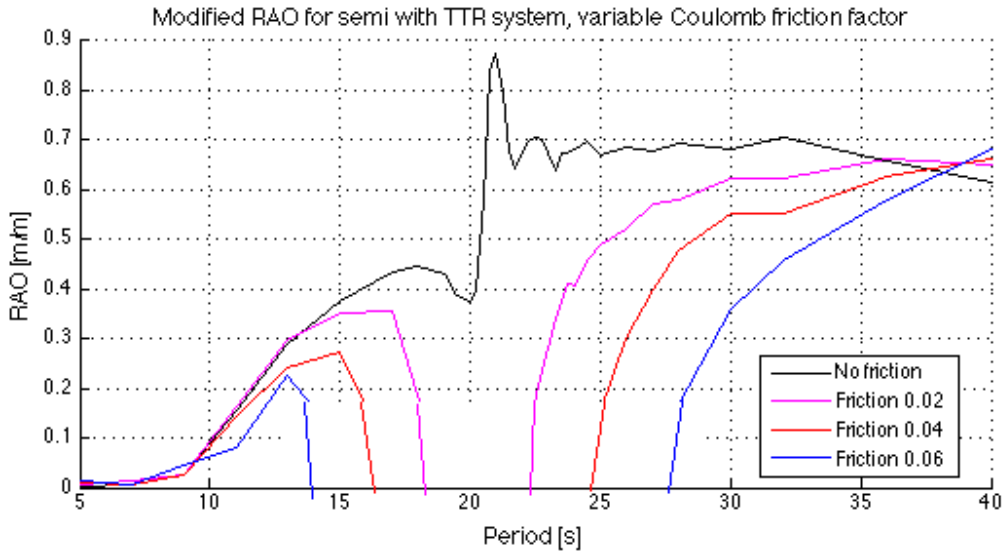

Figure 56: RAOs for semi with variable Coulomb friction factor. Hs=2m

The figure above is a modified version of figure 55, which clarifies the periods and frictional factors where the semi will be ”stuck”.

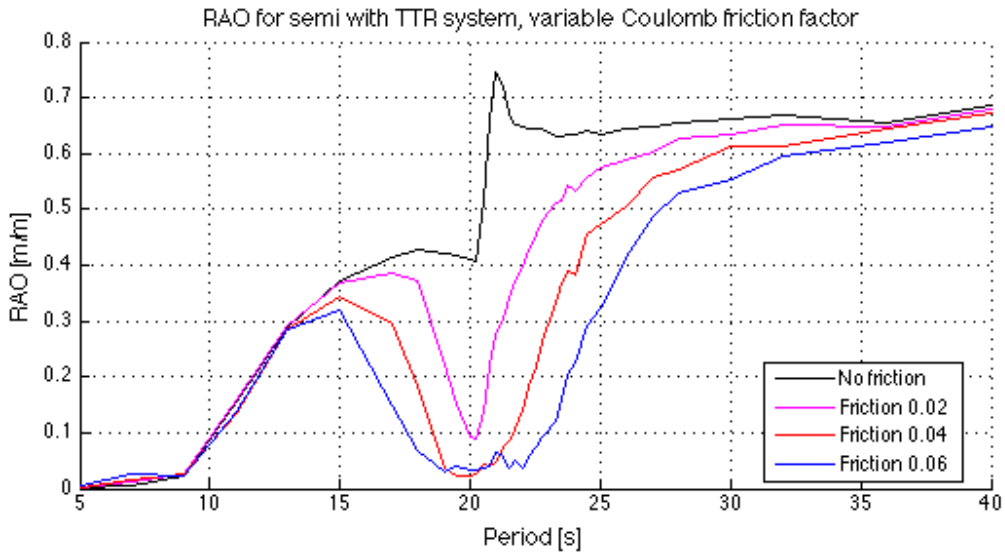

Figure 57: RAOs for semi with variable Coulomb friction factor. Hs = 4m

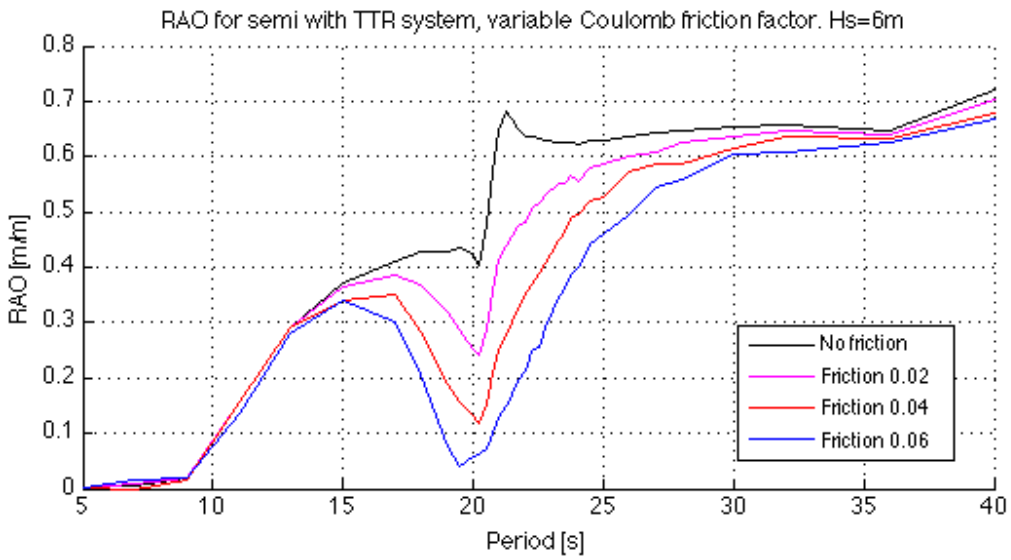

Figure 58: RAOs for semi with variable Coulomb friction factor. Hs = 6m

Figure 57 and 58 show the response in wave heights of 4[m] and 6[m]. For a 6[m] wave height the semi will freely oscillate for all periods by use of friction coefficients between 2-6%. The full overview for stuck states of the semi is given in table 8 below.

Table 8: Range were semi will be moored by risers, due to Coulomb friction

	Period range where semi will be stuck [s]		
Wave height	**Friction 2%**	**Friction 4%**	**Friction 6%**
Hs = 2m	18.0 [s] - 22.5 [s]	16.5 [s] - 24.5 [s]	14.0 [s] - 27.5 [s]
Hs = 4m	No stiction	19.0 [s] - 22.0 [s]	17.0 [s] - 23.0 [s]
Hs = 6m	No stiction	No stiction	18.0 [s] – 22.0 [s]

As mentioned earlier the vertical stiffness will increase drastically for a stuck state, as it is not the compensator system that defines the stiffness, but rather the spring rate of 12 risers in parallel. For a stuck state the natural period in heave will then be, considering a riser stiffness of $k_{riser} = 3600 * 10^3 [N/m]$

$$T_{3,stuck} = 2\pi\sqrt{(m + A_{33})/(K_{33} + (12 * k_{riser}))}$$

$$T_{3,stuck} = 12.65 \text{ [s]}$$

8 – Conclusion

The additional nonlinear stiffness caused by the compression of gas in hydro-pneumatic tensioner system has a big impact on the dry-tree semi response. Response amplitudes in the inertia-dominated range are increased drastically with increased stiffness, meaning a low gas volume. As a consequence of increased stiffness, the natural period in heave is decreased. For a stiff compensator system with gas volume of 4000 litres the natural period will be decreased to 19.21 [s] for a large sea state, compared to 23.4 [s] for the freely floating semi without TTR system.

Linearized values for stiffness and damping caused by the tensioner system can be used with good accuracy for a medium to soft tensioner system. This means that this problem also can be analysed using a frequency domain solver, like WADAM. Making the tensioner system stiffer, by decreasing the active gas reservoir volume, will increase the deviations between nonlinear and linearized results, and time domain simulations must be run in order to get exact results.

It has been shown that for low sea states the friction force found in seal packers of tensioner cylinders and keel guides can overcome the wave excitation forces. The semi will then be effectively moored by the risers. The natural period will be drastically reduced to 12.65[s] due to the elastic stiffness of risers. By considering a friction force of 2-6% of tension loads in a wave range of 2-6[m] it is shown that the semi can be stuck in the period range 14.0[s] - 27.5[s].

By considering a medium soft tensioner system with a gas volume of 7.500 litres, maximum response amplitudes for extreme wave heights of 20 and 30[m] have been found to be 3.88 and 6.13[m]. Without tensioner system the response were found to be 3.49 and 5.90[m]. As the tensioner stroke design amplitude is set to 6.3[m], the semi will do well in theory. Tidal water effects must be considered though, and this causes the initial piston stroke position to vary around 0[m], which shortens the allowed stroke amplitude in one direction.

9 – Suggestions for Further studies

Only heave motions have been examined in this study. Roll and pitch will also have an influence on the tensioner stroke and dynamics of the system, and for further studies a coupled motion analysis is something that should be evaluated and taken into consideration. In roll & pitch the Coulomb friction forces will increase due to increased normal forces, and is something to be considered for further work.

In an early phase of this study, motion analysis by use of irregular waves modelled by different wave spectrums was planned. This was later neglected as regular waves were more suited to clarify trends and contexts, on how the riser tension system affects the response of the semisubmersible. Irregular sea state analysis is still something that is of interest, especially for ”stick-slip” situations where the semisubmersible will change between a static and dynamic condition for some sea states.

The Coulomb friction factor was in this study simplified and set as a constant. In reality there will be more friction in the turning points of response, where the velocity is zero. More accurate friction models including change between static and dynamic friction can be examined and implemented in the equation of motions for the semi.

The hydro-pneumatic tensioner system can be modelled in a more detailed way including valves, bends etc. More exact calculations of pressure loss in the oscillating system might be calculated by use of CFD-simulations. This may show variations from the simplified calculations done in this study.

For this study a passive accumulator compensator system is applied. Even though this is something currently not available, an active system, which controls the pressure on gas side by use of compressors, is something that might be evaluated. In theory the tension variation could then be reduced to zero, given that the system either predicts the future/response or acts infinitely fast. In reality that is very difficult to obtain.

10 – References

Blevins, R. D. (1984). *Applied Fluid Dynamics; Handbook.* Van Nostrand Reinhold Company, Inc.

Chedzoy, C., & Lim, F. (2003). *Design Challenges of Deepwater Dry Tree Riser Systems for Different Vessel Types .* 2H Offshore Engineering Ltd. Honolulu, Hawaii: Proceedings of The Thirteenth International Offshore and Polar Engineering Conference.

Det Norske Veritas. (2010). *DNV-RP-C205: Environmental Conditions and Environmental Loads.*

Det Norske Veritas. (n.d.). SESAM User Manual - WADAM.

Falk, M.-I., & Skorpen, T. (2011). *Project thesis: Semisubmersible challenges; platform-riser interactions.* Trondheim.

Faltinsen, O. (1990). *Sea Loads on Ships and Offshore Structures.* Cambridge, United Kingdom: Cambridge University Press.

Giliomee, L. (2005). *Analysis of a Four State Switchable Hydro-pneumatic Spring and Damper System.* University of Pretoria, Department of Mechanical and Aeronautical Engineering.

Langen, I., & Sigbjörnsson, R. (1979). *Dynamisk analyse av marine konstruksjoner.* Trondheim, Norway: Tapir.

Larsen, C. M. (January 2009). *TMR4180 MARIN DYNAMIKK.* Trondheim, Norway: Department of Marine Technology, NTNU.

MARINTEK. (2007). SIMO - User's Manual Version 3.6. Trondheim: Det Norske Veritas.

White, F. M. (2002). *Fluid Mechanics, 5th edition.* McGraw-Hill.

APPENDIX A: MATLAB Flowchart

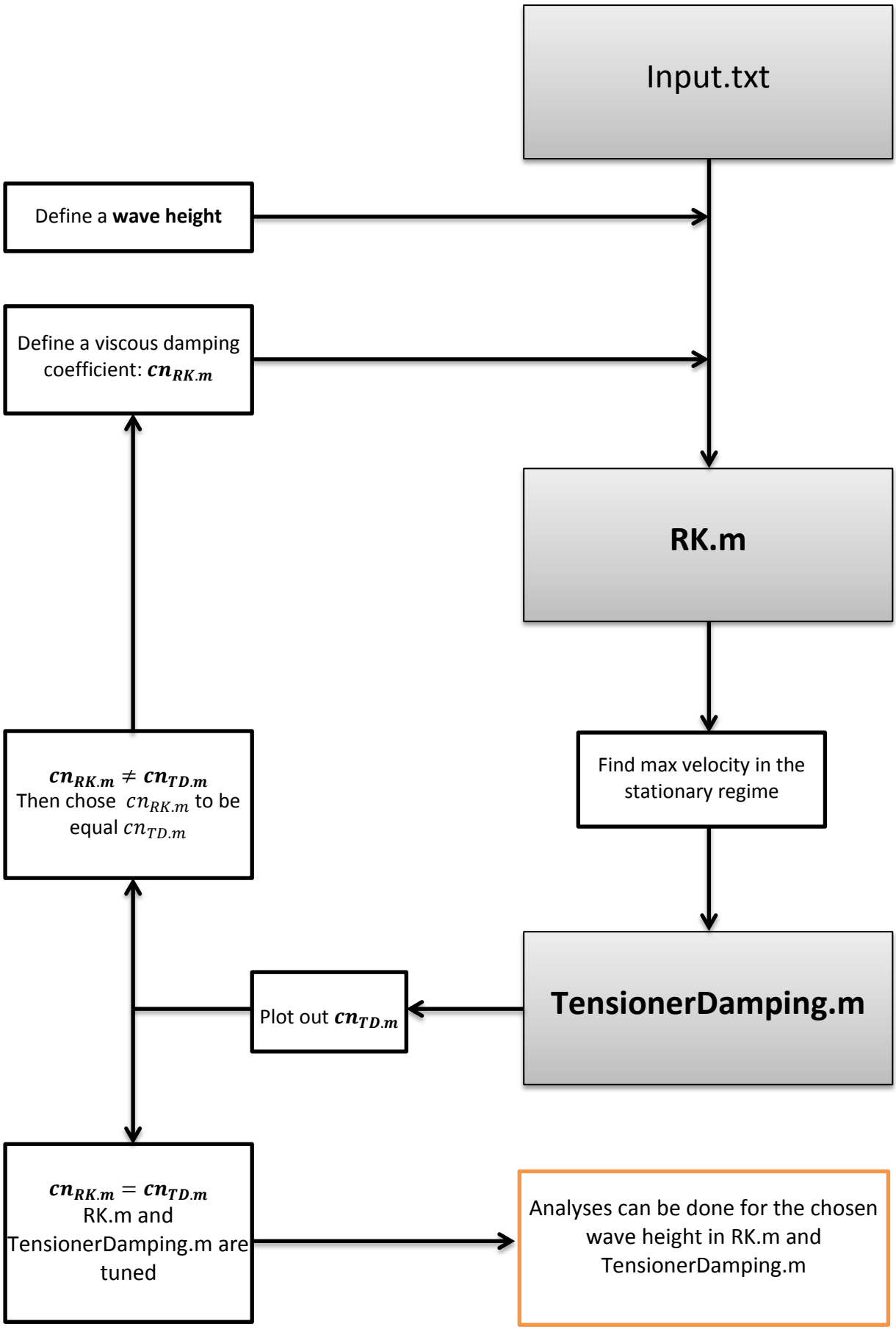

APPENDIX B: Routine for MATLAB code

The following is a routine on how damping coefficients were decided. Internal use.

RK.m - Solving equation of motion in time-domain by use of a numerical Runge-Kutta method. Nonlinear effects can be calculated and accounted for.

TensionerDamping.m - Calculating loss in pipe system for different velocities. Will evaluate a time-varying Reynoldsnumber, Frictionfactor etc and present the tensioner variation for single riser and the whole system as a function of time.

1. Define a waveheight in RK.m. Run analysis and check what velocities is obtained at different frequencies.

** Remember to check that stationary regime is obtained and stable/reasonable results.
** Remember to remove tensioner system!

2. Set amplitude parameter in TensionerDamping.m to get same velocity time function 'vel' as obtained in RK.m for a reasonable period. Check tension variation in

Plot 'resp' against tensiontotal
plot 'vel' against tensiontotal

** Low periods should maybe be used, as they give the highest velocities. But this should be checked in results from RK.m
** Code is unstable for low Reynolds numbers. Higher timesteps give stability.
** Ensure results is in reasonable domain (SESreport, assumed tensioner variation)

3. Insert tension amplitude as damping coefficient in RK.m.

** Remember to insert both colombdamping and TTR spring stiffness (k_TTR)
** For linear damping model remember that higher damping will be given for frequencies with lower velocities
** For nonlinear damping the damping will be pretty good presented for all frequencies/velocities as damping coefficient is multiplied by velocity squared
** For nonlinear c = cn*abs(dx) , linear c = cn

4. Run analysis and verify. If the new velocities are a lot different from results in step 1, follow step 2 again with new velocities and iterate to right solution.

(5.) Run analysis with higher and lower damping coefficients to see how it varies

(6.) For HS=10,20,30 get dimensionless RAOs by dividing RAO by 5,10,15 etc.

APPENDIX C: MATLAB codes

```
%=========================================================================%
%            SOLVE EQUATION OF MOTION USING 4.TH ORDER RUNGE KUTTA        %
%                                                                          %
%®®®®®®®®®®®®®®®®®®®®®®®®®®®®®®®®®®®®®®®®®®®®®®®®®®®®®®®®®®®®®®®®®®®®®®®®®%
%                   mx'' + cx' +kx = Q(t)                                 %
%                                                                         %
%                   x'(k+1)  = x'(k)  + h/6(a1 + 2a2 + 2a3 + a4)          %
%                   x(k+1)   = x(k) + h/6(b1 + 2b2 + 2b3 + b4)            %
%                                                                         %
%®®®®®®®®®®®®®®®®®®®®®®®®®®®®®®®®®®®®®®®®®®®®®®®®®®®®®®®®®®®®®®®®®®®®®®®®®%
%  This program is written for the Master Thesis - 'Responce analysis of  %
%  a deep-draft dry tree semi-submersible' the spring 2012. It solves     %
%  a nonlinear equation of motion in the time domain.                     %
%                                                                         %
%                 Authors: Marianne-Isabelle Falk                         %
%                          Thomas Skorpen                                 %
%®®®®®®®®®®®®®®®®®®®®®®®®®®®®®®®®®®®®®®®®®®®®®®®®®®®®®®®®®®®®®®®®®®®®®®®®®%
%                          Oslo 10.june 2012                              %
%=========================================================================%
%                          DEFINING VARIABLES                             %
%®®®®®®®®®®®®®®®®®®®®®®®®®®®®®®®®®®®®®®®®®®®®®®®®®®®®®®®®®®®®®®®®®®®®®®®®®%
% A33                    : Added mass coefficient in heave                %
% b_pon                  : Bredth of pontoon                              %
% B33                    : Damping coefficient in heave                   %
% beta                   : Frequency ratio                                %
% c_d_equviv             : Drag coefficient upscaled                      %
% c_d_1                  : This should be 2,5 based on DNV rules          %
% c_d_2                  : Approximation based on DNV rules               %
% d_eqviv                : Equvivalent diameter used for upscaled Cd      %
% d_pon                  : Hight of pontoon                               %
% depth                  : Depth from the free surface to the sea floor   %
% draught                : Draugth of semi                                %
% draught_pon            : 'Middle' draugth of semi                       %
% dx                     : Velocity in heave                              %
% eta                    : Damping ratio                                  %
% F3                     : Exciting forces in heave                       %
% g                      : Acceleration of gravity                        %
% h                      : Timestep                                       %
% Hs                     : Significant wave height [m]                    %
% k_wave                 : Wave number                                    %
% K33                    : Restoring term in heave                        %
% L/l_pon                : Length of the pontoons                         %
% lambda                 : Wavelength                                     %
% mass                   : Mass of the semi-submersible                   %
% omega                  : Angular frequency [Hz]                         %
% Period                 : Vector consisting of all periods               %
% phase_angle            : Force phase angle in degrees                   %
% rho                    : Density of sea water                           %
% T                      : Choosen period [s]                             %
% time                   : Length of time interval in [s]                 %
% theta                  : Phase angle                                    %
% vol                    : Displaced volume                               %
% x                      : Displacement in heave                          %
% z_wave_pon1(2)         : Velocity of wave at pontoon 1 (2)              %
%                                                                         %
%®®®®®®®®®®®®®®®®®®®®®®®®®®®®®®®®®®®®®®®®®®®®®®®®®®®®®®®®®®®®®®®®®®®®®®®®®%
%      Variables from the hydropneumatic riser tensioner system           %
%®®®®®®®®®®®®®®®®®®®®®®®®®®®®®®®®®®®®®®®®®®®®®®®®®®®®®®®®®®®®®®®®®®®®®®®®®%
% z_0                    : Air volume column relative to stroke length     %
% n_g                    : Gas constant                                   %
% n_TTR                  : Number of TTRs                                 %
% zmax                   : Max-stroke                                     %
% risertension           : Pretension in each TTR in tonnes               %
% Totaltension           : Calculate total tension for system             %
% k_riser                : Spring rate of riser as N/m                    %
% k_TTR_lin              : Linearized spring stiffness                    %
% cn_tonnes              : Viscous damping coefficient                    %
```

```
% cn_lin                    : Linear Viscous damping coefficient            %
% cn_nonlin                 : Nonlinear viscous damping coefficient         %
% mu_col                    : Coulomb friction as fraction of total tension %
% lindamping                : Linearized damping                            %
% nonlindamping             : Nonlinear damping                             %
% coldamping                : Coulomb damping                               %
% k_TTR                     : Riser tensioner stiffness                     %
% k_TTR_linearized          : Linearized value for k_TTR                    %
% naturalperiodlinearized : Linearized natural period                       %
%                                                                           %
%===========================================================================%

clear all;
clc;
hold on;

%---------------------------------------------------------------------------%
%                Data from the pre-project: RAO_TTR_preproject
%®®®®®®®®®®®®®®®®®®®®®®®®®®®®®®®®®®®®®®®®®®®®®®®®®®®®®®®®®®®®®®®®®®®®®®®®®®®®%
% fid = fopen('RAO_TTR_preproject.txt','r');
% RAO_TTR_preproject = fscanf(fid,'%f',[1 35]);
% fclose(fid);
%®®®®®®®®®®®®®®®®®®®®®®®®®®®®®®®®®®®®®®®®®®®®®®®®®®®®®®®®®®®®®®®®®®®®®®®®®®®®%
%                Uploading environmental and model data                     %
%®®®®®®®®®®®®®®®®®®®®®®®®®®®®®®®®®®®®®®®®®®®®®®®®®®®®®®®®®®®®®®®®®®®®®®®®®®®®%
%                with Morison damping included                              %
% fid = fopen('Runge_Kutta_input_from_HydroD.txt','r');
% temp1                  = fscanf(fid,'%g %g %g %g %g %g %g',[7 1]);
% temp2                  = fscanf(fid,'%f',[1 35]);
% temp3                  = fscanf(fid,'%f',[1 35]);
% temp4                  = fscanf(fid,'%f',[1 35]);
% temp5                  = fscanf(fid,'%f',[1 35]);

%                without Morison damping included                           %
fid = fopen('RK_input_from_HydroD_wo_Morison.txt','r');
temp1                  = fscanf(fid,'%g %g %g %g %g %g %g',[7 1]);
temp2                  = fscanf(fid,'%f',[1 35]);
temp3                  = fscanf(fid,'%f',[1 35]);
temp4                  = fscanf(fid,'%f',[1 35]);
temp5                  = fscanf(fid,'%f',[1 35]);
temp6                  = fscanf(fid,'%f',[1 35]);
% phase_angle            = temp6(1,:); % for force in degrees!!!

%®®®®®®®®®®®®®®®®®®®®®®®®®®®®®®®®®®®®®®®®®®®®®®®®®®®®®®®®®®®®®®®®®®®®®®®®®®®®%
%                         ENVIRONMENTAL DATA & SEMI-SUB
%®®®®®®®®®®®®®®®®®®®®®®®®®®®®®®®®®®®®®®®®®®®®®®®®®®®®®®®®®®®®®®®®®®®®®®®®®®®®%
Period                 = temp2(1,:);
Hs                     = 2;
h                      = 1;
time                   = 400; t = [1:h:time];

%®®®®®®®®®®®®®®®®®®®®®®®®®®®®®®®®®®®®®®®®®®®®®®®®®®®®®®®®®®®®®®®®®®®®®®®®®®®®%
g                      = temp1(1);
rho                    = temp1(2);
depth                  = temp1(3);
vol                    = temp1(5);
L                      = temp1(6);
draught                = 4.41960E+01;
d_pon                  = 10.0584002;
draught_pon            = round(draught-d_pon/2);
l_pon                  = round(79.7724978);
b_pon                  = l_pon/2;
d_equiv                = 0.001;
c_d_equviv             = 56229;
c_d_1                  = 2;
c_d_2                  = 0.29;
%®®®®®®®®®®®®®®®®®®®®®®®®®®®®®®®®®®®®®®®®®®®®®®®®®®®®®®®®®®®®®®®®®®®®®®®®®®®®%
mass                   = temp1(4);
A33_vector             = (rho*vol*temp3(1,:));
B33_vector             = (rho*vol*sqrt(g/L)*temp4(1,:));
```

```
K33                  = temp1(7);
F3_vector            = rho*vol*g/L*temp5(1,:);
fclose(fid);
%@@@@@@@@@@@@@@@@@@@@@@@@@@@@@@@@@@@@@@@@@@@@@@@@@@@@@@@@@@@@@@@@@@@@@@@@@@@@%
%                          HYDROPNEUMATIC RISER TENSIONER SYSTEM            %
%@@@@@@@@@@@@@@@@@@@@@@@@@@@@@@@@@@@@@@@@@@@@@@@@@@@@@@@@@@@@@@@@@@@@@@@@@@@@%
z_0                  = 31.5;
n_g                  = 1.4;
n_TTR                = 12;
zmax                 = 6.3;
risertension         = 840;
Totaltension         = risertension*1000*g*n_TTR;
k_riser              = 3600000;
k_TTR_lin            = 2.3591e+06;

cn_tonnes            = 1180;
cn_lin               = cn_tonnes*10000;
cn_nonlin            = 800*10000;
mu_col               = 0.02;


%--------------------------------------------------------------------------%
%                DEFINING VECTORS USED IN THE FOR-LOOP                    %
%--------------------------------------------------------------------------%
x                    = zeros(1,length(t));
dx                   = zeros(1,length(t));
z_wave_pon1          = zeros(1,length(t));
z_wave_pon2          = zeros(1,length(t));
c_mor1               = zeros(1,length(t));
c_mor2               = zeros(1,length(t));
c_mor3               = zeros(1,length(t));
morison              = zeros(1,length(t));
Tensionvariation     = zeros(1,length(t));
egenperiode          = zeros(1,length(i));
eigenfrequency       = zeros(1,length(t));
eta                  = zeros(1,length(t));
beta                 = zeros(1,length(t));
theta                = zeros(1,length(t));
nodes                = -b_pon:1:b_pon;
z_wave3              = zeros(length(t),length(nodes));

% The following variables are used to plot out data
Vector_beta          = zeros(1,length(Period));
Vector_theta         = zeros(1,length(Period));
Force                = zeros(1,length(Period));
force_max            = zeros(1,length(Period));
Morison_max          = zeros(1,length(Period));
Matrix_t_x           = zeros(length(Period),length(t));
Matrix_t_dx          = zeros(length(Period),length(t));
Matrix_t_c_mor2      = zeros(length(Period),length(t));
Matrix_t_c_mor3      = zeros(length(Period),length(t));
Matrix_t_morison     = zeros(length(Period),length(t));
Matrix_t_wave_pon1 = zeros(length(Period),length(t));
Matrix_t_wave_pon2 = zeros(length(Period),length(t));
Matrix_t_wave_pon3 = zeros(length(Period),length(t));
Matrix_t_theta       = zeros(length(Period),length(t));
Matrix_t_c           = zeros(length(Period),length(t));
Matrix_Tensionvariation                  = zeros(length(Period),length(t));
Matrix_Tensionvariation_tonnes           = zeros(length(Period),length(t));
Matrix_Tensionvariationlinearized_tonnes = zeros(length(Period),length(t));


for r = 1:length(Period)
    T        = Period(r)
    omega    = (2*pi/T);
    k_wave   =(omega^2)/g;


%@@@@@@@@@@@@@@@@@@@@@@@@@@@@@@@@@@@@@@@@@@@@@@@@@@@@@@@@@@@@@@@@@@@@@@@@@@@@%
```

```
    %                          HYDRODYNAMIC COEFFICIENTS
%@@@@@@@@@@@@@@@@@@@@@@@@@@@@@@@@@@@@@@@@@@@@@@@@@@@@@@@@@@@@@@@@@@@@@@@@@@@@@%
    A33      = A33_vector(r);
    B33      = B33_vector(r);
    F3       = F3_vector(r)*sin(omega*t)*Hs/2;
    Wave     = (Hs/2)*sin((2*pi/13)*t);


%@@@@@@@@@@@@@@@@@@@@@@@@@@@@@@@@@@@@@@@@@@@@@@@@@@@@@@@@@@@@@@@@@@@@@@@@@@@@@%
    %                          TO BE USED FOR DECAY-SIMULASJON.
    %                          NOT OTHERWISE
    %                          for normal analyse, uncomment F3 above

%@@@@@@@@@@@@@@@@@@@@@@@@@@@@@@@@@@@@@@@@@@@@@@@@@@@@@@@@@@@@@@@@@@@@@@@@@@@@@%
%     F3        = zeros(1,length(t));
%     F3(1:50)  = 1000000;

%@@@@@@@@@@@@@@@@@@@@@@@@@@@@@@@@@@@@@@@@@@@@@@@@@@@@@@@@@@@@@@@@@@@@@@@@@@@@@%

    disp('Solving the equation of motion with Runge-Kutta iteration ')
    for i = 1:h:length(t)

        z_wave_pon1(i) = omega*(Hs/2)*exp(-
k_wave*draught_pon)*cos((omega*i)-(k_wave*b_pon)-theta(i));
        z_wave_pon2(i) = omega*(Hs/2)*exp(-
k_wave*draught_pon)*cos((omega*i)-(k_wave*(-b_pon))-theta(i));

        if i < (length(t)-1)

            m_TTR       = (Totaltension*(1+(x(i)/z_0)).^n_g)/g;
            k_TTR       = Totaltension*n_g*((z_0.^(n_g))./((z_0-
(x(i))).^(n_g+1)));
            c_mor1(i)   = 6.0431e+006*(z_wave_pon1(i)-
dx(i)).*abs(z_wave_pon1(i)-dx(i));
            c_mor2(i)   = 6.0431e+006*(z_wave_pon2(i)-
dx(i)).*abs(z_wave_pon2(i)-dx(i));
            for j=1:length(nodes)
                z_wave3(i,j) = omega*(Hs/2)*exp(-
k_wave*draught_pon)*cos((omega*t(i))-(k_wave*(nodes(j)))-theta(i));
                sumwave3     = sum(z_wave3')/length(nodes);
                c_mor3(i)    = 2*6.0431e+006*(sumwave3(i)-
dx(i)).*abs(sumwave3(i)-dx(i));
            end
            morison(i) = c_mor1(i)+c_mor2(i)+c_mor3(i);

%               morison_166 = 8.515E+06;
%               morison_1   = 5.1294e+006;
            Matrix_t_c_mor3(r,i)     = c_mor3(i);
            Matrix_t_c_mor2(r,i)     = c_mor2(i);
            Matrix_t_morison(r,i)    = morison(i);
            Matrix_t_wave_pon1(r,i)  = z_wave_pon1(i)-dx(i);
            Matrix_t_wave_pon2(r,i)  = z_wave_pon2(i)-dx(i);
            Matrix_t_wave_pon3(r,i)  = sumwave3(i)-dx(i);


            m = mass + A33;
            c = B33 + cn_lin;
            k = K33 + k_TTR;
            Q = F3 + morison(i)  - Totaltension*mu_col*sign(dx(i));

            eigenfrequency(i)    = (sqrt(k/m));
            beta(i)              = omega/eigenfrequency(i);
            eta(i)               = c/(2*m*eigenfrequency(i));
            theta(i)             = atan((2*eta(i)*beta(i))/(1-(beta(i))^2));
            if theta(i) < 0
                theta(i) = pi + theta(i);
            end
            Matrix_t_theta(r,i)  = theta(i);
            Matrix_t_c(r,i)      = c;
```

```
            a1 = 1/m*(Q(i) - k*x(i) - c*dx(i));
            b1 = dx(i);
            a2 = 1/m*(((Q(i)+Q(i+1))/2) - k*(x(i)+0.5*h*b1) -
c*(dx(i)+0.5*h*a1));
            b2 = dx(i) + 0.5*h*a1;
            a3 = 1/m*(((Q(i)+Q(i+1))/2) - k*(x(i)+0.5*h*b2) -
c*(dx(i)+0.5*h*a2));
            b3 = dx(i) + 0.5*h*a2;
            a4 = 1/m*(Q(i+1) - k*(x(i)+h*b3) - c*(dx(i)+h*a3));
            b4 = dx(i) + h*a3;

            dx(i+1)             = dx(i) + h/6*(a1 + 2*a2 + 2*a3 + a4);
            x(i+1)              = x(i) + h/6*(b1 + 2*b2 + 2*b3 + b4);

Matrix_Tensionvariation(r,i) =
Totaltension+k_TTR*x(i)+cn_lin*dx(i)+Totaltension*mu_col*sign(dx(i));
Matrix_Tensionvariation_tonnes(r,i) =
(Totaltension+k_TTR*x(i)+(cn_lin*dx(i))+Totaltension*mu_col*sign(dx(i)))/100
00;
Matrix_Tensionvariationlinearized_tonnes(r,i) =
(Totaltension+k_TTR_lin*x(i)+(cn_lin*dx(i))+Totaltension*mu_col*sign(dx(i)))
/10000;

        end
%        egenperiode(r,i)         = 2*pi/(sqrt(k/m));
        Matrix_t_x(r,i)         = x(i);
        Matrix_t_dx(r,i)        = dx(i);
        Force(r,i)              = Q(i);
    end
end

disp('Time iteration finished')
disp(' ')
disp(' ')
disp(' ')


disp('Calculating the RAO in the frequency domain');
%-------------------------------------------------------------------------%
%    CALCULATES THE RAO & OTHER VARIABLES THAT VARIES OVER THE PERIOD     %
%-------------------------------------------------------------------------%
x_max  = zeros(1,length(Period));
dx_max = zeros(1,length(Period));

for i = 1:length(Period)
    x_max(i)       = max(Matrix_t_x(i,(time-100):(length(t)/h)));
    dx_max(i)      = max(Matrix_t_dx(i,(time-100):(length(t)/h)));
    force_max(i)   = max(Force(i,(time-100):(length(t)/h)));
    Morison_max(i) = max(Matrix_t_morison(i,(time-100):(length(t)/h)));
end



disp('Calculating the linear and nonlinear damping and K_TTR')
%-------------------------------------------------------------------------%
%           CALCULATES LINEAR AND NONLINEAR DAMPING AND K_TTR             %
%-------------------------------------------------------------------------%
lindamping         = cn_lin.*dx;
nonlindamping      = cn_lin.*dx.*abs(dx);
coldamping         = Totaltension*mu_col*sign(dx(i));
k_TTR              = Totaltension*n_g*((z_0.^(n_g))./((z_0-(x)).^(n_g+1)));

% Using the last period = 40s to calculate the spring rate
k_TTR_linearized   = sum(k_TTR(310:349))/40;
naturalperiodlinearized = (2*pi)*sqrt((mass+A33)/(K33+k_TTR_linearized));



disp(' ')
```

```
disp(' ')
disp(' ')
disp('Analysis finished :)')

%%%%%%%%%%%%%%%%%%%%%%%%%%%%%%%%%%%%%%%%%%%%%%%%%%%%%%%%%%%%%%%%%%%%%%%%%%%
%%%%%%%%%%%%%%%%%%%%%%%%%%%%%%%%%%%%%%%%%%%%%%%%%%%%%%%%%%%%%%%%%%%%%%%%%%%
```

```
%=========================================================================%
%                          TENSIONER DAMPING                              %
%®®®®®®®®®®®®®®®®®®®®®®®®®®®®®®®®®®®®®®®®®®®®®®®®®®®®®®®®®®®®®®®®®®®®®®®®®®®®®®®®®®®®®®%
%  This program is written for the Master Thesis - 'Responce analysis of  %
%  a deep-draft dry tree semi-submersible' the spring 2012. It calculates %
%  the pressure loss in an oscillating accumulator based on the Bernoulli %
%  equation and conservation of mass in the gas and fluid.                %
%                                                                         %
%                 Authors: Marianne-Isabelle Falk                         %
%                          Thomas Skorpen                                 %
%®®®®®®®®®®®®®®®®®®®®®®®®®®®®®®®®®®®®®®®®®®®®®®®®®®®®®®®®®®®®®®®®®®®®®®®®®®®®®®®®®®®®®®%
%                          Oslo 15.june 2012                              %
%                                                                         %
%=========================================================================%
%                          DEFINING VARIABLES                             %
%®®®®®®®®®®®®®®®®®®®®®®®®®®®®®®®®®®®®®®®®®®®®®®®®®®®®®®®®®®®®®®®®®®®®®®®®®®®®®®®®®®®®®®%
%      Variables when calculating loss in each cylinder                   %
%®®®®®®®®®®®®®®®®®®®®®®®®®®®®®®®®®®®®®®®®®®®®®®®®®®®®®®®®®®®®®®®®®®®®®®®®®®®®®®®®®®®®®%
% A_cyl                   : Area of piston in m^2                         %
% A_cyl2                  : Real piston area used for calculating tension %
% amp                     : Amplitude                                     %
% omega                   : Oscillating frequency                         %
% p_oil                   : Density of oil in kg/m^3                      %
% Period                  : Oscillating period                            %
% press_0                 : Initial pressure in system in N/m^3 (Pa)      %
% Q_oil                   : Oil flow m^3/s                                %
% resp                    : Response as function of time                  %
% t                       : Time interval                                 %
% v_oil                   : Viscosity of hydraulic oil in CST             %
% vel                     : Velocity as function of time                  %
% vol_acc                 : Volume of accumulator in m^3                  %
% vol_gas                 : Volume in gas bottles in m^3                  %
%                                                                         %
%®®®®®®®®®®®®®®®®®®®®®®®®®®®®®®®®®®®®®®®®®®®®®®®®®®®®®®®®®®®®®®®®®®®®®®®®®®®®®®®®®®®®®®%
%      Variables when calculating loss in piping/bends for hydraulics     %
%®®®®®®®®®®®®®®®®®®®®®®®®®®®®®®®®®®®®®®®®®®®®®®®®®®®®®®®®®®®®®®®®®®®®®®®®®®®®®®®®®®®®®®%
% A_1                     : Area of piston in m^2                         %
% D_1                     : Diameter of piping in meters                  %
% E_1                     : Surface roughness in m                        %
% L_1                     : Length of piping in meters                    %
% plossbar_1              : Pressure loss given in bar                    %
% rey_1                   : Reynolds number                               %
% vel_1                   : Velocity in piping as function of time        %
%                                                                         %
%®®®®®®®®®®®®®®®®®®®®®®®®®®®®®®®®®®®®®®®®®®®®®®®®®®®®®®®®®®®®®®®®®®®®®®®®®®®®®®®®®®®®®®%
%      Variables when calculating loss in piping/bends for pneumatics     %
%®®®®®®®®®®®®®®®®®®®®®®®®®®®®®®®®®®®®®®®®®®®®®®®®®®®®®®®®®®®®®®®®®®®®®®®®®®®®®®®®®®®®®®%
% A_g1                    : Inside area of piping #1                      %
% D_g1                    : Diameter of piping #1                         %
% dgasvol_acc             : Change of gas volume                          %
% gasvol_acc              : Gas volume in accumulator                     %
% gfriction_1             : Friction factor                               %
% L_g1                    : Length of piping #1                           %
% p0_g1                   : Density of gas                                %
%                                                                         %
%®®®®®®®®®®®®®®®®®®®®®®®®®®®®®®®®®®®®®®®®®®®®®®®®®®®®®®®®®®®®®®®®®®®®®®®®®®®®®®®®®®®®®®%
%      Variables when calculating the Tension variation                   %
%®®®®®®®®®®®®®®®®®®®®®®®®®®®®®®®®®®®®®®®®®®®®®®®®®®®®®®®®®®®®®®®®®®®®®®®®®®®®®®®®®®®®®®%
% tension                 : Tension in each cylinder                      %
% tensiontotal            : Total tension in the system                   %
%                                                                         %
%=========================================================================%

clear all;
clc;

%-------------------------------------------------------------------------%
%                   CALCULATING LOSS IN EACH CYLINDER                     %
%-------------------------------------------------------------------------%
```

```
% Input for oscillation of wave / response
period           = 14;
omega            = (2*pi)/period;
t                = 1:1:100;
amp              = 0.01;
resp             = amp*sin(omega*t);
vel              = amp*omega*cos(omega*t);

% Input for accumulator and hydraulic oil
% Common viscosity of hydraulic oils is in the range 16 - 100 centistokes.
% Optimum viscosity value is 16 - 36 centistokes.
vol_acc          = 6;
vol_gas          = 20;
A_cyl            = 4*0.25*pi*(0.56^2);
A_cyl2           = 0.25*pi*(0.56^2);
v_oil            = 30*(10^-6);
p_oil            = 872;
press_0          = 91.34*(10^5);

% Flow of oil between cylinder and accumulator
Q_oil            = A_cyl*vel;




%-------------------------------------------------------------------------%
%       CALCULATING THE PRESSURE LOSS IN PIPING/BENDS FOR HYDRAULICS      %
%-------------------------------------------------------------------------%

% Component 1
D_1              = 0.2;
A_1              = 0.25*pi*D_1^2;
L_1              = 30;
E_1              = 0.0002;
vel_1            = Q_oil/(A_1);
rey_1            = (vel_1*D_1)/(v_oil);

%®®®®®®®®®®®®®®®®®®®®®®®®®®®®®®®®®®®®®®®®®®®®®®®®®®®®®®®®®®®®®®®®®®®®®®®®®®®®®®®®®%
%                     Different friction models                           %
%®®®®®®®®®®®®®®®®®®®®®®®®®®®®®®®®®®®®®®®®®®®®®®®®®®®®®®®®®®®®®®®®®®®®®®®®®®®®®®®®®%
% Haaland equation for darcys friction
friction_1       = (1./(-1.8*log10((E_1./(D_1*3.7))^1.11+(6.9./rey_1)))).^2;

% Swameee-Jaim implicit darcys friction equation
sj_friction_1    = 0.25./(log10((E_1./(3.7.*D_1))+(5.74./rey_1.^2))).^2;

% Brkic solution for darcys friction factor
brkic_s1         = log(rey_1/(1.816*log((1.1*rey_1)/(log(1+(1.1*rey_1))))));
brkic_friction_1 = (1./(-
2*log10((E_1./(D_1*3.71))+((2.18*brkic_s1)./rey_1)))).^2;
%®®®®®®®®®®®®®®®®®®®®®®®®®®®®®®®®®®®®®®®®®®®®®®®®®®®®®®®®®®®®®®®®®®®®®®®®®®®®®®®®®%

ploss_temp       = 0.5.*p_oil.*((friction_1.*L_1)./D_1).*vel_1.*abs(vel_1);
ploss_temp2      = ploss_temp/4;
ploss_1          = ploss_temp2*2;
plossbar_1       = ploss_1/(10^5);




%-------------------------------------------------------------------------%
%       CALCULATING THE PRESSURE LOSS IN PIPING/BENDS FOR PNEUMATICS      %
%-------------------------------------------------------------------------%

p0_g1            = 1.24;
D_g1             = 0.2;
L_g1             = 20;
A_g1             = 0.25*pi*D_g1^2;

gasvol_acc       = (vol_acc/2)+(resp*A_cyl);
```

```
dgasvol_acc      = vel*A_cyl;

gfriction_1      = 1;


%-------------------------------------------------------------------------%
%                    CALCULATING THE TENSION VARIATION                    %
%-------------------------------------------------------------------------%

tension          = 4*(((press_0)+ploss_1)*A_cyl2);
tensiontonnes    = tension/10000;
tensiontotal     = 12*tensiontonnes;


%-------------------------------------------------------------------------%
%                     PLOTTING THE TENSION VARIATION                      %
%-------------------------------------------------------------------------%

hold on;
figure(1)
plot(resp,tensiontotal)
title('Tension variation in top tensioned risers')
ylabel('Tension in risers [tonnes]')
xlabel('Displacement [m]')

figure(2)
plot(vel,tensiontotal)
title('Tension variation in top tensioned risers')
ylabel('Tension in risers [tonnes]')
xlabel('Velocity [m/s]')

%=========================================================================%
```

APPENDIX D: Results from WADAM

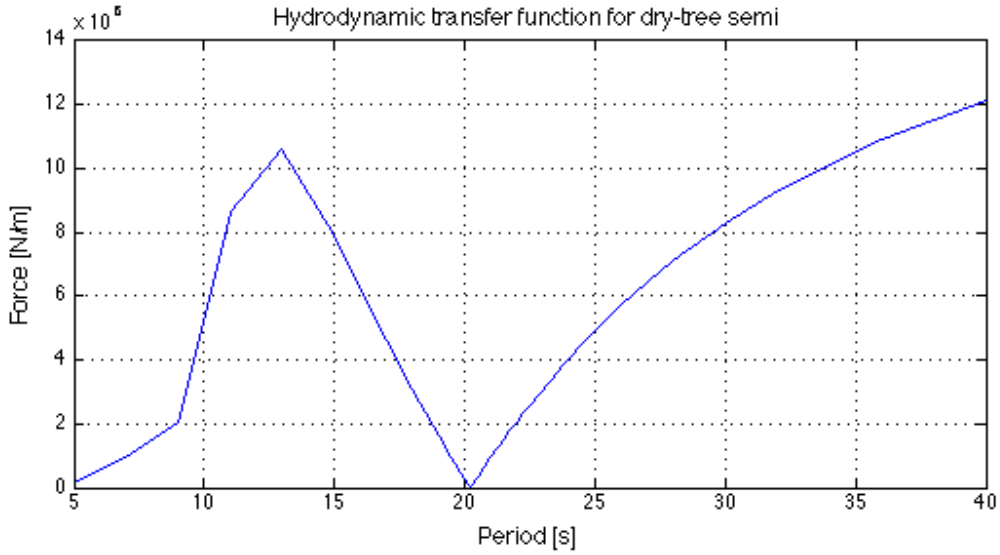

Figure D- 1: Hydrodynamic transfer function for freely floating dry-tree semi

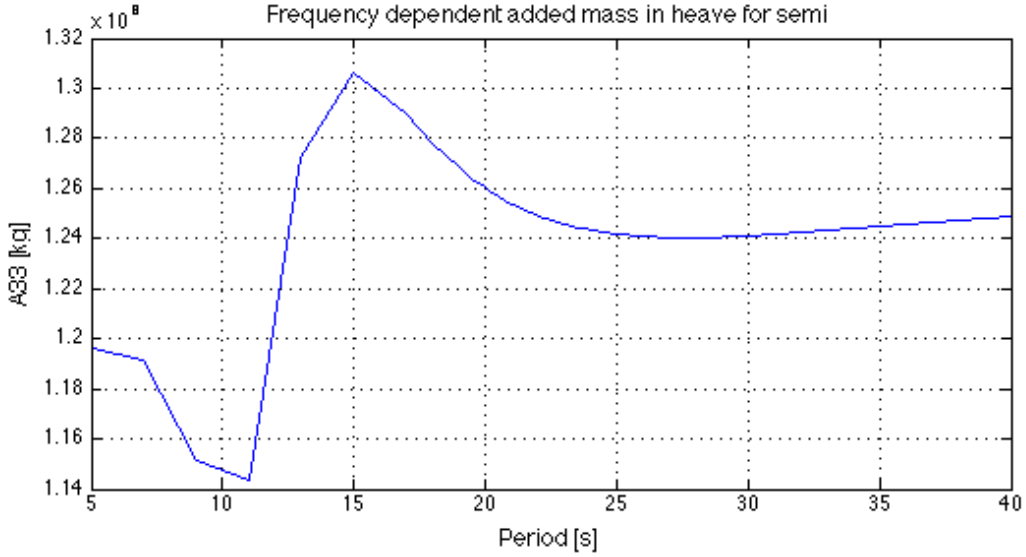

Figure D- 2: Frequency dependent added mass in heave for dry-tree semi

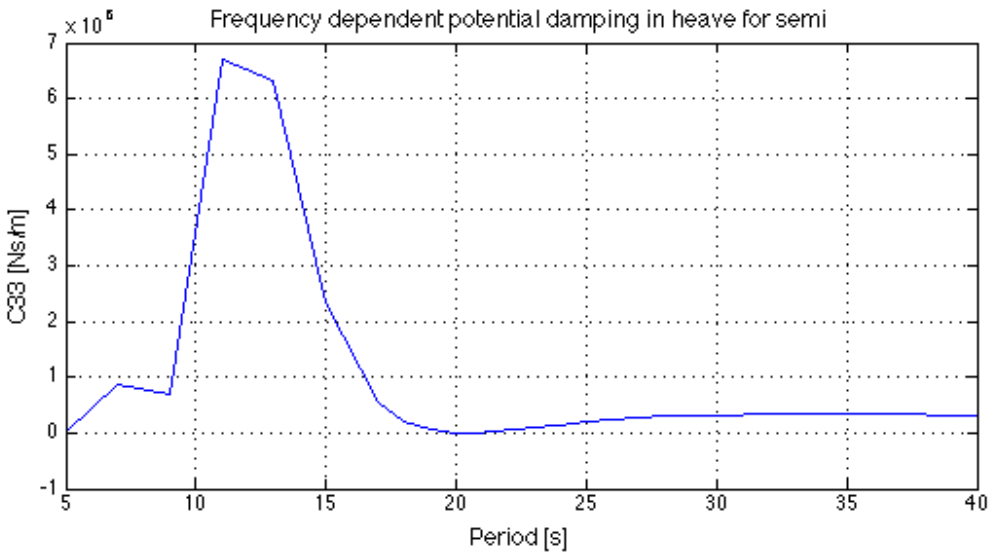

Figure D- 3: Frequency dependent potential damping in heave for dry-tree semi